Investigations on the oligomerization of pyolysin, a cholesterol-dependent cytolysin

by

Lisa A. Pokrajac

A thesis
presented to the University of Waterloo
in fulfillment of the
thesis requirement for the degree of
Doctor of Philosophy
in
Chemistry

Waterloo, Ontario, Canada, 2011

Author's Declaration

I hereby declare that I am the sole author of this thesis. This is a true copy of the thesis, including any required final revisions, as accepted by my examiners.

I understand that my thesis may be made electronically available to the public.

Abstract

The bacterial toxin pyolysin (PLO) is a member of the family of Cholesterol-Dependent Cytolysins, which form large, oligomeric pores in cholesterol-containing membranes. The general CDC structure has an elongated shape and consists of four domains rich in β-sheet structure. Upon binding to a membrane, molecules diffuse laterally on the surface and oligomerize to form a pre-pore complex, then insert into the membrane yielding pores of unusually large size, approximately 30 nm in diameter. In this work, the oligomerization properties of PLO were investigated. In particular, the role of the C-terminal domain in the oligomerization process, the effects of a disulphide-tethered mutant on the activity of the wild type toxin, and the pore-forming ability of oligomers pre-formed in solution were characterized.

Chapter 2 characterizes the functional properties of a recombinant fragment that corresponds to the C-terminal domain 4 of PLO. It is shown that this fragment can form hybrid oligomers with intact PLO toxin molecules, and is also capable of self-oligomerization. The fragment has no haemolytic activity of its own; nevertheless, it can to some degree increase the haemolytic activity of the wild type toxin. In addition, in a mixture domain 4 and wild type interact in such a way as to form unusual shapes on cholesterol crystals that have not been previously observed.

Chapter 3 describes the effects of a disulphide bond linking domain 2 to a membrane-inserting region of domain 3 on the oligomerization process. The disulphide mutant was not able to oligomerize on its own, and when combined with active PLO toxin, the haemolytic activity of wild type was significantly inhibited. Also, the combination of the disulphide-tethered mutant with intact toxin resulted in the formation of hybrid oligomers. This, in turn, caused an increase in incomplete ring formations on cholesterol surfaces which correlate to a reduction in functional pore size, suggesting that insertion of subunits is partially cooperative.

The results of the investigation of the pore-forming ability of solution-derived oligomers (SDO) are described in Chapter 4. Here, the fluorescence emission of an environmentally-sensitive probe on the SDO after membrane insertion was a fraction of that observed with the monomeric control, which was supported by hydrophobic quenching analyses. This suggests that the formation of SDO may block necessary conformational changes in the intact toxin to allow membrane insertion.

Acknowledgements

I would like to thank Professor Michael Palmer for his continual guidance and support during this thesis and all the many interesting discussions we had over the past years. It has been a very rich and fulfilling experience.

I would like to thank my committee members, Professors Elizabeth Meiering, Gary Dmitrienko and Rod Merrill for not only their useful suggestions and comments to assist me in this project, but also for their consideration, support and encouragement during this time. Sincere and special thanks to Professors Eric Jervis and Russel Bishop for their careful examination of my thesis and thoughtful suggestions.

I would like to thank all the members of my research group, Dr Shenhui Lang, Dr Dinath Ratnayake, Dr Naghmeh Sarri-Sarraf, Dr Waseem el Huneidi, David Donkor, Oscar Zhang, Mohammad Khan, Muhamad Salah, Jawad Murrah; all the undergraduate students Clara Baik, Claudia Chien, Tim Ramadhar, Ryan Mui, Gordon Sheffrey, Linda, Ana, Kathy and the exchange students Aurelie and Morgane. You all have made this a nice place to work.

I would also like to thank many of the friends I have made in the department, and my family and friends who provided continual cheers and encouragement. In particular, I want to thank Mom and Dad, Eric, Marc, Heather and the kids, Tim, Jake, Rob, Ron, Tom, JB, Chris and Andrea, CE, AK, Cecile and family, Family Rabak, Kathryn, Sandy, Angie, Farah, Connie and Marie Claire, Kathleen, Richard, Steve, Nick, Pat and Maria, Robin, CM, TM, Karen and Heather and friends, and all the rest (you know who you are). It really meant a lot.

Dedication

To my family

Table of Contents

List of Figures

List of Tables

Chapter 1

Introduction

Pyolysin is a pore-forming toxin secreted by the bacterial pathogen *Arcanobacterium pyogenes*. With its discovery and characterization in 1996 [25, 31] it has been classified as a member of the group of toxins known as Cholesterol Dependent Cytolysins or CDC [12]. Toxins of this group are secreted from a variety of Gram-positive bacteria, are known for causing damage to cell membranes, and are also considered to be important virulence factors for the producing organisms [5]. Although a great deal of study has been conducted on these toxins to understand activity, structure and mechanism of function, many questions still remain. In the present study, the results of an investigation of the oligomerization properties and the pore forming mechanism of the CDC pyolysin are presented.

1.1 PORE-FORMING TOXINS

Out of the over 300 different protein toxins produced by pathogenic bacteria that have been characterized to date, almost one-third cause damage to cellular membranes [5]. These membrane damaging toxins are commonly categorized by their mode of action. They either work enzymatically, by solubilizing the membrane via detergent-like action, or by self-organizing and oligomerizing on the surface to form discrete pores across the lipid bilayer [3]. In the latter case, pore-formation creates an osmotic imbalance, which results in cell swelling, lysis

and death [7, 38]. Bacterial pore-forming toxins are believed to be important virulence factors [116]. Pore-forming proteins do not only occur as bacterial toxins, however. A wide variety of organisms can produce such proteins, including plants, fungi, insects, and also mammals.

Bacterial pore-forming toxins are usually secreted as water-soluble monomers [18, 2] and upon encountering a membrane, binding occurs via a surface receptor. The toxin can then undergo oligomerization with other toxin monomers to form circular or partially formed rings ranging in size from seven, as is the case for the α-haemolysin of *Staphylococcus aureus*, to approximately 50 subunits (for the Cholesterol Dependent Cytolysins) [11, 73, 84].

Pore forming toxins are often classified according to the structural features that form the trans-membrane portion of the pore [42]. An α-pore forming toxin forms pores using α-helices, whereas a β-pore forming toxin forms a membrane-spanning β-barrel. While the membrane-inserted forms of α-pore forming toxins have not been well characterized, much more structural information is available on the membrane-inserted complexes of the β-PFTs [5]. In β-barrel pores, the amino acid residues along the polypeptide chain are alternatingly exposed to aqueous phase inside the lumen of the pore, and the non-polar lipid region of the bilayer core. Figure 1.1 illustrates the crystal structure of the membrane-inserted heptameric complex of the β-pore forming toxin *Staphylococcus aureus* α-haemolysin, with its membrane-spanning β-sheet network. Other members of this group include the Anthrax Protective Antigen (PA) and all members of the large family of toxins known as the Cholesterol Dependent Cytolysins or CDC. The crystal structure of the membrane-inserted Anthrax toxin PA has also been determined which has been found to be similar to α-toxin [91], however the oligomeric structure of the CDC is significantly different and due to their heterogeneity, it is very difficult to determine the crystal structure of CDC oligomers.

1.2 CHOLESTEROL DEPENDENT CYTOLYSINS

The cholesterol-dependent cytolysins (CDCs) constitute a large family of pore-forming toxins that are produced by more than 28 species from the Gram-positive bacterial genera *Clostridium*, *Streptococcus*, *Listeria*, *Bacillus*, *Paenibacillus* and *Arcanobacterium* [2, 39, 48]. Unusual features of toxins from this group include the formation of very large pores with a diameter of approximately 300 Å consisting of up to 50 monomers [11, 73, 84], and the absolute dependence on cholesterol in the target membrane for cytolytic activity. Table 1.1 lists some of the identified cholesterol dependent cytolysins and the originating bacterial pathogen.

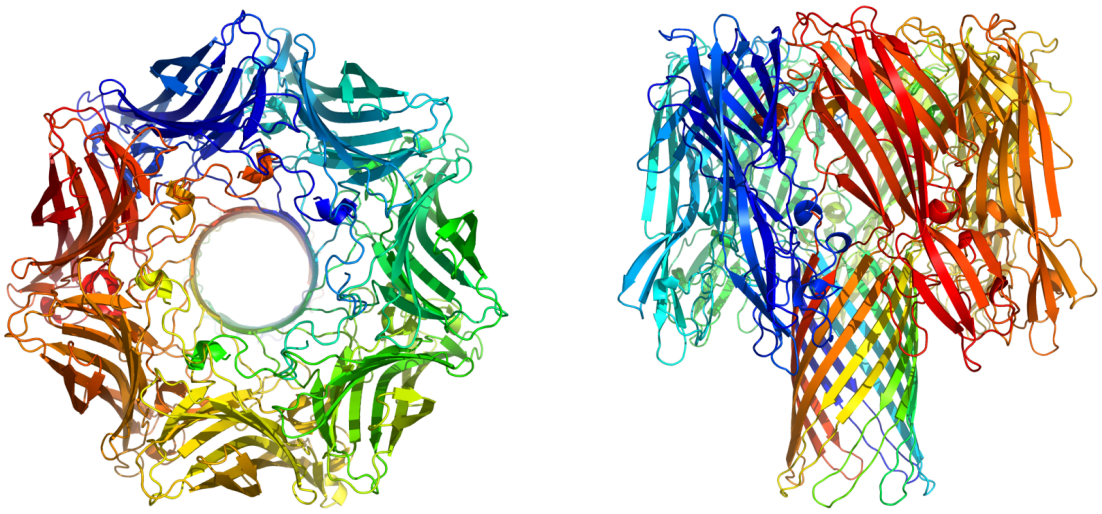

Figure 1.1 The Membrane-Inserted Heptameric Complex of *Staphylococcus* α-Haemolysin. The top and side views of the *Staphylococcus* α-Haemolysin (7AHL) heptameric pore [109]. Each of the seven subunits is shown in a different colour.

1.3 THE CDC MONOMER STRUCTURE

The first crystal structure of a CDC was resolved in 1997 [98]. The monomeric structure of perfringolysin O (PFO) was shown to be elongated (approximately 115 Å in length), rich in β-sheet, and to consist of four domains. Domain 1 is located at one end of the molecule and contains both α-helix and β-sheet elements, while domain 2 is a long, curved single layer of antiparallel β-sheet. Domain 3 consists of a core of five strands of anti-parallel β-sheet surrounded by helical layers on both sides. Two sets of three short α-helices each are found in this domain that convert to transmembrane β-hairpins upon pore formation. Finally, domain 4 has a predominantly β-sandwich structure, which is connected to the rest of the protein through a single peptide link. Domain 4 is the only contiguous domain of the CDC molecule. Found in this domain are three short loops (L1, L2 and L3) and a highly conserved undecapeptide region that are implicated in membrane recognition and binding.

Since the determination of the PFO crystal structure, the monomeric structures of two other CDCs have also been resolved, intermedilysin (ILY)[92] and anthrolysin O (ALO) [17], showing that these toxins adopt a very similar three-dimensional configuration. Considering the similarity of the primary sequence of the CDCs, it is very likely that all members of the CDC family of toxins share similar three dimensional structures and similar modes of pore formation [47, 113].

Table 1.1 The Family of Cholesterol Dependent Cytolysins [97].

Bacterial Genus	Species	Toxin	Acronym
Streptococcus	*S. pyogenes*	Streptolysin O	SLO
	S. equisimilus	Streptolysin O	SLO
	S. canis	Streptolysin O	SLO
	S. pneumoniae	Pneumolysin	PLY
	S. suis	Suilysin	SLY
	S. intermedius	Intermedilysin	ILY
Bacillus	*B. cerus*	Cereolysin O	CLO
	B. anthracis	Anthrolysin O	ALO
	B. thuringiensis	Thuringolysin O	TLO
	B. lacterosporus	Lacterosporolysin	LSL
Clostridium	*C. tetani*	Tetanolysin	TLY
	C. botulinum	Botulinolysin	BLY
	C. perfringes	Perfringolysin O	PFO
	C. septicum	Septicolysin O	SPL
	C. histolyticum	Histolyticolysin O	HLO
	C. novyi A	Novyilysin	NVL
	C. chauvoei	Chauveolysin	CVL
	C. bifermentans	Bifermentolysin	BFL
	C. sordellii	Sordellilysin	SDL
Listeria	*L. monocytogenes*	Listeriolysin O	LLO
	L. ivanovii	Ivanolysin	ILO
	L. seeligeri	Seeligerolysin	LSO
Arcanobacterium	*A. pyogenes*	Pyolysin	PLO

The residues spanning each domain for the CDC pyolysin (PLO) are listed in Table 1.2, and the structure of monomeric PLO (based on the PFO-PLO sequence alignment generated by Swiss Model) is shown in Figure 1.2.

Table 1.2 Assignment of Amino Acid Residues for the Domains of Pyolysin

Domains of PLO	Residues Spanning the Domain
One	58-81, 118-207, 257-303, 373-406
Two	82-117, 407-423
Three	208-256, 304-372
Four	424-534

1.4 MECHANISM OF PORE FORMATION

Four main steps occur in the pore-formation process: 1. membrane binding of the toxin monomer, 2. lateral diffusion on the membrane surface, 3. oligomerization to form the pre-pore, and 4. insertion of the latter into the membrane to form the pore.

The initial binding of the monomer is mediated by the C-terminal domain [81, 114], also known as domain 4. This binding event causes discernible structural rearrangements in the upper domains of the CDC that prepares the toxin for oligomerization [87]. At this time, the bound monomers are able to diffuse laterally on the membrane surface and interact with other bound monomers. In this way, oligomerization of the toxin molecules is initiated.

Within the oligomers, interactions between domains 1 and 3 have been documented [87, 86], and as seen in the current investigation, domain 4 of PLO also participates in the oligomerization process. The subsequent oligomerization of the monomers into pre-pore complexes aligns the twinned domain 3 trans-membrane β-hairpins (TMH) segments of adjacent monomers and triggers their insertion into the membrane to form a large trans-membrane β-barrel [104, 105].

These oligomerized monomers form a *pre-pore* complex. These pre-pores consist of toxin molecules that are in a similar conformation as the monomeric toxin before membrane binding [23, 110]. The oligomerization of the monomers leads to the formation of ring- and arc-like structures on the membrane surface [11, 70, 72, 86, 78, 102], followed by insertion of the transmembrane β-hairpins, forming a membrane-spanning β-barrel pore. A more detailed description of each step of the pore forming mechanism and the domains involved is given below.

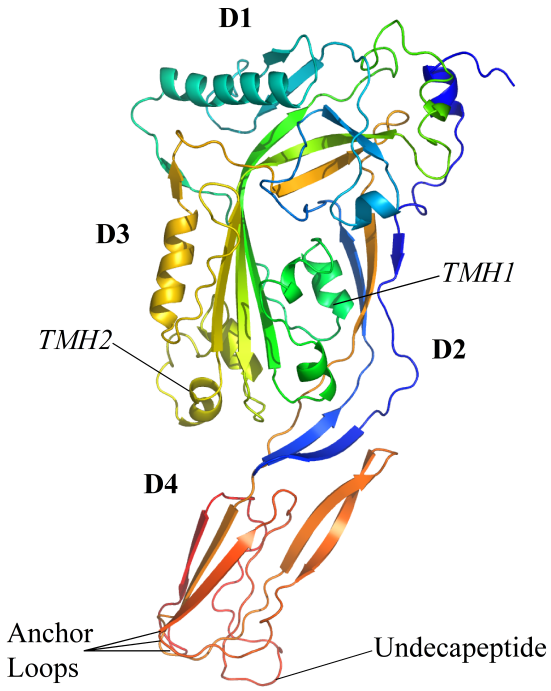

Figure 1.2 Homology Model of Pyolysin. Ribbon representations illustrate the locations of the four domains of the toxin. The positions of both transmembrane β-hairpins, and the binding loops in domain 4 are labelled. The homologous PLO structure was based on the sequence alignment of PFO and PLO using Swiss Model, and the crystal structure of PFO created from pdb records 1PFO (perfringolysin) using PyMOL.

1.4.1 Membrane Binding

In early studies to determine which regions of the toxin were responsible for membrane binding, PFO was proteolytically cleaved to yield two fragments [81, 114]. While the N-terminal fragment lacked any recognizable activity, the C-terminal fragment retained the ability to bind to cell membranes. In 1997, after the determination of the crystal structure of PFO [98], it was postulated that this domain was responsible for spanning the membrane and creating the pore. This theory, however, was inconsistent with previous fluorescence studies conducted on SLO, where it was discovered that residues found in domain 3 inserted into the membrane [86, 87]. Upon further investigation, it was found that the only areas of domain 4 to insert into the membrane were three short loops (L1, L2 and L3) and the undecapeptide region found at the tip of domain 4, and these regions inserted shallowly which could not allow for domain 4 to span the bilayer [94].

The binding event has been shown to be reversible, and it can occur at low temperatures [88]. The reversibility of SLO binding to erythrocytes was observed when the toxin was incubated with the cells at 4 °C and the excess toxin removed after centrifugation. After fresh erythrocyte cells were added to the SLO-bound cells, photometric examination of subsequent haemolysis showed that a greater number of cells lysed than were originally treated. This indicated that the SLO toxin molecules must have migrated to new cells from those to which they were originally bound [88].

In the same study, reversibility of binding was also tested using radio-labelled ^{125}I-SLO. After incubation in the cold and removal of excess toxin, 5,5'-dithiobis-(2-nitrobenzoic acid), (DTNB, Ellmans Reagent) was added to the SLO-erythrocyte mixture. At specific intervals the sample was centrifuged and aliquots of the supernatant were taken and tested for the presence of radio-labelled SLO. With time, increasing amounts of SLO were found in the supernatant, compared to none in the supernatant of the control sample (with no Ellmans Reagent). These tests show that CDCs have the ability to bind to erythrocyte membranes in a reversible manner.

Interestingly, the binding event initiates conformational changes within the CDC molecule seen in both domains 1 and 3, prior to oligomerization [89]. As the oligomerization process is temperature dependent [29, 46, 79], studies were conducted to determine the extent of conformational coupling between the different domains. For toxin incubated with ghost erythrocytes at low temperatures, it was found that four mutants of SLO that were modified with the fluorophore 6-acryloyl-2-dimethyl-amino-naphthalene (acrylodan), whose spectral properties are dependent on the polarity of the surrounding environment, exhibited a distinct shift in fluorescence emission upon binding. The mutants S218C and A266C showed a distinct red-shift in wavelength maxima, or shift to higher wavelengths with membrane binding, signifying these mutants become exposed to regions of greater polarity. The mutants A248C and T277C, on the other hand, gave a blue shift in spectral maxima, or shift to lower wavelength upon binding, denoting exposure to an environment of increasing hydrophobicity, yet the maxima remained greater than those typical of membrane-inserted amino acid residues. These shifts represent a change in polarity of the local environments, and this study concluded that membrane binding conformationally affects a distant part of the molecule involved in later steps of pore formation [89].

1.4.2 Oligomerization and Membrane Insertion

After binding to the membrane, monomers diffuse laterally in order to initiate oligomerization. The binding process confers distinct conformational changes in upper domains of the toxin molecule. It was first discovered that domains 1 and 3 were involved in the oligomerization and membrane insertion steps in 1996 [87]. Here, 19 amino acid residues of SLO, spanning the positions 213 to 305 were replaced with cysteine and labelled with acrylodan. Three residues in domain 3 showed distinct emission blue-shifts, signifying the movement to an area of increased hydrophobicity upon interaction with the membrane. With the addition of dexoycholate solution to the samples to dissolve the membrane, the acrylodan emission exhibited a significant red-shift, or shift to longer wavelengths, denoting that these residues came into direct contact with the lipid bilayer of the membrane.

The residues A213C (found in domain 1) and T245C (at the domain 1-domain 3 interface) also exhibited blue shifts upon membrane binding, illustrating that domain 1 experiences discernable conformational changes as well. When the membrane was solubilized, there was little change in the emission maxima denoting no change in the polarity of the fluorophore environment. This indicates that these residues do not insert into the membrane, but rather move into a proteinaceous apolar environment during oligomerization.

The core of domain 3 consists of five β-strands that are linked to two sets of three short α-helices that later form the transmembrane β-hairpins (TMH) that insert into the bilayer. In Figure 1.3, the loops are labelled $\beta1$ through $\beta5$, with $\beta1$ and $\beta2$ associating with transmembrane β-hairpin 1 (TMH1), $\beta3$ and $\beta4$ associated with TMH2, and $\beta5$ is a short loop covering the outside edge of $\beta4$ [95]. Upon membrane binding, it was found that the outer $\beta5$ strand moves away from the $\beta4$ strand of the core during this process. This motion renders $\beta4$ exposed where it can now interact with the $\beta1$ strand of the adjacent toxin monomer, thus initiating or extending the oligomerization process.

Additional studies using PFO confirmed that the series of small helices on either side of central β-sheet of domain 3 could unfurl into a β-sheet conformation, into the two transmembrane β-hairpins (TMHs) that insert into the membrane and form a β-barrel. This was determined as each residue in both TMH regions of PFO (residues 189-218 for TMH1 and residues 288-312 for TMH2) [104, 105] were replaced with cysteine and chemically modified with the environmentally sensitive fluorophore N'-(7-nitrobenz-2-oxa-1,3-diazol-4-yl)-ethylenediamine (NBD). The changes in the emission spectra after incubation with membranes indicated

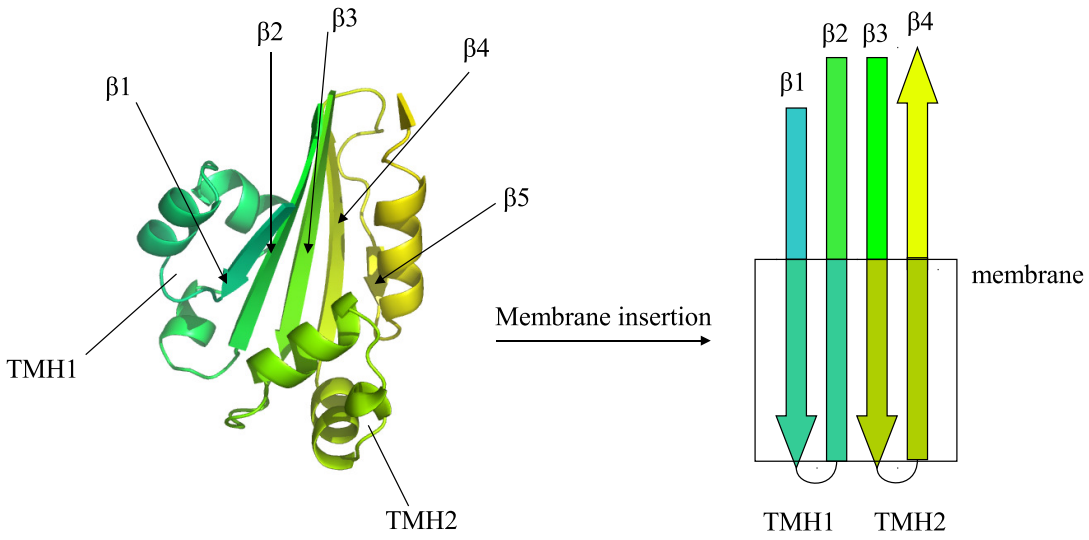

Figure 1.3 Core of Perfringolysin O Domain 3, α-Helices to β-Sheet Transition with Membrane Insertion [95]. Ribbon representation of the domain three core of perfringolysin O (1PFO) in water-soluble monomer form (left). The three short α-helices of TMH1 are in blue, and the helices of TMH2 are in green, with the five β-sheets within the perfringolysin O core labelled. The α-helices undergo structural changes to β-sheet upon membrane insertion. Cartoon representation of the membrane-bound form of the toxin, left.

an alternating pattern of polar and non-polar environments for each stretch of residues tested, signifying that the residues alternated between facing the aqueous phase (forming the lumen of the pore) and the inner lipid bilayer of the membrane core. Figure 1.3 illustrates the conformational changes involved in the core β-strands of domain 3 and the insertion of the TMHs. This conversion from α-helix to β-barrel pore is unique to the CDC pore-forming process. In addition, many other pore forming toxins only contribute one trans-membrane β-hairpin per molecule to the β-barrel structure. Cholesterol dependent cytolysins are so far the only pore-forming toxins that donate two trans-membrane β-hairpins per toxin molecule [104].

Atomic force microscopy (AFM) [23] and fluorescence resonance energy transfer studies [96] have shown that a significant decrease in toxin height occurs after the conversion from monomeric to membrane-inserted states, believed to be caused by the collapse of domain 2 that brings the transmembrane β-hairpins found in domain 3 close to the membrane surface for insertion [96]. It is not yet certain, however, if the collapse occurs in order to bring domain 3 closer to the membrane surface to facilitate insertion, or if the event is a consequence of TMH insertion. Figure 1.4 summarizes the steps of the pore formation process as described.

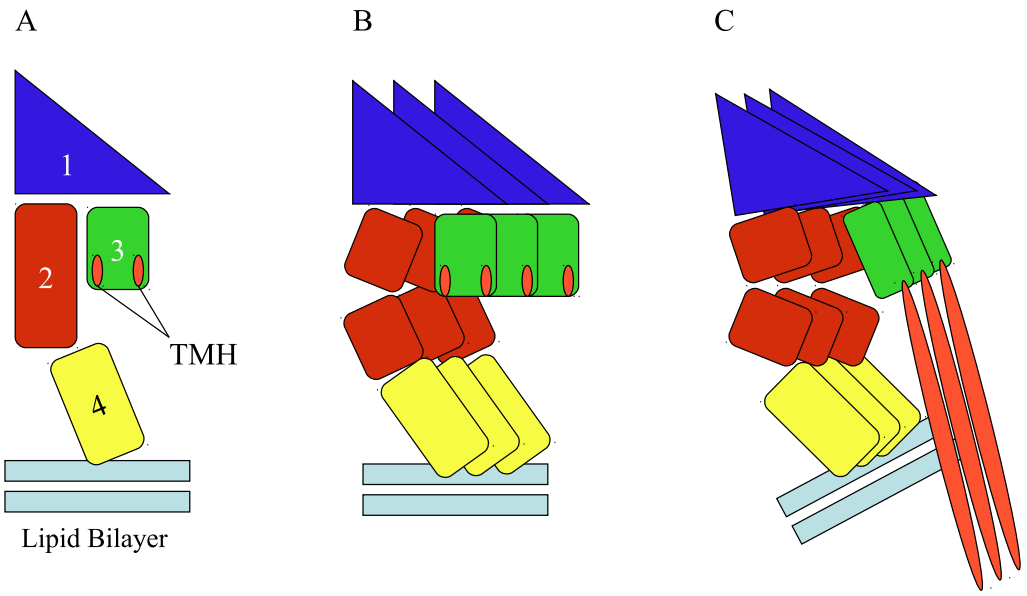

Figure 1.4 The Pore-Forming Mechanism of Cholesterol-Dependent Cytolysins. The binding of the monomers to the lipid bilayer is the first step in the pore forming mechanism of CDC (as seen in panel A). Next, the monomers diffuse laterally across the membrane surface and oligomerize to form a membrane-bound pre-pore (B). The final step involves a conformational change, and the toxin oligomer inserts into the membrane to form a pore (C).[110]

1.5 THE CORRELATION OF OLIGOMERIZATION AND PORE-FORMATION

As mentioned earlier, both circular rings and incomplete rings or "arcs" of CDCs have been observed on membranes using electron microscopy [9, 70, 72, 78, 86, 102]. In addition to this, SLO exhibited irregular-shaped pores that resembled two arcs that have fused together. These features have not been observed in other pore-forming toxins, and their presence has been the topic of much debate over the mechanism of assembly of the oligomeric complexes on the membrane surface. Different models have been proposed to account for this behaviour, as illustrated in Figure fig:IntroductionPoreFormationModels.

One model is based on the observation that PFO can assemble into large oligomeric ring-shaped complexes prior to the insertion of the β-hairpins into the membrane bilayer [106]. This model suggested that the formation of a complete, circular 'pre-pore' complex must be formed before the insertion of the TMHs and formation of the membrane-spanning β-barrel can occur [106].

This completed-ring oligomer model, however, does not take into account the presence of the arcs on the membrane surface and that these arcs give rise to pores of decreased size [86],

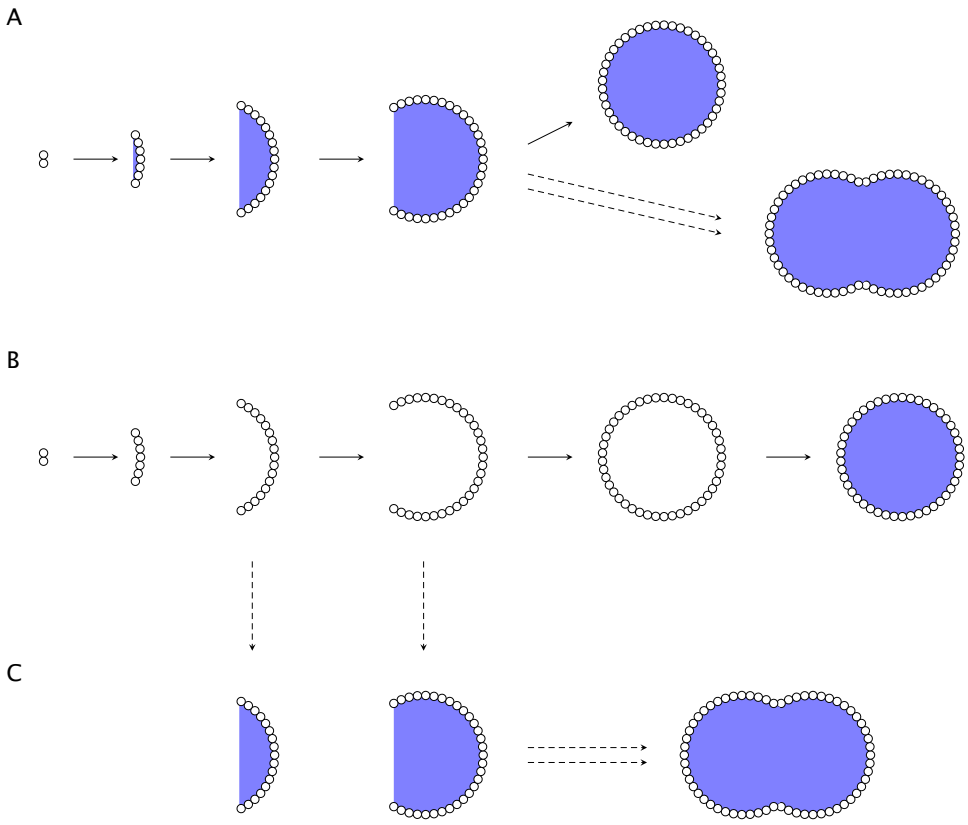

Figure 1.5 Comparison of the Different Proposed Models for Cholesterol Dependent Cytolysin Pore Formation. Top: The Growing Arc Model of pore formation described by Palmer [86] stipulates that toxin oligomerization and pore formation can occur simultaneously. Formation of twin-arcs is driven by the relaxation of line tension which exists at the free membrane edge opposite a single arc. Center: The Completed-Ring Pre-Pore Model of pore formation postulated by Tweten [115] states that oligomerization of CDC monomers must proceed until complete rings are formed before insertion into the membrane can occur. Bottom: A consensus model postulates that oligomerization precedes insertion but does not have to go to completion before insertion occurs [38]. The purple colour indicates toxins that have inserted into the membrane.

suggesting that oligomerization does not need to be complete for insertion to occur. To account for this, a second model proposes that oligomerization and membrane insertion of the CDC molecule can occur in tandem. Here, it is argued that pore formation is commenced by the formation of a dimer that immediately inserts into the membrane and serves as a nucleus for further oligomerization. Further monomers are successively added to the dimer and concurrently insert into the membrane, giving rise to a pore that is lined on one side by toxin and

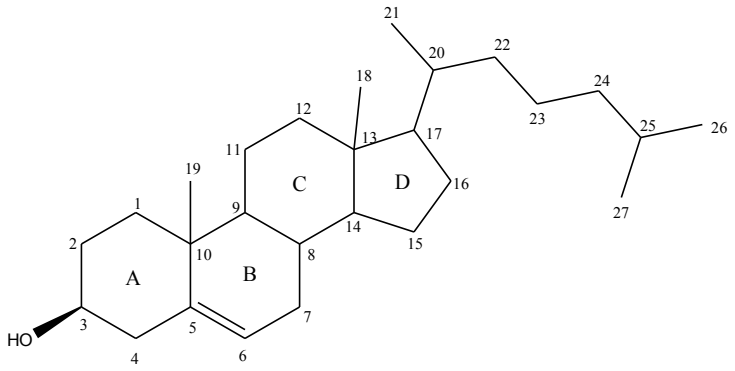

Figure 1.6 Chemical Structure of Cholesterol

on the opposing side by lipid membrane. This growing arc eventually becomes a complete ring-shaped pore [86].

A third model of pore formation has been proposed, which is the only model that accounts for all available experimental evidence. Here, two different oligomeric states can exist, the pre-pore and the pore, and the moment of transition depends on factors other than completeness of the ring. In this model, once membrane insertion has occurred, oligomerization ceases [38].

1.6 ROLE OF CHOLESTEROL IN THE ACTIVITY OF CDCS

The role of cholesterol in pore formation has been found to be primarily in the binding step. This is supported by the observations that the lytic activity of tetanolysin (TLY) [6, 71], cereolysin [21, 103], streptolysin O [26, 93, 103, 119], and listeriolysin (LLO) [33] was inhibited by incubation with free cholesterol, the toxins have no haemolytic activity on prokaryotic or any cells lacking cholesterol, and that the CDCs could bind directly to pure cholesterol and liposomes containing cholesterol [55, 83].

Inhibition of lytic activity has been observed with low (nano-molar) concentrations of not only cholesterol, but with sterols of similar structure. It was found that variations in the sterol structure affected CDC activity. It was found that the hydroxyl functional group in the β-configuration on the C_3 of ring A of the cyclopentanoperhydrophenanthracene, the isooctyl chain on C_{17} of ring D, the methyl group on C_{20}, and an intact B ring are all necessary for interaction with the toxin [93, 118]. The chemical structure of cholesterol is illustrated in Figure 1.6.

With the OH group in the α-position on the C_3 (as in epicholesterol), esterified, replaced with a keto-group or replaced with a β-SH group (thiocholesterol), the inhibitory effects of the incubated sterols on the toxin were not observed [4].

Studies with cholesterol-containing liposomes have shown that a relatively high concentration of cholesterol is required for binding, in the order of 40 mole percent of the total membrane lipid concentration [80]. It has also been shown that the transition from no binding to full binding in liposomes occurs within a narrow range of cholesterol concentration [80]. In fact, this high concentration of cholesterol led some researchers to speculate that the formation of lipid rafts in the membranes may be necessary for binding to occur [117]. However, no conclusive evidence has been shown to support this model. Studies have been conducted to determine if the conditions that promote lipid raft formation would enhance binding of PFO, phospholipids of various acyl chain lengths [30] and degree of saturation [77], as well as various sterols [77]. Here, little correlation was found between the liposome composition expected to promote raft formation and PFO binding.

The role of cholesterol has been examined in three CDCs, PFO, SLO and ILY [34]. Here, each of the toxins was incubated with membranes where the cholesterol content of the membrane was decreased by approximately 90%. It was found that the haemolytic activity of all toxins dramatically decreased, by 90% for both ILY and SLO, and by over four orders of magnitude for PFO compared to wild type activity. It was also found that the decrease in membrane-cholesterol effected an approximate 10-fold decrease in binding of PFO, yet the binding of ILY and SLO was not affected. The latter two toxins were seen to oligomerize into pre-pore complexes, but were not able to insert into the membrane; based on these findings it was proposed that the main role of cholesterol was for membrane insertion of the TMHs. However, this experiment did not completely remove all cholesterol from the membranes and the findings may be a result of the toxins' interaction with the residual sterol in the membrane.

Although the above finding is in agreement with previous studies on PFO that cholesterol is necessary for PFO binding [69, 80, 82], the observation that SLO binds to cholesterol-depleted membranes contrasts with other findings. Previous reports illustrate that SLO has significant affinity to liposomes consisting of cholesterol, and to immobilized cholesterol substrates [43] but not to liposomes without cholesterol [74].

Recently, it was proposed that two residues in one of the loops of domain 4 involved in membrane-binding (L1) are essential for the cytolytic toxin recognition of cholesterol at the membrane surface [28]. The two residues, T490 and L491, in PFO are strictly conserved in

all known CDCs, and conservative changes (to either glycine, alanine or reverse threonine for leucine) result in drastically decreased binding and activity to cholesterol-rich liposomes and human erythrocytes. Although this study shows there is correlation between these two conserved residues and cholesterol dependence, it is unlikely that only two amino acid residues mediate the recognition of cholesterol in the entire toxin molecule.

1.7 PROPERTIES OF SPECIFIC CHOLESTEROL DEPENDENT CYTOLYSINS

The toxins belonging to this family are very similar with respect to structure and mode of action, but many interesting differences exist between them as well. Listed below are some specific cholesterol dependent cytolysins and unusual features not shared with other known family members.

1.7.1 Streptolysin O

Streptolysin O (SLO) is secreted from *Streptococcus pyogenes*, a pathogen frequently associated with dermatological infection [41]. The lytic activity of *S. pyogenes* lysates was first discovered by Marmorek in 1902 [66], and upon further investigation in the 1930's, this lytic activity was attributed to two haemolysins [111, 112, 121]. The haemolysin that became less haemolytically active with increased exposure to air was named streptolysin *O* (SLO) in order to denote it is oxygen-labile, whereas the oxygen-stable haemolysin was named streptolysin *S* (SLS) [111, 112, 121]. Since then, SLO has been one of the most intensively investigated membrane-damaging toxins over the past 60 years and it has been shown to be important to the pathogenesis of *S. pyogenes* [1].

SLO has the longest primary sequence of all the CDCs identified thus far, at 571 residues in length, compared to PFO at 500, and the smallest alveolysin (ALV) at 470 residues [5]. When secreted, SLO contains approximately 60 extra amino acids at its N-terminus that are not found on any other CDC [65]. This N-terminal extension is used in the translocation of the bacterial protein NADH-glycohydrolase (an exoenzyme also produced by S. pyogenes) into human keratinocytes [65]. It was found that when these extra residues were deleted from the SLO sequence, the toxin retained the ability to form pores, but the ability to transport NADH-glycohydrolase was lost. Additionally, when the peptide sequence was added to PFO, translocation of the enzyme did not occur, suggesting that SLO must have additional features to allow this [67].

1.7.2 Pneumolysin

Pneumolysin (PLY) is produced by *Streptococcus pneumoniae*, a pathogen known for several important diseases including pneumonia, bacteraemia, meningitis, and otitis media [85]. *S. pneumoniae* was first reported to produce haemolysin in 1905 [63], and since then PLY has been considered an important virulence factor of pneumococci.

PLY is a 53 kDa toxin produced by almost all isolates of *S. pneumoniae* [59, 90]. Unlike the other known CDCs, PLY lacks an N-terminal signal peptide and as such is not secreted by the usual type II secretion pathway. Instead, PLY accumulates in the cytoplasm of a pneumococcus cell and is released upon bacterial growth and autolysis in most strains [54].

Another distinct feature of PLY is that it contains a region that is capable of activating complement in the absence of specific antitoxin antibodies [68]. This activation in the fluid phase may act to divert complement away from intact bacteria and consume complement components. At higher concentrations, PLY can form oligomeric structures in solution without the presence of a membrane surface and it is postulated that the function of this form may be more effective in activating complement than monomeric toxin [68]. PLY may have evolved in such a way to be more easily triggered to oligomerize in solution so that a fraction of PLY can activate complement but the remainder can still bind to membranes and form pores.

1.7.3 Listeriolysin O

Listeriolysin O (LLO) is secreted from *Listeria monocytogenes*, an important pathogen in humans, known to cause meningitis, encephalitis and intrauterine infections [41]. The production of a haemolysin by this organism was first reported in 1941 [45], and in 1964 it was found that the listerial haemolysin was functionally related to SLO [60]. However, it was not until 1987 that the toxin was purified to homogeneity and categorized as a member of the CDC family [33].

Listeriolysin O is an unusual CDC because of its pH-dependent pore-forming activity. The toxin has a pH optimum at 5.5, much more acidic than for other members of the CDC family, and when the pH is elevated to become neutral, the cytolytic activity is decreased [33]. The discovery of the low pH optimum led researchers to suspect that LLO may be involved in the disruption of phagosomal membranes [60].

Once the bacterium enters a cell, it secretes LLO which becomes activated by the acidic medium of the phagosome (pH 5.5-5.9) [33]. The LLO can then perforate the phagosomal

boundary where the bacterium can gain entry into the cytosol of the host cell. Here, the *L. monocytogenes* can use the cytosol and contents as nutrients, allowing the bacterium to grow and proliferate. As the pH of the intracellular medium of the host is closer to neutral, the activity of LLO is significantly decreased and is not able to lyse the outer membrane of the host cell [40, 8]. In addition to this, LLO contains an N-terminal PEST (proline-glutamic acid-serine-theronine)-like sequence that targets LLO for degradation before excessive damage to the host cell can occur [24]. Living inside the host cell is advantageous to *L. monocytogenes* as here it is protected from extracellular immune system factors [8, 32].

1.7.4 Intermedilysin

Intermedilysin (ILY) is produced by *Streptococcus intermedius*, which was first discovered in human liver abscess in 1996 [75]. The 54 kDa protein is considered to be an atypical cholesterol dependent cytolysin as it is specific to human cells and does not use membrane cholesterol as a receptor for binding [76].

As the toxin activity was only weakly inhibited with incubation with free cholesterol, speculation arose as to the necessity and function of membrane cholesterol [34]. Studies involving ILY and cholesterol-depleted membranes have shown that the activity of the toxin decreased significantly, yet no effect on binding was seen. This signified that the toxin's sensitivity to cholesterol must occur at later steps in the pore-formation process [34].

The binding of ILY on human erythrocytes was shown to decrease when the cells were treated with trypsin, suggesting that ILY uses a surface protein receptor to bind [35]. It was found that the human glycosylphosphatidylinositol (GPI)-anchored membrane protein CD59 acts as the receptor. The CD59 protein of other animal erythrocytes is not susceptible to ILY binding; even primate erythrocytes show a 100-fold decrease in binding compared to human cells. It is believed that this specificity is in part a result of the CD59 peptide sequence from residues 42-59 that is known to bind complement proteins. This region exhibits the greatest level of heterogeneity between human, non-human primate and animal CD59 molecules and may be responsible from the species-selective activity of ILY [35].

Table 1.3 The Conserved Undecapeptide Region of Cholesterol-Dependent Cytolysins [5]. Residues that deviate from the consensus sequence are highlighted.

Toxin	First residue	Sequence
PFO	458	ECTGLAWE-WWR
SLO	529	ECTGLAWE-WWR
PLY	427	ECTGLAWE-WWR
SLY	455	ECTGLAWE-WWR
LLO	483	ECTGLAWE-WWR
LSO	484	ECTGLFWE-WWR
ILO	458	ECTGLAWE-WWR
ALY	460	ECTGLAWE-WWR
CLY	465	ECTGLAWE-WWR
PLO	491	EATGLAWDPWWT
ILY	485	GATGLAWEPW-R

1.8 CHARACTERIZATION OF PYOLYSIN AS A CHOLESTEROL-DEPENDENT CYTOLYSIN

Pyolysin is produced by the bacterial pathogen *Arcanobacterium pyogenes*, and it was first identified as a haemolytic toxin in 1937 by Lovell [64]. The organism *A. pyogenes* is an arc-shaped, non-motile and non-spore forming bacterium that grows under strictly anaerobic conditions, with optimal growth occurring in a CO_2-rich atmosphere [56]. All isolates of *A. pyogenes* show β-haemolysis on agar media containing bovine and ovine blood, with isolates originating from porcine sources exhibiting the greatest haemolytic activity [57, 58].

A. pyogenes is an opportunistic pathogen of economically important livestock, such as dairy and beef cattle and swine. The organism is often found in the mucous membranes and routinely isolated from the udders, urogenital and upper respiratory tracts of healthy animals [15]. As one of the most common opportunistic pathogens of domestic ruminants and swine, it can cause a variety of suppurative infections of the skin, joints and organs. These infections may result in abortion, abscess, arthritis, mastitis, pneumonia and uterine infection which can lead to infertility [12, 51, 53, 56]. As *A. pyogenes* is a very versatile pathogen, infection is not confined to domesticated animals and can cause infection in many species such as antelope,

bison, camel, cat, dog, poultry and horse, among others [15, 56]. While rare, human infection has been reported and is often due to occupational exposure [13, 15, 52].

Pyolysin was classified as a CDC in 1997 by Billington and Jost [12] based on its primary structure, and it was the first CDC to be non-oxygen labile. PLO is considered to be a major determinant in *A. pyogenes* infection [15, 58] and it has been shown to lyse immune cells and erythrocytes, alter host cytokine expression of many different species, and can be dermonecrotic and lethal to test animals when administered through intravenous and intraperitoneal routes [12, 15, 51]. Although the importance of PLO in *A. pyogenes* virulence is well-established, the precise role it plays in pathogenesis, like that of many other CDC, is not exactly clear [12].

The amino acid sequence alignment shows PLO as one of the most divergent members of the CDC family, exhibiting only 31-41% similarity. In addition, PLO possesses an undecapeptide sequence that diverges significantly from the consensus for CDC, as seen in Table 1.3. Here, the sequence for PLO has an alanine residue substituted for the common cysteine found in other CDC sequences. As with the other CDC members, the undecapeptide sequence is important in the activity of PLO, especially the three tryptophan residues [16]. When the undecapeptide sequence of PLO is replaced with the consensus sequence, the haemolytic activity of PLO is significantly reduced. In addition to this, it appears that the D1 region of PLO is also important for its function.

As PLO is a relatively new addition to the CDC family, little research has been conducted to determine the functional assignments of its specific domains. Considering its divergent primary sequence from the other CDCs, especially in its undecapeptide region, it is reasonable to believe that the functionality of the domains of PLO may also differ from that of cholesterol-dependent cytolysins more commonly studied.

1.9 RESEARCH OBJECTIVES

In this research work, various fluorescence analysis and electron imaging techniques have been employed to investigate the oligomerization properties of PLO. The work encompasses three main topics. In the first section, the C-terminal domain or domain 4, the domain originally believed to be responsible for membrane recognition and binding, is shown to play a role in the oligomerization process, and its ability to form hybrid oligomers with active wild type toxin is discussed. The second topic focuses on the effects of an engineered disulfide bridge tethering domain two and a portion of domain three that inserts into the membrane (transmembrane β-

hairpin 1) on the oligomerization and resulting pore size. Finally, the last chapter focuses on the membrane-inserting regions and pore-forming mechanism of PLO oligomers pre-formed in solution, or solution-derived oligomers, in order to ascertain how these oligomers retain partial activity. Together, the results of these studies provide further insight and increase our understanding into the function of cholesterol dependent cytolysins as pore forming toxins.

Chapter 2

Oligomerization Properties of the C-Terminal Domain of Pyolysin

2.1 INTRODUCTION

Many studies have been conducted on various cholesterol-dependent cytolysins in order to determine functional assignments of the different domains of this class of toxin: domain 3 is responsible for oligomerization and membrane insertion, while initial membrane recognition and binding is mediated by domain 4 (D4) [56, 95, 104, 105]. Previous studies on the role of domain 4 in the pore-forming process have used C-terminal fragments of two other CDCs, namely a recombinant fragment encompassing domain 4 of streptolysin O (SLO-D4) [120] and a C-terminal proteolytic fragment of perfringolysin O (PFO-T2) [114] that contains domain 4 and the adjoining parts of domain 2, the latter most likely in unstructured form. Both fragments were found to inhibit the haemolytic activities of their corresponding wild type toxins. This observation was attributed to the ability of the C-terminal region to form a complex with intact toxin at a stage in the oligomerization step which terminated the process. Considering that each oligomer subunit must have two separate oligomerization interfaces to interact with its two neighbours, it was proposed that the fragments may retain only one of these, enabling them to associate with a growing end of an oligomer but then interfering with continued oligomer growth.

In this study, the functional role of domain 4 has been revisited, especially its involvement in the oligomerization process, and its effect on the haemolytic activity. The findings show

that not only can it form hybrid oligomers with wild type toxin, but it is also capable of self-oligomerization. Moreover, the haemolytic activity of wild type toxin is not only retained but even enhanced by the presence of domain 4 fragments. Hence, compared to other CDC toxins, the isolated domain 4 of PLO retains a greater scope of function. The findings reported in this chapter indicate a greater functional role of domain 4 in the overall activity of CDC than previously reported.

2.2 MATERIALS AND METHODS

2.2.1 Protein Expression and Purification

The plasmid pJGS59 encoding the PLO gene containing a histidine purification sequence was used to create a cysteine-containing intact-toxin mutant (N90C) [50] and the C-terminal fragment that corresponds to domain 4, also containing a single cysteine residue to enable covalent labelling.

The recombinantly expressed C-terminal fragment, PLO-D4, comprises residues 421 to 534 of the native sequence. The PCR primers were extended in order to N-terminally insert a thrombin cleavage sequence for removal of the purification tag, and a cysteine residue to allow for chemical modification. The primers used are listed in table 2.1.

PCR products were used to transform the *E. coli* XL1 Blue strain, cultured on LB ampicillin plates and incubated at 37 °C for 12-18 hours. After sequence verification, recombinant plasmids were transformed into *E. coli* BL21 and cultured in 2×YT broth supplemented with 0.5 mM IPTG (BioShop, Burlington ON) for protein expression. After harvesting, cells were lysed using the Emulsiflex C5 Emulsifier (Avestin, Ottawa ON) and the protein was purified using a BioRad Biologic LP liquid chromatography system (Mississauga ON) with nickel agarose column (Qiagen, Mississauga ON). To remove the hexa-histidine purification tag for the PLO-D4 toxin fragment, the protein was equilibrated by gel filtration with thrombin cleavage buffer consisting of 50 mM Tris (BioShop, Burlington ON), 150 mM NaCl (BioShop, Burlington ON) and 2.5 mM $CaCl_2$ (Fisher Chemicals, Fair Lawn NJ) pH 7.5. Human plasma thrombin (Sigma Chemicals, St Louis MO) was added to 1 µg for every 100 µg protein, incubated 12-18 hours at 4 °C with cleavage monitored using SDS-PAGE. Protein molecular masses were determined on a MicroMass QToF quadropole time of flight mass spectrometer (Montreal QC).

Table 2.1 Primers used for the construction of the PLO cysteine mutant N90C and the domain 4 fragment by PCR mutagenesis. Cysteine codons and anticodons are underlined.

Mutation	Sequence
N90C-forward	5′–TCA ATT GAA TGT GTG CCG GTT ACC AAG GAT C–3′
N90C-reverse	5′–ACA TTC AAT TGA CTC ACC CTT GAC TGC AAG–3′
Domain 4-forward	5′–CTG GTA CCC AGG GGG TCC TGC TAC AAG TCT GGT GAA ATC ACC–3′
Domain 4-reverse	5′–GCA GGA CCC CCT GGG TAC CAG ACC ACC ATG ATG ATG ATG ATG ATG AGA ACC–3′

2.2.2 Chemical Modification of Cysteine Residues

Protein samples were transferred to labelling buffer consisting of 50 mM Tris, 150 mM NaCl, 1 mM EDTA (BioShop, Burlington ON) pH 7.5 using gel filtration. The samples were supplemented to 1 mM of either Fluorescein-5-Maleimide (Biotium Inc, Hayward CA) or Rhodamine Red Maleimide (Invitrogen, Burlington ON). The samples were incubated at 25 °C for 60 minutes and the excess label was removed using gel filtration. To determine the labelling efficiency, the ratio of the concentration of fluorophore to protein was calculated using UV-Vis absorbance with extinction coefficients of 83,000 $/_{mol \cdot cm}$ for fluorescein at 490 nm and 91,000 $/_{mol \cdot cm}$ for rhodamine at 540 nm. The extinction coefficient of PLO was determined to be 68,480 $/_{mol \cdot cm}$ at 280 nm. As both fluorescein and rhodamine also absorb at 280 nm, the absorbance value at 280 nm for the protein was corrected by subtracting the absorbance value contributed by the dye (with fluorescein and rhodamine extinction coefficients of 35,115 $/_{mol \cdot cm}$ and 17,697 $/_{mol \cdot cm}$, respectively). Labelling efficiencies of 85-90% for fluorescein and 70-80% for rhodamine, as determined by UV-Vis absorbance were found.

2.2.3 Preparing Red Blood Cells and Membrane Ghosts

To prepare red blood cells, aliquots of 400 µL sheep red blood cells were made up to 1 mL with PBS buffer (16 mM K_2HPO_4 150 mM NaCl, 1 mM EDTA, pH 7.5), centrifuged at 380 x*g* for 4 minutes, and the supernatant was removed to yield approximately 100 µL RBC pellet. The pellet was washed by resuspending with PBS and centrifugation until the supernatant remained clear. The pellet was resuspended again to a final volume of 1 mL to a concentration of 10%. From this, 1% RBC working solutions were made. To prepare membrane ghosts, 400 µL sheep

RBC were mixed with 600 µL cell lysis buffer (5 mM NaCl, 5 mM Na_2HPO_4 pH 7.0) and centrifuged at 16,060 x*g* for 10 minutes. The supernatant was removed and the pellet washed until both the supernatant became clear and the pellet translucent. The pellet was made up to 1 mL with PBS buffer.

2.2.4 Haemolysis Assay

Wild type PLO (10 µL) was admixed with PLO-D4 to ratios of 1:1, 1:4 and 1:16. Two-fold serial dilutions were made in a 96-well plate with PBS buffer. Sheep red blood cells were added to each well to a final concentration of 0.5% and incubated at 37 °C for 30 minutes. Haemolysis causes a decrease in cell turbidity, which was monitored at a wavelength outside the absorbance of hemoglobin (650 nm) using a SpectroMax Plus 384 Microplate Spectrophotometer (Molecular Devices, Sunnyvale CA). Haemolytic activity of the wild type–PLO-D4 mixtures was compared to wild type alone and PLO-D4 alone. The same samples were tested for lysis kinetically at 25 °C for 30 minutes.

2.2.5 Fluorescence Measurement and Data Analysis

All samples containing labelled protein were made to a final concentration of 1 µM with 1% (v/v) of red cell membrane ghosts. For hybrid oligomer analyses, the samples containing fluorescein-labelled PLO-N90C (PLO-N90C-F) and rhodamine-labelled PLO-N90C (PLO-N90C-R) were mixed to a 1:2 ratio (where PLO-N90C-F concentration was 0.33 µM and PLO-N90C-R concentration was 0.66 µM). The hybrid samples containing rhodamine-labelled PLO-D4 (PLO-D4-R) and fluorescein-labelled (PLO-N90C-F) were also mixed to a 1:2 ratio (where PLO-D4-R concentration was 0.33 µM and PLO-N90CF-F concentration was 0.66 µM). For all other fluorescence assays, fluorescein- and rhodamine-labelled toxin was combined in a 1:1 ratio (0.5 µM each). After incubation at 37 °C for 30 minutes, the protein-membrane samples were centrifuged at 16,060 x*g* for 10 minutes, the supernatant removed, and the pellet resuspended with PBS. Steady state fluorescence spectra were recorded for soluble toxin controls, membrane-bound samples, and the centrifugation supernatant. The intensity of the membrane-bound samples was corrected for incomplete binding toxin according to the following equation:

$$F_{\text{membrane,corrected}} = \frac{F_{\text{membrane}}}{F_{\text{soluble}} - F_{\text{supernatant}}} \tag{2.1}$$

Steady state fluorescence measurements were conducted on a PTI QuantaMaster spectrofluorimeter using an excitation wavelength of 465 nm with emission scans recorded from 485 to 630 nm, using 1 mm slit widths. Time-resolved fluorescence was measured using an FT-100 compact fluorescence lifetime spectrometer (PicoQuant, Berlin, Germany) using an LDH-P-C-470 LED laser light source. Fluorescein emission was isolated using a 520±5 nm bandpass filter (Andover Corporation, New Hampshire). Decays were fitted using Fluofit software (PicoQuant) using three exponential lifetime components, from which the average lifetime $<\tau>$ was calculated according to

$$<\tau> = \frac{\sum \alpha_i \tau_i}{\sum \alpha_i} \tag{2.2}$$

where α_i is the intensity contribution of the lifetime component τ_i at $t = 0$, with the three-exponential fits producing χ^2 values between 1.0 and 1.2.

2.2.6 Oligomer Size Characerization by Size Exclusion Chromatography

In order to determine relative sizes of hybrid oligomer complexes formed, samples of labelled PLO-N90C-F or PLO-D4-F were made to 1 μM concentration, with varying concentrations of unlabelled PLO-D4 added as indicated in the Results section. Membrane ghosts were added to a final concentration of 20% (v/v). Samples were incubated at 37 °C for 30 minutes, centrifuged at 16,060 xg for 10 minutes, after which the supernatant was removed. Membranes were dissolved using 5% sodium deoxycholate, and the samples were brought to a final volume of 1 mL. Size exclusion chromatography was performed on a BioRad BioLogic chromatography system using a Sephacryl S-400 column equilibrated with elution buffer consisting of 20 mM Tris, 150 mM NaCl, 1 mM EDTA and 0.25% (w/v) sodium deoxycholic acid (BioShop, Burlington ON) pH 8.5. Eluted fractions were collected and analyzed for fluorescein fluorescence.

2.2.7 Transmission Electron Microscopy

Wild type PLO and the C-terminal fragment PLO-D4, alone or in mixtures as indicated in the Results section, were incubated at a total protein concentration of 0.125 $^{mg}/_{mL}$ with cholesterol crystals 0.5 $^{mg}/_{mL}$, prepared according to Harris [43] for 30 minutes at room temperature. The samples were subjected to negative staining with 2% uranyl acetate according to Harris [43]. Transmission electron microscopy study of the negatively stained specimens was performed by a Phillips CM 100 transmission electron microscope at 100 kV. Digital images were recorded using an Optronics 1824×1824 pixel CCD camera with an AMT40 version 5.42 capture engine

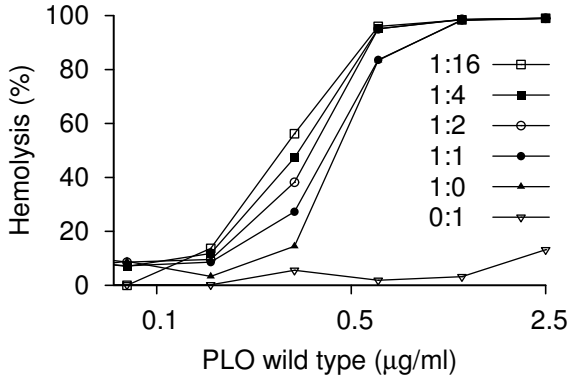

Figure 2.1 Haemolytic activity of wild type PLO with increasing ratios of PLO-D4. The extent of haemolysis of 0.5% sheep red blood cells after incubation at 37 ℃ for 30 minutes was determined by the decrease in turbidity (OD_{650}). The concentration of PLO-WT was held constant at 10 µg/mL; the concentration of PLO-D4 in the mixed samples is implied by the molar ratios indicated on the graph (PLO-WT:PLO-D4). The sample containing PLO-D4 had a concentration of 5 µg/mL.

supplied by Deben (Bury St. Edmunds, UK). All TEM analyses were performed by J. R. Harris at the University of Newcastle upon Tyne, Newcastle upon Tyne, UK.

2.3 RESULTS

2.3.1 Haemolytic Activity of Wild Type Toxin with PLO-D4

In order to test the activity of PLO-D4, the protein was combined with sheep erythrocytes, and the extent of cell lysis was determined by the decrease in turbidity as illustrated in Figure 2.1. In this assay, wild type PLO (PLO-WT) achieves 50% haemolysis at approximately 400 ng/mL, similar to previous measurements [51]. As expected from previous studies on perfringolysin O and streptolysin O [114, 120], PLO-D4 alone shows no haemolytic activity. However, when the fragment is combined with PLO-WT, the haemolytic activity of the mixture exceeds that of PLO-WT alone.

Independent repetitions of the experiment showed considerable variation in the extent of haemolysis which may be attributed to the age or difference between erythrocyte batches. Despite this however, the relative order of the individual samples within sets was reproducible such that a higher excess of domain 4 over wild type PLO always produced a greater extent of haemolysis.

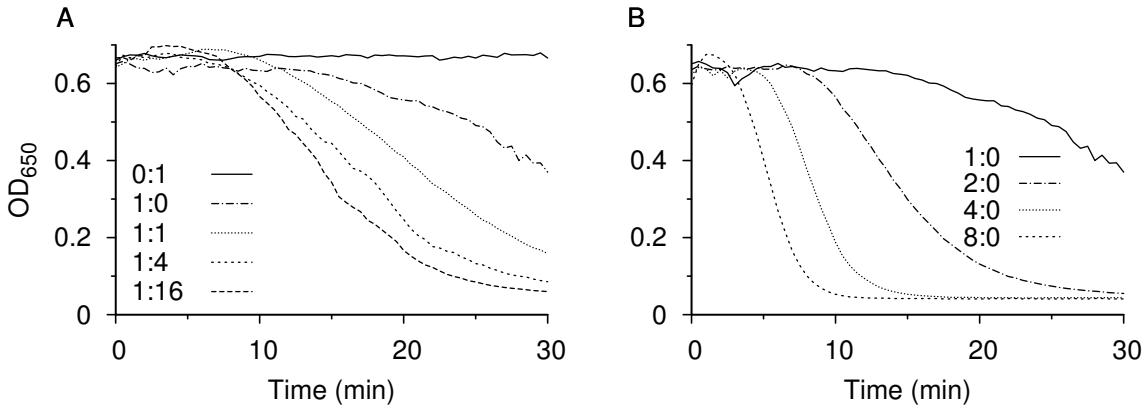

Figure 2.2 Time Course of haemolysis of wild type PLO with increasing ratios of PLO-D4. In (A), wild type PLO at 0.625 µg/mL was incubated with 0.5% RBC's at room temperature, and the progress of hemolysis was monitored by the decrease in turbidity (OD_{650}). The toxin was present alone (1:0) or with PLO-D4 at various molar proportions (1:1 to 1:16). The sample labelled 0:1 contains PLO-D4 only. In (B), wild type toxin alone was used at various multiples of the initial concentration (1:0 again equals 0.625 µg/mL).

Although under the experimental conditions of Figure 2.1, the enhanced haemolytic activity is visible only at one concentration of the wild type toxin (312 ng/mL), it is, however, also visible at other concentrations in kinetic assays, as seen in Figure 2.2A. As in the endpoint assay, the incremental effect of domain 4 is limited and levels off at a large excess of the fragments over wild type PLO. For comparison, the time course of haemolysis observed with various amounts of PLO-WT is shown in Figure 2.2B. The effect of a single additional equivalent of PLO-WT on the rate of haemolysis appears similar to that of 16 equivalents of PLO-D4, and higher concentrations of wild type toxin increase the speed of haemolysis even further. The observation that the promotion of haemolysis by domain 4 can be saturated suggests that its productive interaction with PLO-D4 is limited by the amount of the latter. Nevertheless, the finding that PLO-D4 increases the haemolytic activity of wild type PLO is in stark contrast with previous observations on the isolated domain 4 of streptolysin O, which inhibits rather than augments the activity of the wild type toxin [120].

2.3.2 Oligomerization of PLO-D4: FRET Studies

To examine the ability of PLO-D4 to oligomerize with itself and the full length toxin, both molecules were thiol-specifically labelled with fluorescein and rhodamine, respectively. The two labels form a donor-acceptor pair for fluorescence energy transfer (FRET) studies with a

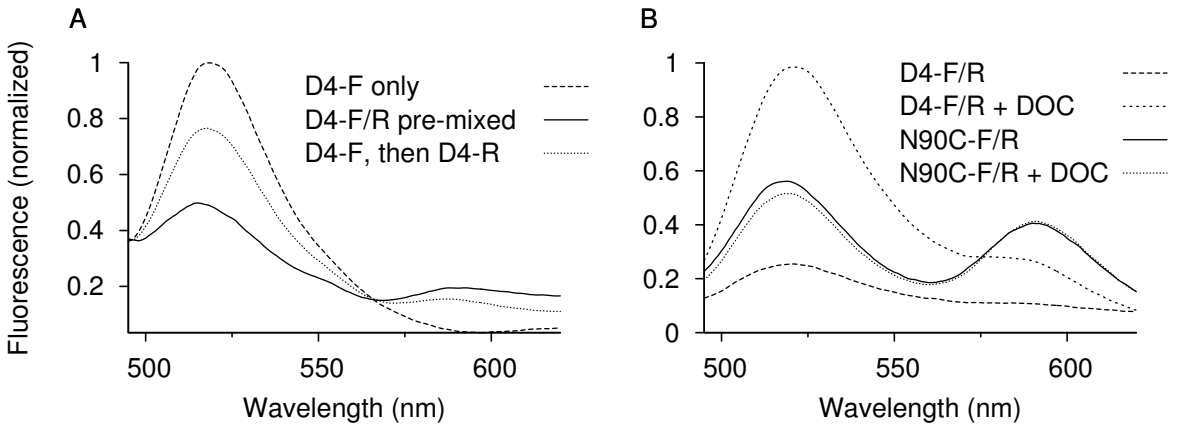

Figure 2.3 Characterization of domain 4 fragment oligomers by FRET. **A**: PLO-D4 labelled with fluorescein (D4-F) alone or in combination with rhodamine (D4-R) were incubated with sheep erythrocyte ghosts. Addition of D4-R prior to incubation with membranes greatly reduces the fluorescence of D4-F due to FRET, indicating oligomerization. If PLO-D4-R is added after incubation for 30 minutes with D4-F alone, the extent of FRET is reduced, indicating that the two species remain partially segregated. **B**: A mixture of fluorescein- and rhodamine-labelled PLO-D4 was incubated with membranes as before and the sample solubilized with deoxycholate (DOC). FRET is reversed, indicating dissociation of the oligomer. The same treatment does not change the fluorescence of a sample of N90C-F and N90C-R.

Förster distance (R_0) in the range of 50 Å [122]. The fluorescein-labelled (PLO-D4-F) and the rhodamine-labelled fragment (PLO-D4-R) were mixed and then incubated with sheep erthyrocyte membrane ghosts, and the fluorescence emission was measured. The pronounced decrease in the donor (fluorescein) signal when combined with acceptor (rhodamine), as illustrated in Figure 2.3A indicates that PLO-D4 fragments can associate with each other and thereby engage in FRET. When the two species were applied to the membranes sequentially rather than simultaneously, the donor signal was weaker than with PLO-D4-F alone but stronger than with the pre-mixed sample. This suggests that at least some of the molecules in the initially applied sample are sequestered in oligomers and are no longer available for the formation of hybrid oligomers at the time of the second application. The results are consistent with the formation of oligomers that are stable on the time scale of the experiment. The attenuation of donor fluorescence in the combined samples is not the result of competition for binding sites by the acceptor-labelled fragments, as application of two equivalents of donor also doubles the donor intensity (data not shown).

Oligomers of SLO and PFO are stable after membrane disruption with detergents, and solubilization with deoxycholate has been used to isolate and characterize these oligomers [87].

In order to test the stability of the domain 4 oligomers towards dissociation by detergents, PLO-D4-R and PLO-D4-F were incubated with membrane ghosts and subsequently with deoxycholate to dissolve the membranes. Fluorescence spectra were obtained before and after deoxycholate solubilization as illustrated in Figure 2.3B. The intensity of the fluorescein peak increases greatly upon membrane solubilization, indicating disruption of the oligomers and abolition of FRET. In contrast, the oligomers of full-length toxin readily withstand membrane solubilization, as evident from the continued existence of FRET before and after solubilization. This indicates that oligomers formed by domain 4 alone are linked by forces weaker than those formed by wild type toxin.

2.3.3 Oligomerization of PLO-D4: Electron Microscopy

Cholesterol crystals have been established as a useful model system to study the oligomerization of CDCs by EM [26, 43]. Looking at TEM images of PLO on a crystalline cholesterol surface, the consistent ring- and arc-structures seen with the oligomerization of wild type PLO illustrated in Figure 2.4A, yet PLO-D4 on the same surface results in a striped pattern of toxin fragments arranged in a linear array across the surface, as seen in Figure 2.4B. Evidently, the absence of the first three domains influences the size and shape of the resulting oligomers formed by PLO-D4. At the same time, it is clear that the presence of these domains does not abolish interaction between the toxin molecules.

2.3.4 Hybrid Oligomer Formation by PLO-D4 and Wild Type PLO

From the observation of oligomers of both PLO-D4 and of the full-length molecule, the question arises if the two can also form hybrid oligomers. The enhancement of the haemolytic activity of wild type PLO by PLO-D4 suggests that this is possible. In order to directly detect such hybrids, PLO-D4-R was mixed with PLO-N90C-F, and the mixture incubated with membranes. Formation of hybrid oligomers should result in FRET between the two species, and this is indeed apparent from the reduction in PLO-N90C-F fluorescein emission as illustrated in Figure 2.5. FRET occurs only when the two species are applied simultaneously, but not sequentially, which corroborates the conclusion that this is due to the formation of hybrids, as opposed to FRET between segregated donor- and acceptor-labelled oligomers that happen to be located in close proximity to each other.

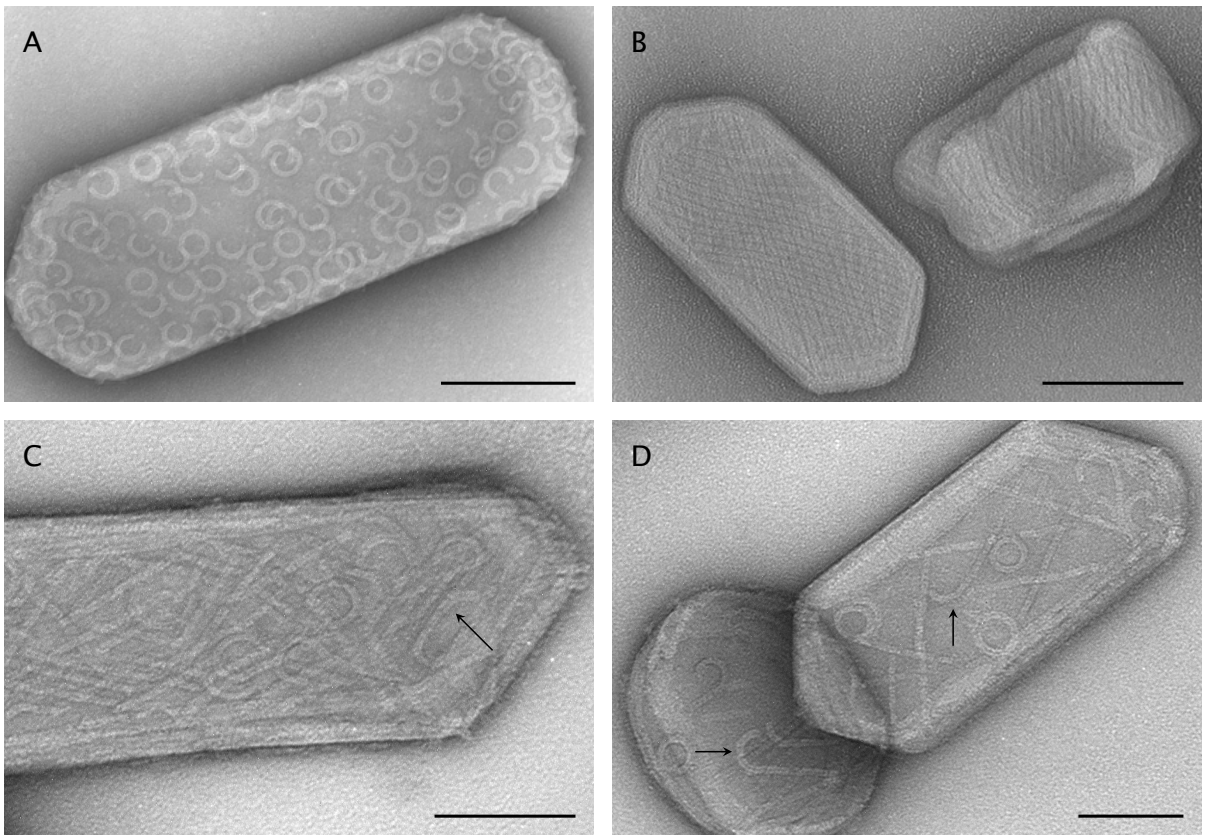

Figure 2.4 Electron microscopy of wild type PLO and domain 4 oligomers on cholesterol crystals. **A**: Wild type PLO alone. The rings and arcs resemble those previously described for other CDCs. **B**: PLO-D4 alone. Instead of rings and arcs, straight rods in parallel arrangement are seen. **C** and **D**: Mixtures of wild type with PLO-D4 in twofold or fivefold excess, respectively. In addition to the arcs, the rings and rods are also observed in A and B, 'walking canes' and other hybrid shapes are seen, some of which are marked with arrows. Black scale bars correspond to 100 nm. All TEM analyses were performed by J. R. Harris at the University of Newcastle upon Tyne, Newcastle upon Tyne, UK.

In hybrid oligomers, the domain 4 fragment may be restricted to terminal positions, or alternatively it might intercalate between two molecules of full-length toxin. In order to determine whether such intercalation occurs, fluorescence measurements were performed on an equimolar mixture of PLO-N90C-F and PLO-N90C-R, to which increasing amounts of unlabelled PLO-D4 were added. The rationale here is that intercalation of PLO-D4 between the donor- and acceptor-labelled full-length molecules should reduce FRET between the donor- and acceptor-labelled intact molecules. Figure 2.5B shows that, with increasing PLO-D4 concentration, the donor signal also increases, and the acceptor signal decreases. This change is

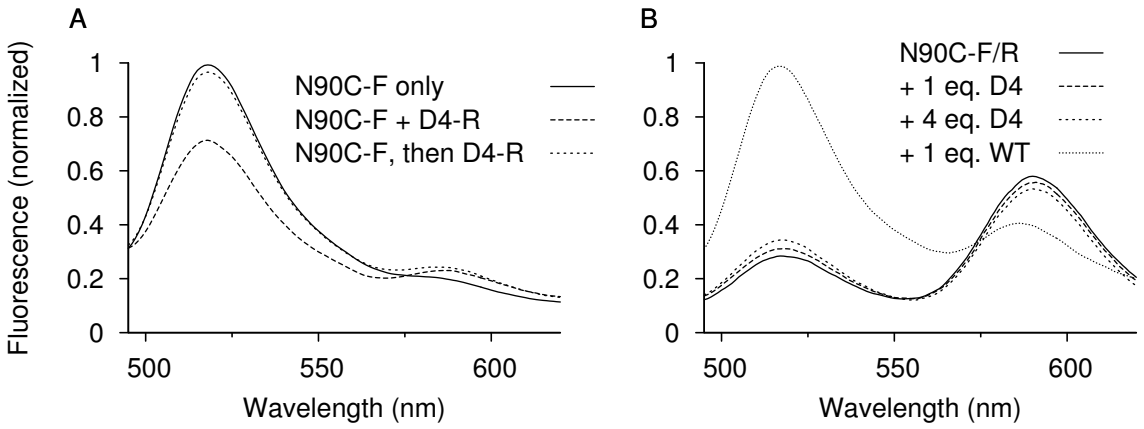

Figure 2.5 Formation of hybrid oligomers from wild-type PLO and the domain 4 fragment (FRET). **A**: PLO-N90C labelled with fluorescein (PLO-N90C-F) and rhodamine (PLO-N90C-R) were incubated with sheep erythrocyte ghosts. FRET (as detected by a decrease of fluorescein fluorescence) only occurs if the two proteins are applied simultaneously. The absence of FRET observed with sequential application, with incubation for 30 minutes between the two species, likely indicates the formation of segregated oligomers. **B**: FRET between N90C-F and the rhodamine-labelled species (N90C-R) is effectively suppressed if the labelled toxin is admixed with an equivalent amount of unlabelled wild type toxin before addition to membranes. In contrast, only a very slight reduction of FRET is observed even with a 4-fold excess of unlabelled D4 fragment. This indicates that the fragment does not efficiently intercalate between N90C subunits in hybrid oligomers.

very small but reproducible, and is indicative of a slight increase in the average spacing between the labelled full-length toxin monomers. However, as also shown in Figure 2.5B, the decrease in energy transfer was far more pronounced when unlabelled wild type PLO was employed instead of the unlabelled D4 fragment.

These observations are corroborated by time-resolved fluorescence measurements (Table 2.2).[1] Fluorescein-labelled N90C alone yields a fluorescein lifetime of 2.8 ns, whereas the mixture of N90C-F and N90C-R alone yields a lifetime of 1.1 ns, corresponding to the maximum FRET effect. When the unlabelled D4 fragment is added, the fluorescein lifetime rises slightly, while a much greater increase is seen with unlabelled wild type PLO. Independent repetitions of this experiment showed slight variations in absolute lifetime values, however the overall order was reproducible where a greater concentration of domain 4 gave consistently higher lifetime values. The collective results indicate that the domain 4 fragments can interca-

[1]The parameters for the individual components obtained from the fit are listed in tables A.1 and A.2 on page 98.

Table 2.2 N90C-fluorescein fluorescence lifetimes in hybrid oligomers. An equimolar mixture of the fluorescein-labelled and rhodamine-labelled forms of mutant N90C was incubated with membranes, either alone (leftmost column) or with the D4 fragment or wild type PLO added at different molar excess over the labelled N90C. The fluorescein time-dependent fluorescence decay was fit with a three-exponential model, and the average lifetimes $<\tau>$ calculated according to equation 2.2 on page 25. The fluoresence lifetime of N90C-F alone after incubation with membranes is shown for comparison. The χ^2 values report the goodness of the three-exponential fit.

	N90C-F/R	D4			WT			N90C-F
unlabeled protein (mol/mol)	–	1	2	4	1	2	4	–
$<\tau>$ (ns)	1.10	1.23	1.25	1.29	1.87	2.23	2.14	2.77
χ^2	1.15	1.12	1.07	1.15	1.12	1.06	1.13	1.03

late between full length toxin molecules, but with a greatly reduced efficiency relative to the intact toxin molecules themselves.

One possible explanation for the low efficiency of domain 4 incorporation into oligomers of full-length toxin is related to the rates of oligomerization. If one species undergoes oligomerization much faster than the other, this would favour the formation of segregated oligomers. To compare the rates of oligomerization, the time course of fluorescein fluorescence was monitored in mixtures of PLO-N90C-F and PLO-N90C-R, and of PLO-D4-F and PLO-D4-R, respectively, during incubation with membrane ghosts (Figure 2.6). Progress of oligomerization is evident from the decrease in fluorescein fluorescence due to FRET. While the kinetic curves of the different samples vary somewhat in shape and slope, overall the rates of oligomerization appear to be of comparable magnitude. This suggests that effects other than differences in the rate of oligomerization are responsible for the relatively low efficiency of intercalation of domain 4 between full-length toxin molecules mixed in samples.

2.3.5 Morphology of Hybrid Oligomers

On crystalline cholesterol surfaces, mixtures of PLO-WT and PLO-D4 yield both rings and arcs as expected for PLO-WT alone. However, in addition to these two elementary shapes, the two shapes are seen to combine into walking-cane like formations, as seen in Figure 2.4 on page 30. It is likely that the arc portion of the walking stick oligomer is formed predominantly by wild type molecules, whereas the stick consists mostly of domain 4 fragment. Some

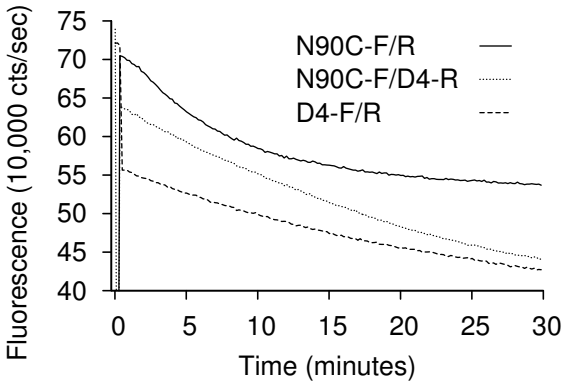

Figure 2.6 Kinetics of oligomer formation on membrane ghosts by FRET. The progress of oligomerization of full-length PLO, the domain 4 fragment and of hybrid oligomer formation was monitored by FRET. Fluorescein- and rhodamine-labelled N90C or D4 fragment were mixed as indicated. At t=0, RBC membrane ghosts were added to 1%, and the sample mixed by pipetting. The spikes at t=0 are artifacts caused by opening and closing the sample compartment.

additional variations occur, as illustrated in Figures 2.4C and D, in which multiple changes of curvature give rise to horseshoe-like formations or other irregular shapes. In some sections of those structures, the curvature appears to be smaller than in regular arcs, suggesting that these sections may contain both PLO-WT and intercalated domain 4 molecules.

The observed structures are compatible with the notion of a limited but measurable ability of domain 4 to form hybrid oligomers with PLO-WT, as inferred from fluorescence experiments (see Figure 2.5B).

2.3.6 Reduced Size of Hybrid Oligomers and PLO-D4 Oligomers

In order to determine the relative size of the D4-WT PLO hybrid oligomers, fluorescein-labelled intact toxin, PLO-N90C-F was incubated with membranes with a twofold molar excess of domain 4, and after the membranes were dissolved using deoxycholate, size exclusion chromatography was performed. The elution profile of the hybrid oligomers of 1:2 PLO-WT to PLO-D4 ratios is compared to PLO-WT oligomers and monomer, as seen in Figure 2.7. The hybrid oligomer gives a peak maximum at a higher elution volume as compared with that obtained with wild type oligomers alone, and the control sample of WT monomer eluting at a high volume (indicating a very low relative molecular weight). After the main peak, the size of the hybrid oligomers gradually trails off. This range of elution volumes may be a result of

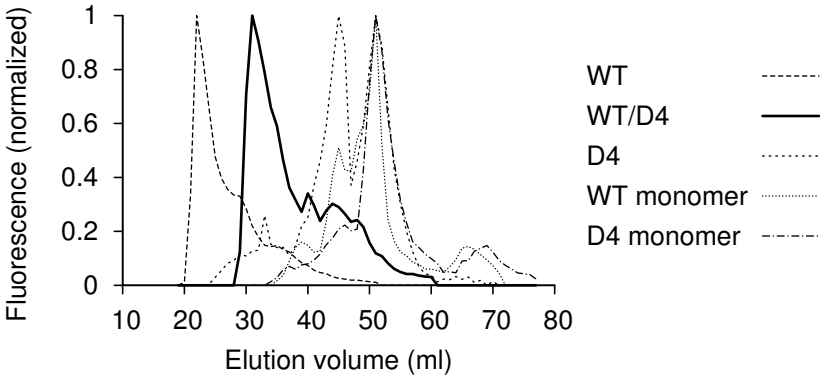

Figure 2.7 Characterization of PLO-D4 homogenous and hybrid oligomers by size exclusion chromatography. N90C and D4, respectively, were labelled with fluorescein and incubated with membrane ghosts for 30 minutes at 37 ℃. The sample representing the hybrid oligomers were prepared from fluorescein-labelled PLO-N90C with a twofold molar excess of unlabelled D4. After incubation, the membranes were dissolved with 5% deoxycholate, and the samples were run through a Sephacryl S-400 column in the presence of 6 mM of the detergent. Fluorescein fluorescence was measured in the eluate fractions.

the relative instability of the oligomers formed by PLO-D4 after membrane solubilization by deoxycholate, as previously seen (refer to Figure 2.3).

Looking at the homogenous PLO-D4 oligomers, there is a double maximum with the first peak eluting at a higher elution volume than seen for the WT-D4 oligomers and the second peak eluting at a volume corresponding to the peak maxima of PLO-WT monomers and the PLO-D4 monomer control. Therefore, the second peak may be assigned to un-complexed PLO-D4 fragments. (As the molecular weight separation range of the resin Sephacryl S-400 does not differentiate between PLO-WT (57000Da) and PLO-D4 (15000Da), both peaks are eluted at the same volume.) This suggests that the PLO-D4 oligomers have an overall lower molecular weight than the wild type-domain 4 hybrid oligomers, and that the oligomerization of PLO-D4 alone is not as efficient as oligomerization between wild type and PLO-D4, or with PLO-WT alone.

2.4 DISCUSSION

The pore-forming mechanism of CDCs and the role each domain plays in the binding, oligomerization, and insertion steps have been the topic of numerous research studies and publications. As mentioned earlier, it was found that domain 3 is the main participant in the oligomer-

ization and insertion steps, while the role of domain 4 is reserved for membrane-recognition and binding. The function of domain 4 was initially discovered with the analysis of trypsin-digested toxin fragments where the C-terminal fragment was able to retain the ability to bind to the membrane surface [82, 114], and after the determination of the CDC crystal structure, it was found that domain 4 was the only contiguous domain of the toxin [98]. In a study by Weis and Palmer [120], it was found that domain 4 alone was responsible for membrane binding, whose function mimicked those of larger fragments. Later, it was discovered that only the bottom tip of domain 4 inserts into the membrane, where three hydrophobic loops, L1, L2 and L3, and the highly conserved undecapeptide sequence bind to the membrane surface [94].

Mutations in the highly conserved undecapeptide sequence, especially the three tryptophan residues contained within, resulted in dramatically decreased haemolytic activity [14, 101], showing the region's importance in the pore-forming process. In order to determine the function of the undecapeptide sequence, studies conducted on the CDC intermedilysin (ILY), a toxin that does not depend on membrane cholesterol to bind, illustrated that the role of the undecapeptide region was not directly for membrane-cholesterol recognition, but instead to initiate the conformational changes necessary to commence the oligomerization and TMH insertion events [108]. Together, these results helped to define the primary role of domain 4 as membrane-recognition and binding. Some studies, however, were conducted to examine the role of domain 4 in the oligomerization process. The proteolytic fragment of perfringolysin O (PFO-T2) containing domain 4 and the adjoining parts of domain 2 [114], and the recombinant fragment encompassing domain 4 of streptolysin O (SLO-D4) [120] was investigated for oligomerization ability by fluorescence analysis. Here, both PFO-T2 and SLO-D4 exhibited an inhibition of lytic ability when combined with wild type toxin, and neither retained the ability to self-associate.

However, in this study, fluorescence analysis and TEM imaging show strong evidence for domain 4 self-association. When fluorescein- and rhodamine-labelled PLO-D4 were combined on a membrane surface, a decrease in fluorescein signal is clearly seen, indicating the donor- and acceptor-labelled toxin fragments are within the 50Å Förster distance. Also, TEM images demonstrate the interaction of PLO-D4 fragments to associate into linear, rod-shaped complexes. The forces binding these complexes, however, were found to be much weaker than those supporting the intact toxin oligomer, as demonstrated by the disruption of the PLO-D4 oligomer using deoxycholate.

The combination of intact toxin and domain 4 gave surprising results. As expect, D4 alone shows little haemolytic activity, yet the combination of the two enhanced the lytic ability of wild type toxin, a result not seen in other CDC studies. By comparison, the C-terminal fragments of PFO [114] and SLO [120] showed an inhibitory effect when combined with their respective wild type toxins. Although PLO-D4 causes an increased rate of wild type lysis, it is not to the same extent as wild type alone at increased concentrations indicating that the interaction is not as efficient as with other wild type molecules. However, the results observed are significant, and two possible explanations can be proposed to account for this behaviour. The first possibility is that D4 on the membrane surface could act to initiate wild type oligomerization, and the second mechanism is via the formation of wild type PLO and D4 functional hybrid oligomers where the increase in overall toxin concentration would cause an increase in the overall number of pores formed. The current study offers strong evidence that the intact PLO and domain 4 can form functional hybrid oligomers.

Fluorescence resonance energy transfer analysis (FRET) show that wild type can associate with domain 4 fragments as a decrease in fluorescein intensity was observed when fluorescein-labelled intact toxin was combined with rhodamine-labelled D4 on a membrane surface, signifying a close proximity between the two species. This result was also supported by an observed decrease in FRET when fluorescein- and rhodamine-labelled intact toxin was combined with increasing amounts of unlabelled domain 4, indicating an increase in spacing between the labelled intact toxin molecules. TEM images show rather unusual and unique structures are formed by intact PLO and D4 hybrid oligomers; elongated arcs, canes, and horseshoe patterns are observed here that have not been reported elsewhere.

Size exclusion data suggest that the molecular weight of the hybrid oligomers are reduced in size compared to the oligomers formed by wild type toxin, although TEM images show the hybrid structures to be of similar size or larger. The formation of hybrid oligomers which caused an inhibition of activity as described with the C-terminal fragment of PFO [114] suggested that the fragment must possess at least one complementary oligomerization site, while lacking the corresponding sites for continued oligomer growth. In the current study, continued oligomer growth is observed, suggesting that domain 4 does in fact possess required sites to continue the oligomerization process, as illustrated in Figure 2.8.

The frequency of occurrence and the consistent shapes observed suggest that the interaction of intact toxin and D4 is not random. In each image, the ‘arc’ of the cane and its ‘shaft’ always align to form an angle close to 180°, random interactions of these two structures would most

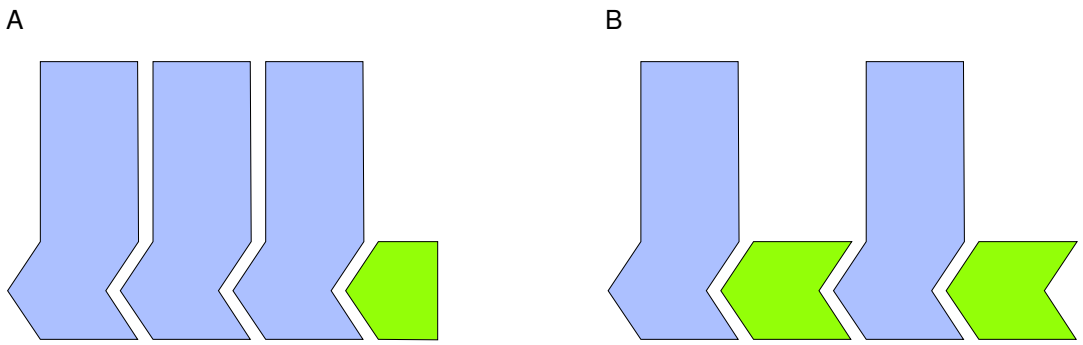

Figure 2.8 Possible modes of interactions between intact PLO and the domain 4 fragment. Each subunit of the oligomer requires two faces for interaction with the neighbouring subunits. In the isolated domain 4 fragment, either only one face (A) or both faces (B) may be preserved. In the case that only one oligomerization site exists on the domain 4 fragment, its interaction with wild type toxin would result in the termination of the oligomerization process, and the domain 4 fragment being restricted to the terminal positions of the oligomer. In contrast, if the domain 4 fragment possesses both faces necessary for oligomerization, then intercalation of the fragment between intact toxin molecules is possible. (Intact PLO molecules are depicted in blue, while domain 4 fragments are in green.)

certainly result in formations of arcs and rods interacting or touching at more acute angles, and possibly having the rods spanning across the arcs to touch at both terminal ends.

In summary, these results show that the C-terminal domain of PLO retains the ability to not only bind to target membranes, but also oligomerize with intact toxin moleculess to the point of enhancing activity, and oligomerize with other C-terminal fragments. This evidence shows that D4 is involved in the oligomerization process, and the intact toxin in hybrid oligomers maintain the ability to undergo the appropriate conformational changes and rearrangement to insert into membranes to form functional pores. This behaviour is quite different than that seen of two other CDC's studied, where little self-association was seen, and an inhibition of activity was observed. These findings signify that the functional role of domain 4 in CDC pore formation may be more profound than previously believed.

Chapter 3

Partial Oligomerization of Pyolysin Induced by a Disulfide-Tethered Mutant

3.1 INTRODUCTION

In the previous chapter, a novel role of domain 4 in the CDC pore formation mechanism not previously observed in other studies was discussed. Here, it was discovered that domain 4 of PLO participates in the oligomerization process. The process of oligomerization is complex, and fluorescence experiments have been conducted to elucidate the progression and points of contact between adjacent monomers during oligomerization. Briefly, once a toxin molecule binds to a membrane, conformational changes occur throughout the molecule that allow core β-strands of one monomer to interact and form hydrogen bonds with adjacent toxin monomers [95]. In order for the two sets of short α-helices in domain 3 to undergo the transition to form β-sheets, domains 2 and 3 must first uncouple, so that the transmembrane β-hairpins can insert into the membrane and form a pore.

In a previous study on the homologous toxin perfringolysin O (PFO) , it had been reported that the introduction of a disulfide bond between domains 2 and 3 prevented membrane insertion, while still allowing the assembly of pre-pore oligomers [49]. This observation suggests that conformational flexibility of domain 2 relative to domain 3 is not a requirement up to the pre-pore stage. In this study, it was found that a homologous disulfide mutant derived from the toxin pyolysin formed by substituting cysteine residues for glycine 85 of domain 2 and arginine

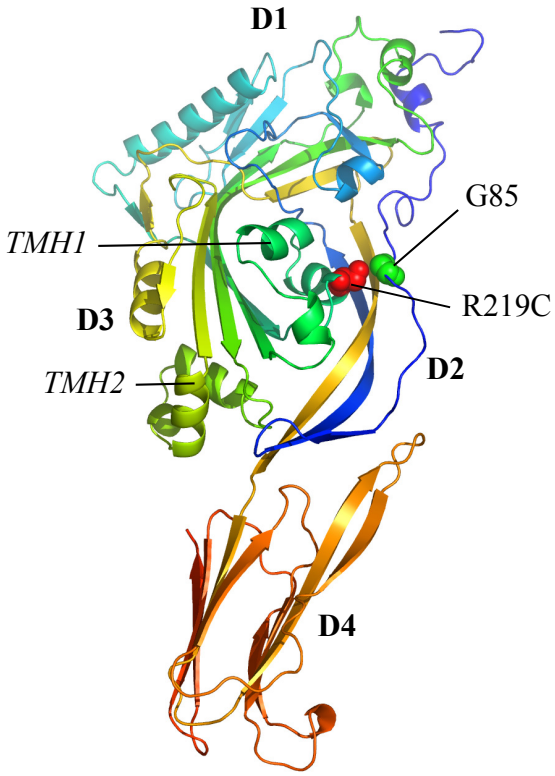

Figure 3.1 Location of the Disulfide Bond in the Structure of Pyolysin. The disulfide bond is formed between the residues G85 in domain 2 and R219C in the first transmembrane β-hairpin region in domain 3. Rendered from 1PFO.pdb with PyMOL (DeLano Scientific LLC, 2005).

219 in domain 3, as illustrated in Figure 3.1 fails to oligomerize. The mutant also interferes with the activity of wild type pyolysin in a dose-dependent manner. At large molar excess over the latter, inhibition of haemolysis is virtually complete, whereas at equimolar ratio, haemolysis is partially preserved, but both oligomer and pore size are reduced. These findings indicate that conformational flexibility between domains 2 and 3 is required for proper oligomerization. Furthermore, they show that membrane insertion of oligomers is co-operative, yet completion of oligomerization to ring shape is not necessary.

3.2 MATERIALS AND METHODS

3.2.1 Plasmid Expression and Protein Purification

All mutants were created using the plasmid pJGS59 [12] encoding the PLO gene containing a histidine purification sequence. The first mutant is a cysteine-containing double mutant

designed to have one cysteine residue located in domain 2 in close proximity to the second cysteine residue at the start of the TMH1 sequence found in domain 3 so that a disulfide linkage could form within one toxin molecule. To create this mutant, the wild type toxin was first modified to replace the arginine residue at position 219 with cysteine using the forward primer 5'-ACG TCA AAG TGT CAA CTG GAG GCA AAG C-3', and 5'-CAG TTG ACA CTT TGA CGT CAC CAG AGT C-3' as the reverse primer (PLO-R219C), followed by replacement of the glycine residue at position 85 with cysteine using the forward primer 5'-GCA GTC AAG TGC GAG TCA ATT GAA AAT GTG C-3' and the reverse primer 5'-TTC AAT TGA CTC GCA CTT GAC TGC AAG TAC ACC-3'. This disulfide mutant will be referred hereinafter as PLO-DS. The third mutant is a triple mutant, that was generated using the above disulfide PLO-DS gene, and replacing the lysine 328 residue with cysteine using the forward primer 5'-AGC GGC CTG TTC TGC GCT AAG TTC GGC AAT CTT TCC ACA-3', and the reverse primer 5'- TCT GGA AAG ATT GCC GAA CTT AGC GCA CAA CAG GCC GCT-3' (PLO-DS-K328C or PLO-TS). The K231C mutant in the first transmembrane β-hairpin was formed using the forward primer 5'-GGA TTT GAA TGC GTC TCA GCC AAG CTC AAC-3' and the reverse primer 5'-GCA TTC AAA TCC GAG GCC AAG CTT TGC CTC-3'. Finally, the A329C mutant in the second transmembrane β-hairpin region replaces the alanine residue in the 329 position with cysteine using 5'-TTT AGC GGC CTG TTC AAA TGC AAG TTC GGC AAT CTT TCC-3' and 5'-GGA AAG AAT GCC GAA CTT GCA TTT GAA CAG GCC GCT AAA-3' as the forward and reverse primers, respectively. The PLO-R219C and PLO-DS mutants were created by C. Baik. The active mutant N90C was created as described in Chapter 2.

3.2.2 Chemical Modification of Cysteine Residues

Protein samples were transferred to labelling buffer consisting of 50 mM Tris, 150m M NaCl, 1 mM EDTA (BioShop, Burlington ON) pH 7.5 using gel filtration. The single cysteine mutants were supplemented to 1 mM of either Fluorescein-5-Maleimide (Biotium Inc, Hayward CA), Rhodamine Red Maleimide (Invitrogen, Burlington ON) or N,N'-dimethyl-N-(iodoacetyl)-N'-(7-nitrobenz-2-oxa-1,3-diazol-4-yl)ethylenediamine (IANBD, Cedarlane, Hornby ON). The samples were incubated at 25 °C for 60 minutes and excess label was removed using gel filtration chromatography. Labelling efficiencies were calculated as described in the Materials and Methods section of Chapter 2. IANBD concentrations were calculated according to UV-Vis

absorbance using 24,667 L/mol·cm at 490 nm and 1218 L/mol·cm at 280 nm. Labelling efficiencies of 85-90% were obtained for fluorescein, and effciencies of 70-80% were obtained for both rhodamine and IANBD.

3.2.3 Haemolysis Assay

Two-fold serial dilutions were made of PLO-DS (initial concentration 60 $\mu\text{g/mL}$) in a 96-well plate with PBS buffer, in the presence and absence of 5% (v/v) β-mercaptoethanol (EM Science, Gibbstown NJ). Incubation of PLO-DS was conducted by incubating the toxin at room temperature for 30 minutes. Sheep red blood cells were added to each well to a final concentration of 0.5% and incubated at 37 °C for 30 minutes. The decrease in cell turbidity corresponding to haemolysis was monitored at a wavelength outside the absorbance of hemoglobin (650 nm) using a SpectroMax Plus 384 Microplate Spectrophotometer (Molecular Devices, Sunnyvale CA).

The effect of the PLO-DS on the haemolytic activity of active toxin was determined by mixing fluorescein-labelled PLO-N90C-F with disulphide mutant at 1:1, 1:2, 1:3 and 1:4 ratios with a constant PLO-N90C-F concentration of 1 $\mu\text{g/mL}$. Samples were incubated with sheep erythrocytes at 0 °C for 30 minutes, were pelleted and the supernatant removed. The fluorescein emission of the supernatant was recorded (excitation at 465 nm) along with unbound PLO-N90C-F at 1 $\mu\text{g/mL}$, which was used to calculate the extent of active toxin binding. The pellet was resuspended in PBS buffer and the haemolytic activity of the mixtures was measured at 25 °C. The time-dependent decrease in cell turbidity corresponding to haemolysis was monitored at 650 nm, using a SpectroMax Plus 384 Microplate Spectrophotometer (Molecular Devices, Sunnyvale, CA). Haemolysis assays of PLO-N90C-F alone was run at 0.25, 0.50, 0.75 and 1.0 $\mu\text{g/mL}$ to compare activity with that of the active toxin-disulphide mutant mixtures.

3.2.4 Fluorescence Experiments

All samples containing labelled protein were made to a final concentration of 1 µM, with 1% (v/v) of red cell ghost membranes. For all fluorescence resonance energy transfer (FRET) assays, fluorescein- and rhodamine- labelled toxins were combined at a 1:1 ratio (0.5 µM each). For NBD-emission assays, labelled toxins were mixed at a 1:2 ratio with either unlabelled wild type PLO (PLO-WT) or with unlabelled disulfide mutant (PLO-DS). Chemical modifica-

tion, erythrocyte membrane ghost preparation steps, correction for incomplete binding, and the steady state and time resolved fluorescence analyses procedures are as described in Chapter 2.

After incubation with membranes, any remaining unbound toxin was removed by centrifugation. The fluorescence emission of the resuspended membranes was recorded with excitation at 465 nm. Fluorescence spectra were obtained of the supernatants and were used to correct those of the membrane samples for incomplete toxin binding.

3.2.5 Size Exclusion Chromatography

In order to determine relative sizes of hybrid oligomer complexes formed, samples of labelled PLO-K219C-F were made to 1 μM concentration, with an equal amount of unlabelled PLO-DS. Ghost membranes were added to a final concentration of 20% (v/v). Samples were incubated at 37 °C for 30 minutes, centrifuged at 16,060 x*g* for 10 minutes, after which the supernatant was removed. Membranes were dissolved using 5% sodium deoxycholate, and the samples were made to a final volume of 1 mL. Size exclusion chromatography was performed on a BioRad BioLogic FPLC using a Sephacryl S-400 column equilibrated with elution buffer consisting of 20 mM Tris, 150 mM NaCl, 1 mM EDTA and 0.25% (w/v) sodium deoxycholic acid (BioShop, Burlington ON) pH 8.5. Eluted fractions were collected and the fluorescein fluorescence was measured.

3.2.6 Transmission Electron Microscopy

Sample preparation and instrumentation for electron microscopy are as described in Chapter 2.

3.2.7 Osmotic Protection Assay

A standard buffer of 10 mM K_2HPO_4, 25 mM NaCl at pH 7.5 was supplemented with either Dextran 6 or Dextran 40 (both, Fluka Biochemika, Switzerland) to a final concentration of 13% or 17% (w/v), respectively, as these concentrations were found to give sufficient osmotic protection to erythrocytes. Washed sheep erythrocytes were made in the above buffers to a final concentration of 0.5% and 100 μL of each RBC-dextran mixture was added to wells of a 96-well microtitre plate and supplemented with wild type PLO to a final concentration of 2.5 μg/mL, as well as mixtures of 1:1 and 1:2 wild type PLO and PLO-DS. Kinetic analyses were conducted using the SpectroMax Plus 384 Microplate Spectrophotometer at an absorbance of 650nm at 25 °C for 30 minutes.

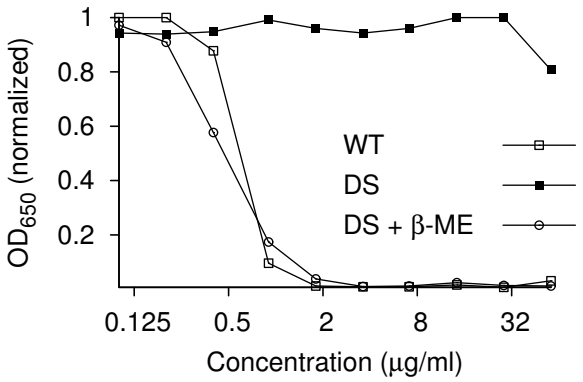

Figure 3.2 Hemolytic Activity of Oxidized and Reduced PLO-DS. The extent of hemolysis of a 0.5% sheep RBC solution was read as the decrease in OD_{650} after incubation at 37 ℃ for 30 minutes. Sheep RBC (0.5% in PBS) were incubated with the indicated amounts of PLO-WT or PLO-DS and incubated at 37 ℃ for 30 minutes. The OD_{650} reflects the fraction of cells that remain intact after the incubation; hemolysis is apparent as a drop in the OD_{650}.

3.3 RESULTS

3.3.1 Haemolytic Activity of the Disulfide-Tethered Mutant

In keeping with previous results, wild type PLO (PLO-WT) exhibits 50% haemolysis at approximately 400 ng/mL. In contrast, the disulfide mutant, or PLO-DS, shows no haemolytic activity up to a concentration of 5 µg/mL. However, when PLO-DS is reduced with β-mercaptoethanol, the haemolytic activity was restored to a level similar to that of wild type pyolysin, as illustrated in Figure 3.2. This indicates that the functional impairment is due to the disulfide bond and not to the substitutions of residues R219C or G85C individually. These findings are entirely analogous to those reported previously for the homologous mutant of perfringolysin O [49].

3.3.2 Oligomerization of PLO-DS

The disulfide mutant of perfringolysin O was reported to form pre-pores on membranes, with the same circular shape and diameter that also characterizes the final, membrane-inserted perfringolysin pores [49]. In contrast to these findings, PLO-DS did not form any distinct, regular ring-shaped oligomers on liposomes containing phosphatidylcholine and cholesterol (data not shown). Similarly, on cholesterol microcrystals, which provide a minimal but viable model substrate for CDCs [26, 43], the mutant failed to form typical oligomers as illustrated in Figure 3.3B. Therefore, the mutant is deficient not only in its ability to undergo membrane insertion,

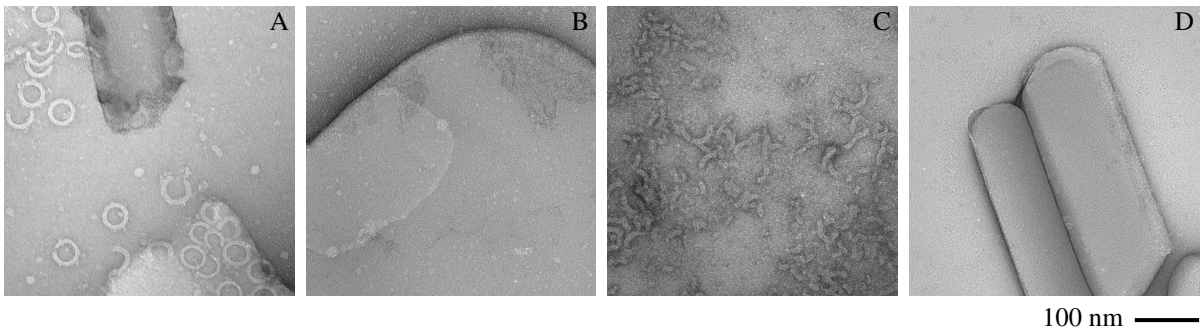

Figure 3.3 Electron microscopy of wild type PLO and of PLO-DS, alone and in mixtures, on cholesterol crystals (negative staining with 2% uranyl acetate). The protein (0.125 mg/mL) and cholesterol crystals (0.5 mg/mL) were incubated for 30 minutes at room temperature. **A**: Wild type PLO, **B**: PLO-DS, **C**: Wild type PLO and PLO-DS 1:1, **D**: Wild type PLO and PLO-DS 1:10. All TEM analyses were performed by J. R. Harris at the University of Newcastle upon Tyne, Newcastle upon Tyne, UK.

but is already unable to properly oligomerize. Oligomerization of the mutant was restored upon reduction which is in agreement with the observed restoration of hemolytic activity.

The lack of oligomerization of PLO-DS is also apparent in fluorescence resonance energy transfer (FRET) experiments. Here, PLO-DS was modelled with the triple mutant PLO-DS-K328C (or PLO-TS), which in addition to the disulfide bond contains another cysteine residue amenable to covalent labelling. In both labelled and unlabelled form, the triple mutant functionally behaves like PLO-DS, exhibiting haemolytic activity only upon disulfide reduction.

The mutants were labelled with fluorescein and rhodamine, respectively. Fluorescein and rhodamine form an efficient donor-acceptor pair for FRET, with an R_0 distance of approximately 50 Å [122], which is well above the distance of two adjacent subunits in CDC oligomers [44, 110]. Accordingly, when mixtures of fluorescein- and rhodamine-labelled N90C are incubated with membranes, the formation of hybrid oligomers results in a strong reduction of the fluorescein emission, as seen in Figure 3.4A. In contrast, no such reduction is apparent with the triple mutant, indicating the decreased extent of oligomerization, shown in Figure 3.4B.

3.3.3 The Effect of PLO-DS on the Oligomerization of Wild Type PLO

When PLO-DS was added to wild type PLO at equal amounts or in slight excess, oligomers were observed, but these were mostly incomplete and arc-shaped, indicating that oligomerization was partially inhibited by the mutant, shown in Figure 3.3C. With PLO present in ten-fold excess, oligomerization was virtually completely inhibited, seen in Figure 3.3D.

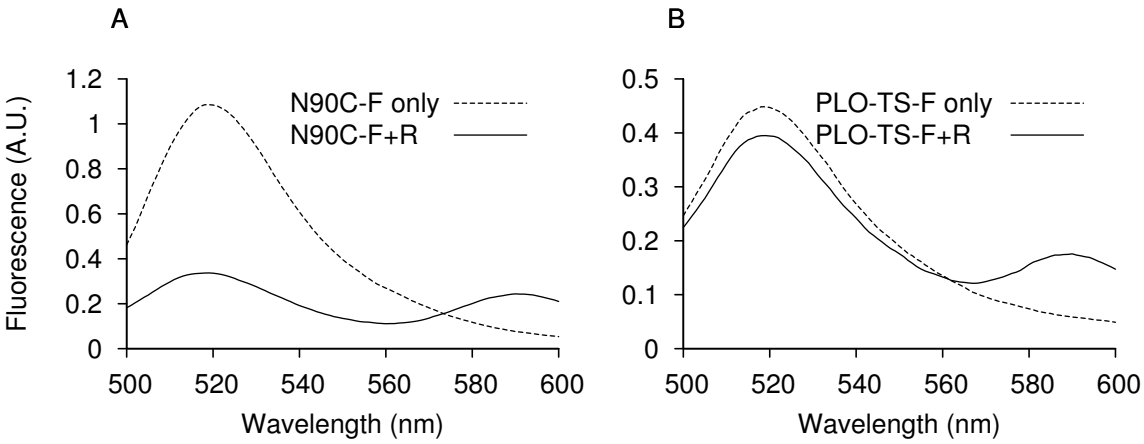

Figure 3.4 FRET experiments on the oligomerization of PLO-DS on erythrocyte ghost membranes. The active single cysteine mutant N90C and the triple mutant PLO-DS-K328C (PLO-TS) were labelled with fluorescein (F) or rhodamine (R). The labelled species were then mixed and incubated with membranes. Spectra were corrected for incomplete binding of labelled protein. **A**: Oligomerization of the active mutant N90C is evident by the suppression of fluorescein emission due to FRET to rhodamine. **B**: The triple mutant does not show significant FRET, indicating inhibition of oligomerization.

The formation of oligomers of reduced size in mixtures of PLO-WT and PLO-DS was confirmed with size exclusion chromatography. In these experiments, wild type PLO was replaced with the haemolytically active fluorescein-labelled cysteine PLO mutant (R219C). This mutant was incubated, with or without added PLO-DS, with sheep red cell membranes to induce oligomerization. The membranes were then solubilized with deoxycholic acid before application to a Sephacryl S-400 column. Oligomers formed from an equimolar mixture of PLO-DS and the active toxin elute between the monomeric toxin and oligomers formed from the active toxin mutant alone, illustrated in Figure 3.5. Since the fluorescence signal tracks the labelled active mutant only, the slowed elution indicates that the disulfide mutant indeed causes the active toxin to result in oligomers of reduced size.

FRET experiments combining fluorescein-labelled PLO-N90C (PLO-N90C-F) and the rhodamine triple mutant PLO-TS show an efficiency of FRET that is intermediate between those of the active mutant, seen in Figure 3.6A, and the inactive mutants alone. When unlabelled disulfide mutant or wild type PLO is added to a mixture of PLO-N90C-F and PLO-N90C-R, FRET is reduced between the two labelled species, indicating the intercalation of unlabelled molecules between those labelled in hybrid oligomers, as illustrated in Figure 3.6B.

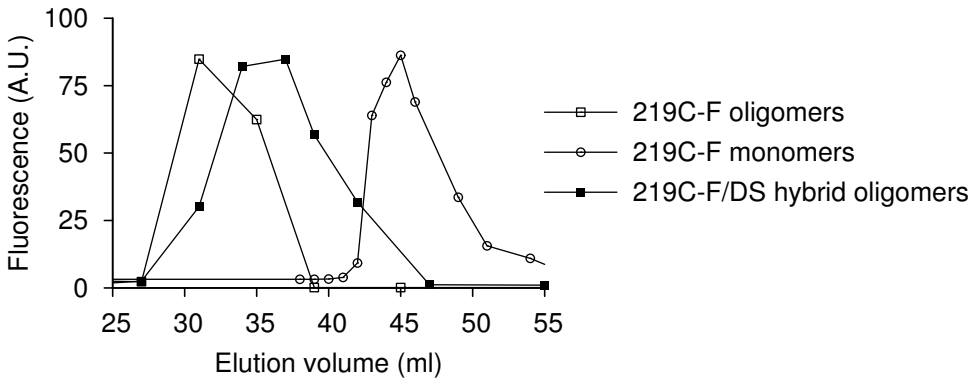

Figure 3.5 Reduced size of wild type PLO/PLO-DS hybrid oligomers, detected by gel filtration. The active mutant R219C was labelled with fluorescein (R219C-F). To induce oligomerization, the mutant was incubated with membranes at 37 ℃ for 30 minutes, alone or as a mixture with an equal amount of unlabelled PLO-DS. The membranes were solubilized with deoxycholate, and the oligomers were applied to a Sephacryl S400 column. The fluorescence of the eluate fractions was measured to detect the labelled protein. For comparison, a sample of labelled R219C not incubated with membranes is shown.

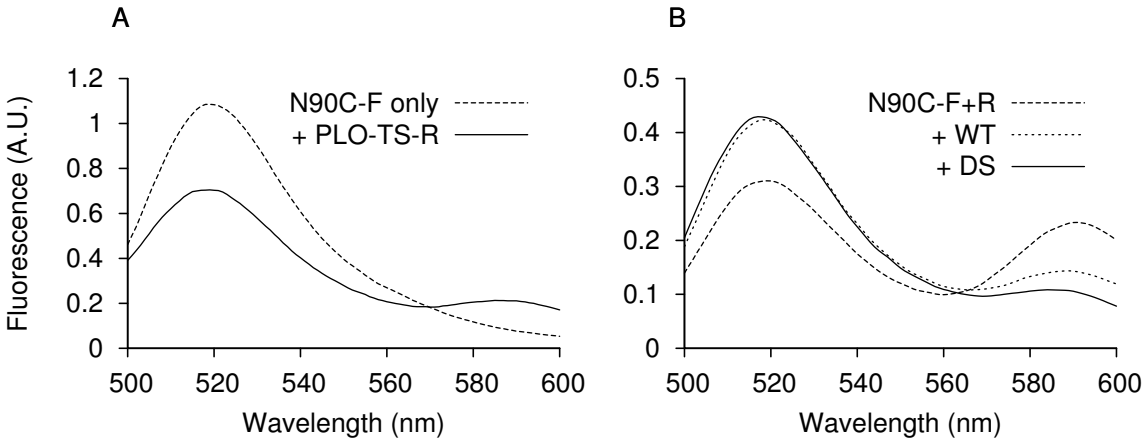

Figure 3.6 FRET experiments on the formation of hybrid oligomers from active PLO and PLO-DS. **A**: The fluorescein-labelled active toxin (PLO-N90C-F) was incubated with membranes alone and after mixing with the rhodamine-labelled triple mutant (PLO-TS-R), respectively. The decrease of fluorescein fluorescence due to FRET indicates the formation of hybrid oligomers. **B**: FRET of fluorescein- and rhodamine-labelled PLO-N90C incubated with membranes, alone and together with unlabelled PLO-DS or PLO-WT. Where present, the amount of unlabelled toxin is equal to the total of the labelled species. The reduction of FRET between N90C-F and N90C-R with both proteins indicates that both can intercalate with the labelled active toxin. PLO-DS is therefore not restricted to terminal positions in hybrid oligomers with wild type toxin.

3.3.4 Membrane Insertion of Active Subunits in Hybrid Oligomers

With the disulfide mutant of PFO, it was shown that the loss of haemolytic activity correlated with the loss of insertion activity of the two β-hairpins in domain 3 into the membrane [95]. From the observation of hybrid oligomers forming between active PLO and PLO-DS, the question arises concerning to which extent the active protein subunits in such hybrids may insert into membrane. The membrane insertion of the two β-hairpins in domain 3 can be detected by labelling mutant cysteine residues with the environmentally-sensitive fluorophore nitrobenzoxadiazole (NBD), whose fluorescence emission undergoes a pronounced increase in intensity and excited state lifetime, and a blue shift upon transition from an aqueous to non-polar environment [19, 22]. The insertion of hybrids was studied using the NBD-labelled mutants K231C and A329C, whose cysteine residues are located within the first and second transmembrane β-hairpin, respectively. When either NBD-labelled mutant was mixed with a twofold excess of the unlabelled PLO-DS, the NBD fluorescence emission was reduced significantly compared to samples that were prepared in the same manner but with unlabelled PLO-WT instead of PLO-DS. This is shown in Figure 3.7A for PLO-K231C-NBD, and in Figure 3.7B for PLO-A329C-NBD. However, in both cases, the NBD fluorescence was still greater than that observed with the equivalent amount of toxin in the absence of membranes. The steady-state spectra are in line with time-resolved fluorescence measurements. For mutant K231C, the average excited state lifetime of NBD was 4.0 ns when mixed with wild type toxin, 3.2 ns when mixed with disulfide mutant, and 1.7 ns in the absence of membranes. For A329C, the lifetimes were 6.2 ns, 2.9 ns and 2.1 ns, respectively. These findings indicate that PLO-DS inhibits but does not completely abrogate membrane insertion of wild type PLO in hybrid oligomers.[1]

3.3.5 Haemolytic Activity of Wild Type PLO and PLO-DS Mixtures

In order to determine the effect of PLO-DS on the haemolytic activity of active toxin, the degree of binding to erythrocyte membranes was first determined by incubation at 0 °C of fluorescein-labelled PLO-N90C and disulphide mutant with membrane, where the incubation of toxin at low temperatures allows for binding but prohibits oligomerization and membrane insertion. Using the supernatant of each sample, the fluorescein emission was recorded and compared to that of a sample of soluble PLO-N90C-F. These values were then used to determine the amount

[1] The parameters for the individual components obtained from the fits for K231C and A329C are listed in Tables A.3 and A.4, respectively.

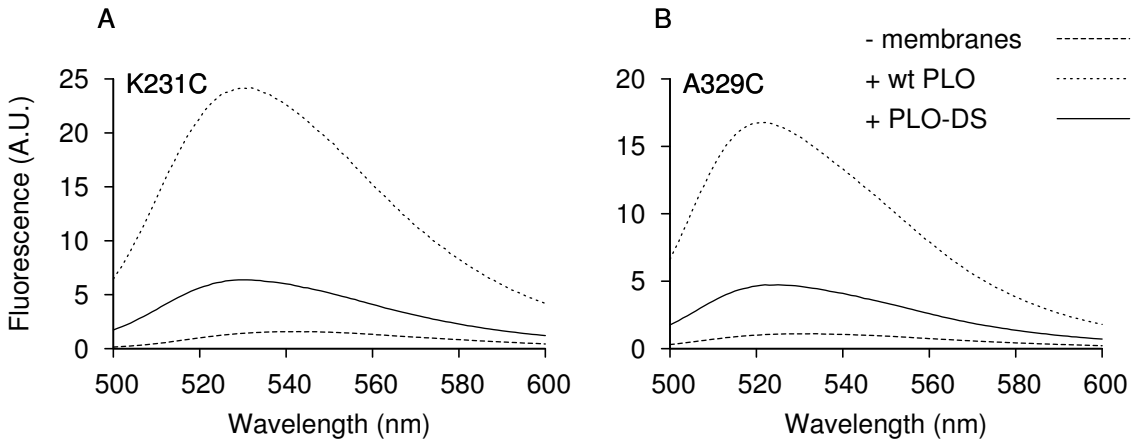

Figure 3.7 Membrane insertion of domain 3 in hybrid oligomers. The mutant residues K231C in TMH1 and A329C in TMH2 were labelled with NBD, and the fluorescence emission was measured in the absence of membranes, and after incubation with membranes after addition of either wild type toxin or of unlabelled PLO-DS in twofold molar excess. The fluorescence increase after incubation with membranes reflects the extent of membrane insertion of the labelled residues.

of protein that remained bound on the surface. It was found that the 1:1 sample retained 94% of the active toxin, corresponding to 0.94 µg/mL, while the 1:2 sample retained 92% of active toxin, or 0.92 µg/mL. The samples with a three- and four-fold excess of disulphide mutant retained concentrations of active toxin at 0.86 and 0.81 µg/mL, respectively.

Considering the haemolytic activity of the mixtures of active and PLO-DS, all mixed samples retained an active toxin amount greater than 0.75 µg/mL, yet show a lysis rate slower than that observed for the active toxin at the same concentration. This suggests that the decrease in haemolytic activity seen by a mixture of PLO-WT and PLO-DS is caused by the association between the wild type and the mutant, and is not due to a simple displacement of active toxin from the membrane surface. The time course for haemolysis of the fluorescein-labelled PLO-N90C-F standard and the mixtures of active-toxin and disulphide mutant are seen in Figures3.8, respectively.

3.3.6 Reduction of Average Pore Size by PLO-DS

When PLO-DS is combined with active PLO, it is likely that only a small fraction of all resulting oligomers will not contain any PLO-DS at all. This suggests that the remaining extent of membrane insertion and pore formation observed with such mixtures is at least in part as-

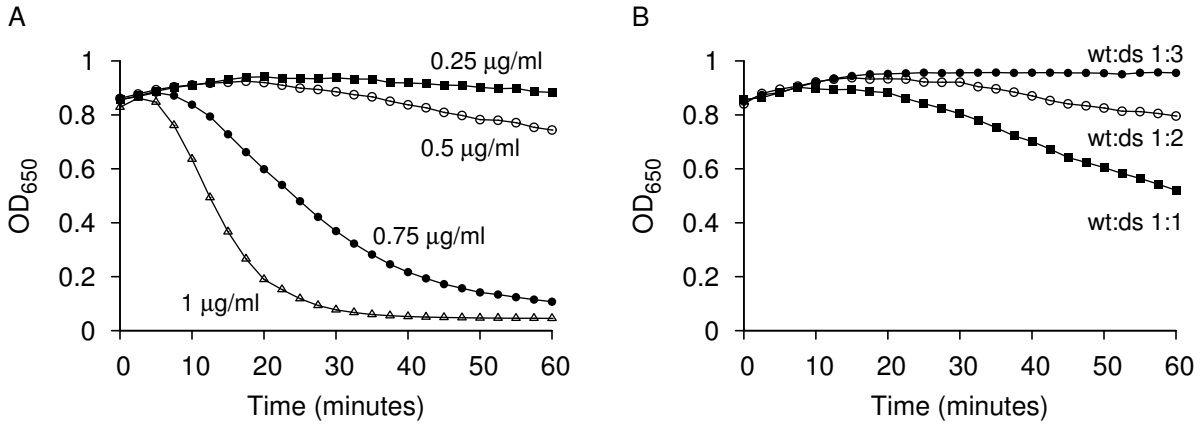

Figure 3.8 Haemolytic activity of wild type PLO in the presence of PLO-DS. Sheep erythrocytes (0.5% v/v) were incubated at 0 ℃ with fluorescein-labelled PLO-N90C with various amounts of PLO-DS. Unbound toxin was removed by centrifugation, and the time course of hemolysis recorded by the decrease in cell turbidity (OD_{650}). **A**: Control experiment with various amounts of PLO-N90C-F alone. **B**: PLO-N90C-F at 1 µg/mL in the presence of 1,2 or 3 equivalents of PLO-DS.

sociated with hybrid oligomers. Since these hybrid oligomers are reduced in size, the pores associated with them should be smaller than those formed by full-size, ring-shaped oligomers formed by wild type PLO alone.

Differences in functional pore size can be studied in haemolytic assays using osmotic protection [86]. In this method, the extracellular medium is supplemented with inert macromolecular solutes such as dextran that counteract the osmotic activity of the intracellular hemoglobin. When pore formation occurs, haemolysis will result only if the pores are large enough to permit equilibration of the macromolecular solutes across the membrane, so that they no longer maintain the balance with haemoglobin. On the other hand, if the effective diameter of the protecting solutes exceeds that of the pores, the solutes will remain excluded from the cell and continue to protect it from osmotic lysis. Differential protection by macromolecular solutes varying in size can be used to characterize the pore size.

In the experiment shown in Figure 3.9A, wild type PLO was incubated with red cells with dextran 6 or dextran 40. The dextrans cause only a very slight delay in the time course of haemolysis. This is consistent with the fact that the hydrodynamic diameters of dextran 6 (Mr 6 000) and dextran 40 (Mr 40 000) at approximately 3 and 10 nm, respectively [100], are smaller than the diameter of ring-shaped PLO oligomers [11] and therefore do not afford osmotic protection against the latter.

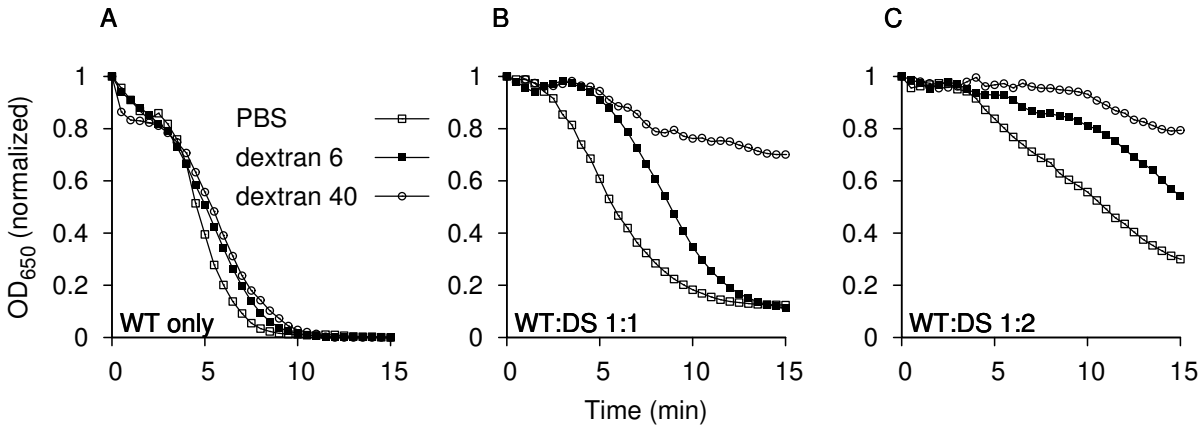

Figure 3.9 Osmotic protection of red cells against mixtures of wild type PLO and PLO-DS by dextran 6 and dextran 40. Wild type PLO (2.5 μg/ml) alone (**A**) or with the same amount (**B**) or twice the amount (**C**) of PLO-DS was incubated in phosphate-buffered saline, with or without dextran 6 or dextran 40. The OD_{650} was followed over time; a drop in the OD_{650} indicates hemolysis.

The results change, however, with the addition of one and two equivalents of disulfide mutants, as illustrated in Figures 3.9B and 3.9C, respectively. Here, the time course of haemolysis is markedly slowed by dextran 6, and even more so by the larger dextran 40. This divergence indicates that some of the pores are no longer permeable to the dextran molecules, or they are sufficiently reduced in size to significantly decrease the rate of permeation of dextran. On the other hand, with both dextran 6 and dextran 40, haemolysis ultimately occurs, which means that some pores are still large enough to allow permeation of dextran. The pores formed by the mixtures of PLO-WT and PLO-DS therefore are heterogenous in size yet smaller on average than those formed by wild type PLO alone. This supports the conclusion that oligomers that contain both wild type PLO and PLO-DS can insert into the membrane and form pores. It also confirms the previous contention that incomplete, arc-shaped oligomers can indeed form functional trans-membrane pores [86].

3.4 DISCUSSION

In this study, PLO was rendered inactive by the introduction of a disulphide bond between domain 2 and the membrane-inserting region of domain 3, the first transmembrane β-hairpin (TMH1). Alone, the disulfide mutant does not retain the ability to oligomerize on membranes or crystalline cholesterol surfaces as determined by electron microscopy, and as such no

haemolytic activity is seen. However, upon reduction of the disulfide bond, activity is restored indicating that the disulfide link is the cause of inactivity, and not the individual R219C and G85C mutations. These results differ from the study on perfringolysin O (PFO) [49] where the disulfide mutant was able to form distinct ring-shaped pre-pore oligomers. (The PFO disulfide mutant was able to trap the monomers in the water-soluble conformation, but enough movement was retained to allow the necessary interaction with adjacent toxin molecules and form rings on the membrane surface, and prevented only the insertion into the membrane.)

The fact that the mutant toxin of PFO was able to assemble into complete, ring-shaped pre-pores on membranes, while the PLO-DS mutant did not retain the ability to oligomerize on its own was remarkable and surprising. The differences between the two toxins may be related to subtle but long-ranging conformational changes that occur in domain 4 upon membrane binding which are translated to the upper regions of the toxin. It is possible that the disulfide bond alters the ability of PLO to oligomerize to an extent that is significantly different than that observed in PFO.

Another interesting finding of this study is that the PLO-DS mutant can form hybrid oligomers with wild type toxin, as evidenced by the occurrence of fluorescence energy transfer and the reduction of haemolytic activity in hybrid oligomer analysis. A possible explanation for this is that upon interaction with wild type toxin, 'hemiplegic' inactivation (which renders one half of the toxin molecule much weaker than the other) may occur. Here, the PLO-DS mutant would be able to attach to a growing oligomer of wild type molecules using its 'active' face while leaving the inactive side exposed, thus terminating further growth of the oligomer. However, this does not appear to be the case as experiments show that PLO-DS retains the ability to intercalate between active subunits; therefore both faces of PLO-DS must preserve some degree of activity. An alternative explanation takes into account the different kinetic stages of oligomerization of CDC toxins [88]. Briefly, the three-stage process involves the rate-limiting initiation reaction (the spontaneous interaction of two or more monomers on the membrane surface into a dimeric or small oligomeric complex), an extension stage (successive addition of monomers onto the growing oligomer) and finally, the oligomer completion stage. When the disulfide mutant is introduced to the membrane surface in the presence of wild type, this initiation reaction would take a considerably greater amount of time to occur as the mutant molecules interact with other toxin molecules to create the initial complex. In addition, the PLO-DS mutant molecules would slow the subsequent extension phase of oligomer growth since at least one participant contains the kinetic obstruction (although this phase is affected to

a lesser extent than the initial reaction stage described above). As a result, the formation of hybrid oligomers is somewhat inhibited, yielding increasing numbers of incomplete, arc-shaped oligomers. What is seen in the hybrid oligomers is that the wild type toxin promotes the oligomerization of disulfide-tethered toxins, while the DS mutants inhibit the oligomerization of wild type toxin. Both toxins play active roles in the other's ability to oligomerize.

In addition to the decreased haemolytic activity observed with the hybrid oligomers is the pattern of membrane insertion. The combination of wild type toxin and disulfide mutant may produce a distribution of oligomers which vary in both shape and size, with some oligomers containing a higher proportion of DS mutant than others. In other words, at similar wild type-PLO-DS concentrations, some oligomers which consist of only wild type protein should form. However at even a two-fold excess of PLO-DS over wild type, the number of wild-type only oligomers would be small, yet this combination results in considerable haemolytic activity and membrane insertion. At 50% activity, this significant level of function must be attributed to the action of hybrid oligomers. This conclusion is supported by the fact that pores formed under these conditions are smaller on average than those formed by wild type toxin only.

These results signify that, with respect to membrane insertion as with oligomerization, neither the wild type toxin nor PLO-DS is clearly dominant over the other. Insertion of hybrids formed at moderate proportions of PLO-DS indicates that not all subunits of an oligomer need to participate in its membrane insertion. Conversely, its suppression by PLO-DS in greater proportion indicates that membrane insertion requires a certain critical proportion of active subunits. Overall, these findings suggest that membrane insertion requires the co-operation of a number of adjacent subunits within the oligomer.

In conclusion, this study provides additional insights into the mechanism of oligomerization and pore formation by CDCs. The initial conformational change that is associated with membrane binding and sets the stage for oligomerization involves conformational flexibility between domains 2 and 3. The complementation of PLO-DS oligomerization by wild type PLO supports a two-step model of oligomerization that to date has been based primarily on kinetic modelling [88]. The fact that membrane insertion and pore formation can occur in oligomers that contain some insertion-deficient subunits suggests that the process of insertion is only partially co-operative.

Chapter 4

The Pore-Forming Activity of Solution-Derived Oligomers of Pyolysin

4.1 INTRODUCTION

Thus far in this thesis, the oligomerization process of cholesterol dependent cytolysins has been investigated in regards to the monomer-monomer interactions and the roles specific domains play in oligomerization that lead to pore formation. In this section, a different aspect of CDC oligomerization is investigated, namely the self-association of toxin molecules in solution that form oligomeric complexes in the absence of membrane surfaces, and the mechanism by which these complexes can form functional pores.

As CDCs are released from the originating organism as a water-soluble monomer, it was believed that most CDCs possess a mechanism which protects against the premature oligomerization of the monomers while in solution, before a host membrane is encountered [39, 95]. However, several CDCs have shown the ability to form oligomeric complexes in solution, including pneumolysin (PLY) [37], cereolysin (CLO) [21], and streptolysin O (SLO) [78]. Recent studies on the CDC pyolysin (PLO) show that it too can spontaneously undergo oligomerization in solution to consistently form complexes averaging six subunits [27], as compared to the dimers formed by PFO [39] or trimers of SLO found in solution [78]. Also, it has been found that the oligomeric complexes of PLO retain some haemolytic activity, around

one-quarter to one-third of that observed with wild type toxin [27], in contrast to the inactive oligomeric complexes formed by the previously mentioned CDCs.

In this study, the pore forming mechanism of the *solution-derived oligomers* or SDO, of pyolysin was investigated. Here, specific residues within both trans-membrane β-hairpins of domain 3 in the SDO sample were monitored for membrane insertion using cysteine-scanning mutagenesis and covalent modification with the environmentally-sensitive fluorophore NBD, with the results compared with monomeric PLO samples. It was found that although the residues of SDO inserted into the membrane in a fashion similar to that seen with the monomeric toxin samples, fluorescence analysis suggests that only a fraction of the SDO subunits insert into the membrane leaving the remainder idle or uninserted. This action may be the direct cause of the decrease in haemolytic activity.

4.2 MATERIALS AND METHODS

Unless stated otherwise, the experimental methods used in this study are the same as those in the preceding chapters. The following describes only changes and extensions to those previously described methods.

4.2.1 Plasmid Preparation and Protein Expression

Mutagenesis and protein preparation were performed as described in Chapter 2. After purification of the protein by metal-chelating chromatography and, where applicable, covalent labelling with fluorescent dyes, the solution-derived oligomers, or SDO[1] were isolated by gel filtration chromatography (see below). The primers for the site-directed mutagenesis are listed in Table 4.1.

4.2.2 Chemical Modification of Cysteine Residues with IANBD

The mutant proteins were thiol-specifically labelled with 0.5 mM N,N'-dimethyl-N-(iodoacetyl)-N'- 3-(7-nitrobenz-2-oxa-1,3-diazol-4-yl)ethylenediamine (IANBD, Cedarlane, Hornby

[1]In order to distinguish between monomeric and SDO samples, the prefix "M" will be used for monomeric toxins, while the prefix "SDO-" will be used for oligomeric toxins for the remaining text of this chapter. Also, NBD-labelled toxins will have the suffix -NBD. For example, the monomeric toxin with the point mutation A329C that has not been derivatized with IANBD will be referenced as PLO-A329C. The SDO sample of this toxin that has been labelled with NBD is known as SDO-A329C-NBD.

Table 4.1 Primers for site-directed mutagenesis. For each mutant, one forward primer and one reverse primer span the site of the mutation. The cysteine codons and anticodons are underlined.

Mutation	Sequence
R219C Forward	5′–ACG TCA AAG TGT CAA CTG GAG GCA AAG C–3′
R219C Reverse	5′–CAG TTG ACA CTT TGA CGT CAC CAG AGT C–3′
K231C Forward	5′–GGA TTT GAA TGC GTC TCA GCC AAG CTC AAC–3′
K231C Reverse	5′–GCA TTC AAA TCC GAG GCC AAG CTT TGC CTC–3′
V232C Forward	5′–GGC CTC GGA TTT GAA AAG TGC TCA GCC AAG CTC AAC GTG–3′
V232C Reverse	5′–CAC GTT GAG CTT GGC TGA GCA CTT TTC AAA TCC GAG GCC–3′
F327C Forward	5′–GCG GCT TTT AGC GGC CTG TGC AAA GCT AAG TTC GGC AAT–3′
F327C Reverse	5′–ATT GCC GAA CTT AGC TTT GCA CAG GCC GCT AAA AGC CGC–3′
K328C Forward	5′–AGC GGC CTG TTC TGC GCT AAG TTC GGC AAT CTT TCC ACA–3′
K328C Reverse	5′–TCT GGA AAG ATT GCC GAA CTT AGC GCA CAA CAG GCC GCT–3′
A329C Forward	5′–TTT AGC GGC CTG TTC AAA TGC AAG TTC GGC AAT CTT TCC–3′
A329C Reverse	5′–GGA AAG AAT GCC GAA CTT GCA TTT GAA CAG GCC GCT AAA–3′
K330C Forward	5′–TTC AAG GCC TGC TTC GGC AAT CTT TCC–3′
K330C Reverse	5′–GCA GGC CTT GAA CAG GCC GCT AAA AGC CGC–3′
F331C Forward	5′–GGC CTG TTC AAA GCT AAG TGC GGC AAT CTT TCC ACA GAG
F331C Reverse	5′–CTC TGT GGA AGG ATT GCC GCA CTT AGC TTT GAA CAG GCC–3′

ON) as described in Chapter 2. In order to limit the extent of NBD labeling which might lead to self-quenching within SDO, IANBD was admixed with a four-fold molar excess of iodoacetamide (Sigma Chemicals, St Louis MO). The protein sample which includes the monomeric and SDO forms was labelled with NBD, and then was subject to size exclusion chromatography to separate the monomers from the oligomeric complexes.

4.2.3 Size Exclusion Chromatography

Size exclusion chromatography was performed using a Superdex 200 column (400 x 8 mm) which was pre-equilibrated with PBS, operated by an ÄKTApurifier Chromatography system (GE Healthcare, Baie d'Urfe, QC). PBS flow rate was maintained at 0.5 $^{mL}/_{min}$, with the elution profile monitored online by UV-Vis spectrophotometry at 280 nm. The eluate was collected in fractions of 0.3 mL and analysed by SDS-PAGE.

4.2.4 Gel Electrophoresis

SDS-PAGE was performed according to Laemmli [61], using polyacrylamide concentrations of 4% for the stacking gel and 12% for the resolving gel. The gel was stained using a solution of Coomassie Blue G-250 (Fisher Scientific, Fairlawn NJ).

4.2.5 Cholesterol Assay

The concentration of erythrocyte membrane ghosts was standardized between experiments using the Amplex Red Cholesterol Assay Kit (Molecular Probes, Eugene, Oregon). The membrane samples were mixed with the 1x Reaction Buffer provided (KH_2PO_4 0.5 M, NaCl 0.25 M, cholic acid 25 mM, Triton X-100 0.5%, pH 7.4), mixed with equal volumes of Amplex Red Reagent (horseradish peroxidase, cholesterol oxidase, cholesterol esterase) in a microtitre plate. The reaction was protected from light, incubated for 30 minutes at 37 °C and the fluorescence was measured with a fluorescence microplate reader (SpectraMax Gemini XS, Molecular Devices Corporation) with an excitation wavelength of 525 nm and emission wavelength of 590 nm.

4.2.6 Fluorescence Measurements on NBD-Labelled Mutants

All samples containing labelled protein were made to a final concentration of 1 µM. (For samples where the labelling efficiency of monomeric and oligomeric species differed, the protein concentration was adjusted to create samples with equal NBD concentrations.) Monomeric toxin and SDO samples were made up to volume with PBS, while protein-membrane samples were made up to 1% (v/v) with membrane ghosts. After incubation at 37 °C for 30 minutes, the protein-membrane samples were centrifuged at 13,000 RPM for 10 minutes, the supernatant was decanted, and the pellet was resuspended with PBS. Steady state fluorescence and time resolved measurements and data analysis were performed as described in section 2.2.5 on page 24.

4.2.7 Fluorescence Quenching Analysis

Monomeric toxin and SDO samples were mixed with 1% membrane ghosts to a final concentration of 1 µM and incubated at 37 °C for 30 minutes. Unbound toxin was removed by centrifugation at 16,060 x*g* for 10 minutes, after which the supernatant was decanted. The

membrane-toxin pellet was resuspended in PBS and the fluorescence emission was measured. The hydrophobic quencher, 5-doxyl stearic acid, was added to the sample in increments of 0.05 $\mu mol/_{mg\ cholesterol}$ up to a final concentration of 0.25 $\mu mol/_{mg\ cholesterol}$. This procedure was repeated for 16-doxyl stearic acid.

In Figure 4.7 in the Results section, the data were plotted according to the Stern-Volmer equation [62]:

$$\frac{F_0}{F} - 1 = k_a[Q] \tag{4.1}$$

where F is the fluorescence intensity in the presence of quencher at concentration $[Q]$, F_0 is F for $[Q] = 0$, and k_a is the quenching constant.

Most data series produced non-linear Stern-Volmer plots (see Results section). Therefore, the data were fitted using a model in which only a fraction of the fluorophores can be quenched, as expressed in the equation

$$F = \frac{F_0 f_q}{1 + k_a[Q]} + (1 - f_q)F_0 \tag{4.2}$$

where f_q is the fraction quenchable fluorescence. Fitting was performed with Gnuplot.

4.3 RESULTS

4.3.1 Experimental Rationale

In order to determine if an amino acid side chain is located in a polar or non-polar environment, the residue can be covalently modified with an environmentally sensitive fluorophore. These dyes are sensitive to the presence of water, and their emission properties are altered when they move from an aqueous region to an non-aqueous area. Examples of environmentally sensitive dyes include N-iodoacetyl-N-(5-sulpho-1-naphthyl)ethylenediamine (IAEDANS), 6-acryloyl-2-dimethylaminonaphthalene (acrylodan) and N,N'-dimethyl-N-(iodoacetyl)-N'-(7-nitrobenz-2-oxa-1,3-diazol-4-yl)ethylenediamine (IANBD).

The fluorophore NBD was utilized in the study of PFO to establish the membrane-inserting regions of this toxin [43, 104, 105]. In these studies, residues of both trans-membrane hairpins were replaced by a cysteine residue, covalently modified by NBD, and bound to liposomes.

The increase in the emission intensity and the lifetime decay values were examined to show which residues inserted into the lipid core of the bilayer. When examining the change in intensity and lifetime values of the NBD-labelled residues it was found that the residues of the TMH sequences alternated between polar (facing the pore) and non-polar (facing the membrane bilayer), yielding an insertion pattern typical of that seen for β-sheet.

PLO has a similar primary sequence in the TMH regions in domain 3 as PFO, and it is assumed that all members of the CDC family share the same mechanism of pore formation. Using sequence alignment with PFO, homologous residues of PLO were identified, and select residues in each TMH were replaced with cysteine and chemically modified with NBD and tested for membrane insertion. PLO-SDO was labelled with NBD, and was tested for NBD fluorescence emission in its membrane-bound and water-soluble forms. These results were compared with the same residues in the monomeric form of PLO to determine the insertion pattern of PLO-SDO which may be used to account for the decrease in haemolytic activity of the SDO compared to wild type toxin.

4.3.2 Size Exclusion Chromatography

As the oligomeric complexes form spontaneously in the *E. coli* cells and are extracted from the lysates, no external preparation is needed for their formation, and as such the SDO only need be separated from the original protein sample containing PLO in monomeric form. Figure 4.2 shows the elution profile of a sample of wild-type PLO resolved on a Superdex 200 size exclusion column. The main peak corresponds to a molecular weight of 57 kDa, indicating elution of the monomeric species, while the smaller peak ahead of this corresponds to a molecular weight of approximately 350 kDa, indication that the SDO complex is formed by approximately six to eight monomer subunits.

SDS-PAGE analysis of the SDO fractions confirms a molecular weight of the individual subunits of the SDO of 57 kDa, and indicates that the interactions between SDO subunits in the complex are not sufficiently strong to withstand the denaturing properties of SDS. Oligomer size is consistent and reproducible, and does not change significantly between preparations of the same or different mutants.

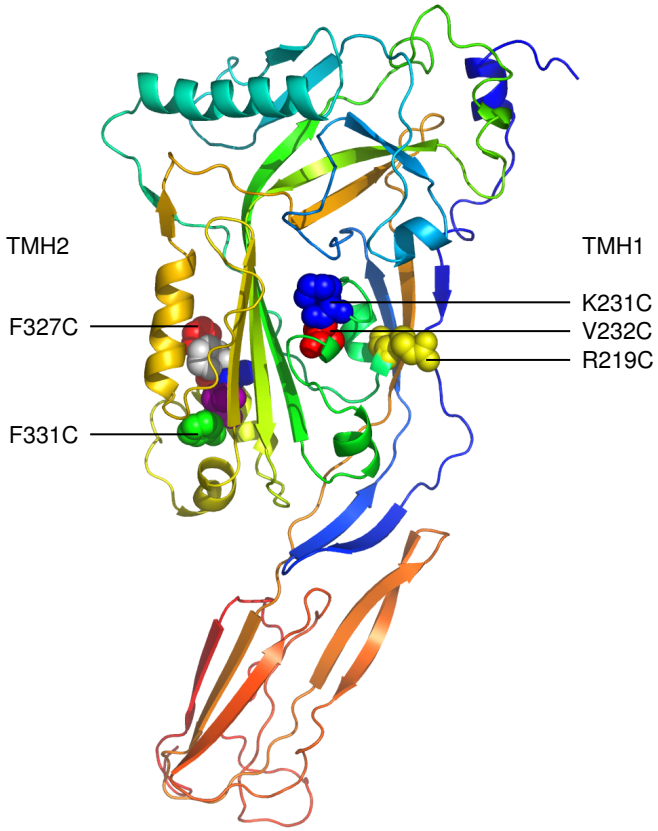

Figure 4.1 Cysteine Mutants in Trans-Membrane Hairpins TMH 1 and TMH 2. The residues that were singly mutated to cysteines are shown in space-filling mode. (In TMH 2, residues 327 and 331 are indicated; all intervening residues were mutated as well.)

4.3.3 Labelling Efficiency of Monomers and SDO with IANBD

NBD has been reported to undergo concentration-dependent self-quenching [99]. To minimize self-quenching between adjacent SDO subunits, the labelling reactions were performed with a mixture of NBD and iodoacetamide at a molar ratio of 1:4. In this manner, approximately one in four subunits should be covalently modified with IANBD, while the remainder will be blocked from IANBD reaction with free iodoacetamide.

After the SDO were separated from the original protein mixture by size exclusion chromatography, the protein concentrations of both SDO and monomeric toxin fractions were determined, and the efficiencies of labelling with IANBD were calculated. The labelling efficiencies for the monomeric mutants ranged from 11% in the case of M-K328C-NBD to a maximum of 41% for M-V232C-NBD, confirming that only a fraction of the monomeric toxin was labelled with the fluorophore. Many of the SDO species exhibited the similar labelling efficiency

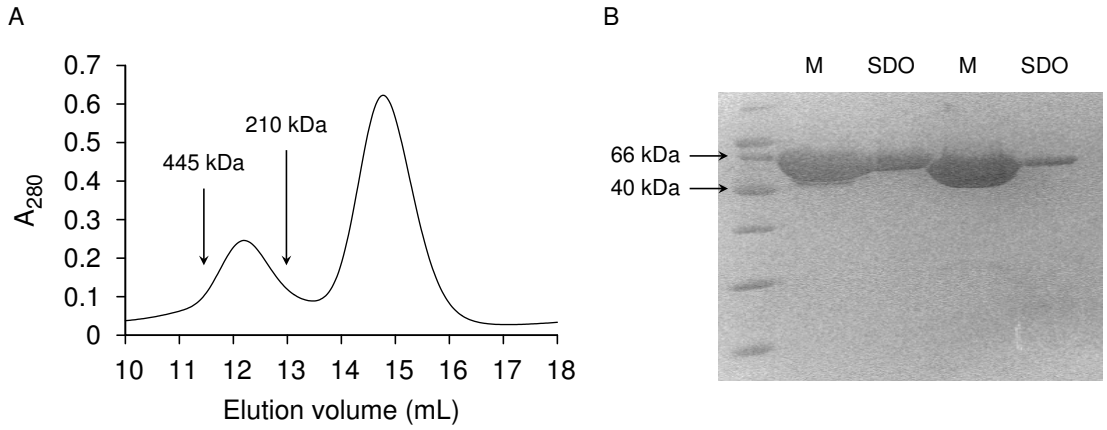

Figure 4.2 Size exclusion chromatogram (A) and SDS-PAGE (B) of wild type PLO expressed in *E. coli*. **A**: The large peak contains the toxin monomer with a molecular weight of 57 kDa. The elution volume of the smaller peak corresponds to a molecular weight of approximately 350 kDa. The vertical lines indicate the elution positions of apoferritin (443 kDa) and amylase 210 kDa). To ensure no cross-contamination of monomer and SDO samples, only fractions that are sufficiently separated were used in haemolysis and fluorescence analysis. **B**: SDS-PAGE of monomer (M) and SDO fractions from the chromatography experiment in A.

as their corresponding monomeric toxin sample, except for SDO-F331C-NBD which showed a 12% decrease in labelling as compared to the monomeric M-F331C-NBD. Monomers and SDO of the mutant M-F327C-NBD showed a negligible NBD absorbance after chemical modification. The results are tabulated in Table 4.2.

The labeling efficiency results show that for most mutants, the cysteine mutant is as accessible for labeling in the monomer as in the SDO form; in other words, the SDO formation does not block or shield the cysteine residue from reaction with the iodoacetamide functional group on the IANBD.

4.3.4 Haemolytic Activity of SDO

To test the activity of the solution-derived oligomers, a haemolysis assay was conducted on sheep erythrocytes and compared to that of monomeric wild type PLO. The specific activity of monomeric and SDO PLO here is defined as the concentration of toxin required to achieve 50% erythrocyte lysis after 30 minutes. As previously reported [27], it was found that the SDO from wild type PLO exhibit a haemolytic activity approximately one-fourth of that of monomeric PLO (400 $^{ng}/_{mL}$ of wild type PLO is needed to achieve 50% haemolysis [51]) (see Figure 4.3). With NBD labelling, most monomers show a slight change in activity. M-R219C-NBD and M-

Table 4.2 NBD labeling efficiencies of PLO cysteine mutants. PLO samples in monomeric and SDO forms were labelled with a 1:4 ratio of NBD to iodoacetamide. The labeling yield is determined by the ratio of NBD concentration of a sample and the overall protein concentration. Two independent series of samples were labelled, and the average value reported.

TMH 1			TMH 2		
Mutant	Monomer	SDO	Mutant	Monomer	SDO
R219C	24%	19%	F327C	<1%	ND
K231C	39%	39%	K328C	11%	12%
V232C	41%	44%	A329C	35%	31%
			K330C	23%	18%
			F331C	23%	11%

V232C-NBD exhibit a two-fold increase in activity, requiring only 220 ng/mL for 50% lysis, and a four-fold increase is seen with M-A329C requiring only 120 ng/mL. In contrast M-K328C-NBD and M-K330C-NBD exhibited a decrease in activity upon labelling, at 910 ng/mL and 2600 ng/mL, respectively. Some SDO demonstrate an increase in activity compared to that of wild type SDO, except for SDO-R219C-NBD giving one-quarter the activity of wild type, and SDO- K330C-NBD with only one-fifth the activity of wild type SDO. Table 4.3 lists the monomeric and SDO concentrations necessary to achieve 50% erythrocyte haemolysis.

4.3.5 Membrane Insertion Behaviour of Monomeric and SDO PLO

4.3.5.1 Fluorescence changes upon membrane binding. As described in section 4.3.1 above, selected residues located within both transmembrane β-hairpins were individually replaced with cysteine and labelled using NBD. Monomers were separated from the SDO, and both samples were incubated with membranes, pelleted and the supernatant was removed. After resuspension of the pellet, NBD fluorescence was examined on the membrane-bound samples and the supernatant, which was then compared to unbound toxin in order to determine the binding efficiency of each sample. For almost all mutants tested, the SDO consistently showed a 30% decrease in binding efficiency compared to the monomeric counterparts. M-V232C, M-A329C and M-F331C bound to membranes with 90% efficiency, while only 60% of the SDO mutants bound to membranes. M-R219C, M-K231C and M-K330C bound with approximately 70% efficiency while each of the SDO bound at 40%. The only exception was SDO-K328C which showed a decrease of 50% binding compared to M-K328C.

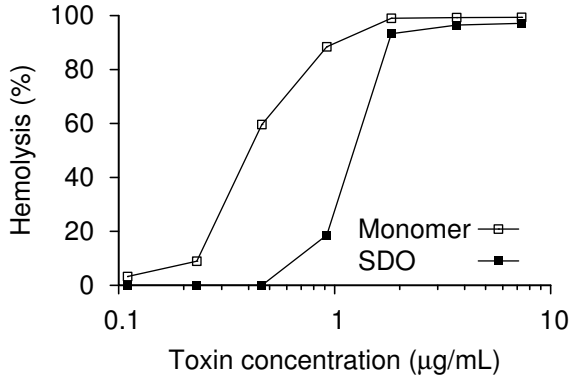

Figure 4.3 Haemolytic activities of wild type PLO monomers and SDO. The concentration of monomeric PLO-WT needed for 50% haemolysis is 400 ng/mL, while the concentration of PLO-SDO is 1250 ng/mL.

Transmembrane β-hairpin 1. The steady state fluorescence spectra of all tested residues comparing the soluble- and membrane bound samples of monomeric toxin and SDO complexes are illustrated in Figure 4.4. Considering the transmembrane β-haripin 1 monomeric species, M-R219C-NBD and M-K231C-NBD both showed a significant increase in fluorescence intensity when combined with membrane ghosts, indicating a change in environment from an area of high polarity to an increasingly non-polar one, which is most probably the result of insertion into the membrane lipid bilayer.

The change in polarity in the NBD environment is also seen in the change in lifetimes. Here, M-R219C-NBD displays an increase in lifetime from 1.0 ns in the soluble state to 2.6 ns in the membrane-bound form, and M-K231C-NBD increases from 2.4 to 4.1 ns during the transition from soluble to membrane-bound states. Conversely, the M-V232C-NBD monomeric toxin showed a decrease in fluorescence intensity and excited state lifetime when incubated with membrane ghosts, suggesting that this residue moves from a relatively apolar location within the protein structure to a more solvent-exposed environment upon membrane interaction.

These observations are in accord with the homologous mutations of PFO [105]. The V202C residue of PFO (homologous with the K231C residue of PLO) is shown to move into an environment of increased hydrophobicity after incubation with liposomes, and has a lifetime decay value of approximately 5 ns. Also, the PFO-L203C residue (corresponding to the M-V232C reside) experiences a change to a more polar environment with liposome interaction. (The residue S190C of PFO, homologous to M-R219C was not tested for membrane-insertion.) Comparing these results to those obtained for the oligomeric species, the SDO-V232C-NBD

Table 4.3 Haemolytic Activities of Mutant Monomers and SDO. The concentrations needed of monomer and SDO, recorded in ng/mL were determined at 50% haemolysis for each sample. The concentration to achieve 50% haemolysis for monomeric wild type PLO is 400 ng/mL, and 1250 ng/mL for wild type PLO in SDO form. The values are reported as averages of two independent experiments.

TMH 1			TMH 2		
Mutant	Monomer	SDO	Mutant	Monomer	SDO
R219C	220	6600	F327C	ND	ND
K231C	425	1300	K328C	910	1400
V232C	220	780	A329C	120	400
			K330C	2600	6800
			F331C	230	1500

sample also shows a decrease in fluorescence intensity and decrease in decay lifetime, yet the extent of the changes are smaller than with the monomeric toxin.

For the samples that exhibit membrane-insertion behaviour, the membrane-bound SDO-R219C-NBD and SDO-K231C-NBD both display an increase in NBD fluorescence intensity over the unbound soluble forms, although to a considerably smaller extent than that seen with the monomeric toxins. The monomeric M-R219C-NBD toxin exhibits an increase in fluorescence intensity of a factor 2.5 when in membrane-bound form over the soluble toxin, whereas the membrane-bound SDO-R219C-NBD species yields a 1.5-fold increase compared to soluble SDO. In a similar fashion, the monomeric M-K231C-NBD gives a three-fold increase in fluorescence of membrane-bound toxin over soluble form, while the same SDO sample gives only an increase of 2. In addition to this, the increases in lifetime values are not as high as with the monomeric toxin. Table 4.4 summarizes the fluorescence decay values obtained for the TMH1 monomeric and SDO toxins.[2]

The differences seen in the time resolved and steady state fluorescence data suggest that only a fraction of the SDO complexes insert into the membrane or undergo the conformational changes necessary to introduce the NBD label into the same environment as seen with monomeric toxin.

[2]Please refer to Tables A.5, A.6 and A.7 for the fit parameters for R219C, K231C and V232C, respectively.

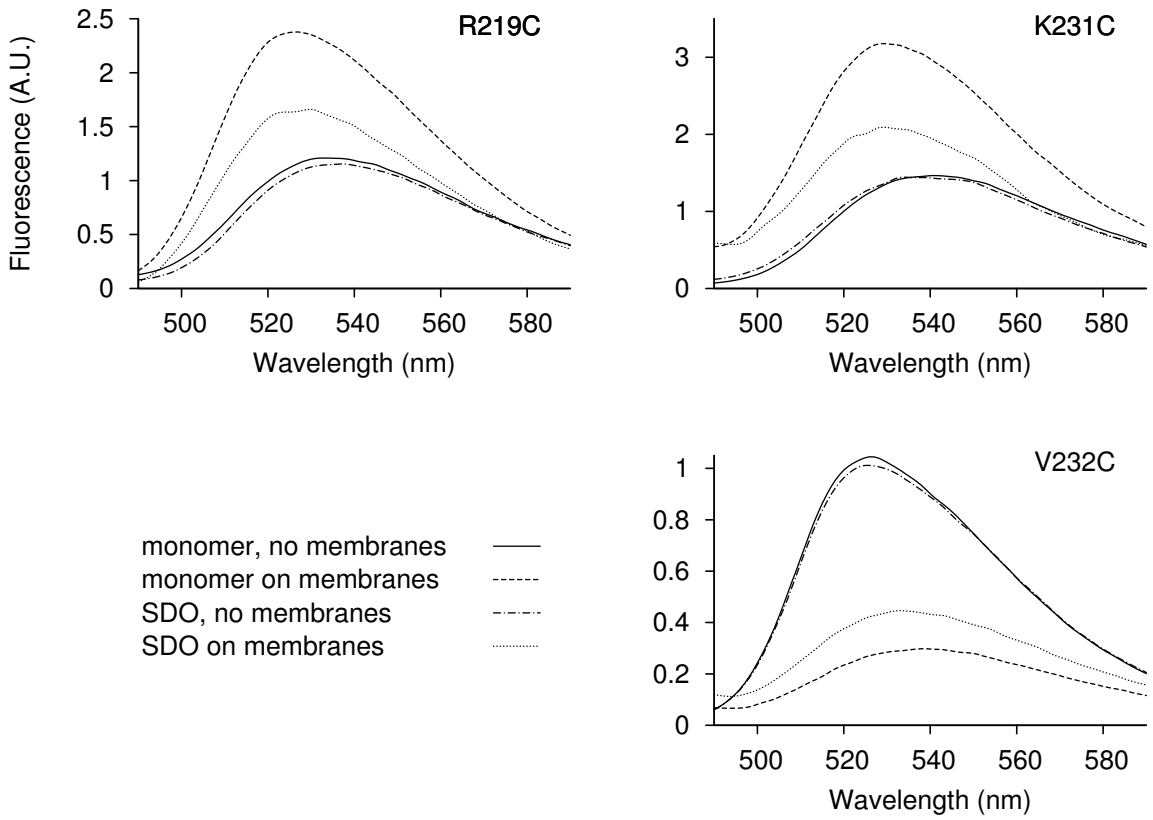

Figure 4.4 Fluorescence emission spectra of NBD-labelled PLO mutants in TMH 1, as monomers and as SDOs, in solution and after incubation with erythrocyte membrane ghosts. With each mutant, the amounts of monomer and SDO were normalized to the same amount of NBD label. The spectra of the membrane-bound samples were corrected for incomplete binding as described in section 2.2.5 on page 24.

Table 4.4 Fluorescence lifetimes of membrane-bound and -unbound NBD-labelled TMH1 mutants in monomeric and SDO form. Average lifetimes were calculated from 3 fitted exponential components, and are given in nanoseconds. The fluorescence lifetime decay analysis of transmembrane β-hairpin 1 residues show that the difference between soluble- and membrane-bound toxin is much less for the SDO complexes than for monomeric toxins. The average values of two sets of independent tests results are reported.

Mutant	Monomer	Monomer on Membranes	SDO	SDO on Membranes
R219C	1.2	2.6	1.2	1.7
K231C	2.3	4.0	2.4	2.9
V232C	3.4	1.6	3.3	1.7

Table 4.5 Lifetime values for soluble and membrane-bound TMH2 mutants in monomeric and SDO form. As with the TMH1 lifetimes, average lifetimes (in nanoseconds) were calculated from 3 fitted exponential components. The fluorescence lifetime decay analysis of transmembrane β-hairpin 2 residues also show a greater difference between soluble- and membrane-bound in monomeric toxin than for SDO complexes. The average values of two sets of independent tests results are reported.

Mutant	Monomer	Monomer on Membranes	SDO	SDO on Membranes
K328C	2.2	1.3	2.0	1.7
A329C	2.1	6.6	2.1	4.0
K330C	1.8	2.8	1.4	1.3
F331C	4.2	3.5	3.8	2.6

Transmembrane β-hairpin 2 Membrane Insertion Patterns. Turning attention to the residues contained in the second transmembrane β-hairpin or TMH2, the NBD intensity of monomeric M-K328C-NBD decreases significantly upon membrane binding, indicative of movement into an environment of greater polarity. The intensity of the M-F331C-NBD sample also decreased with membrane binding. However, the NBD intensity of M-A329C-NBD and M-K330C-NBD increase with membrane interaction. In addition to this, these latter two proteins experienced a considerable increase in fluorescence lifetime was observed, consistent with the observation of movement into an area of greater non-polarity, such as into a lipid bilayer. Comparing these observations with the oligomeric counterparts, SDO-A329C-NBD and SDO-K330C-NBD gave greater NBD intensity and fluorescence lifetime measurements when bound to membrane than the soluble form, but to a lesser extent than that seen with the monomeric counterparts. SDO-F331C-NBD gave a greater decrease in NBD intensity and lifetime than that seen for the monomeric M-F331C-NBD sample, which contrasts with the observation of the SDO-K328C-NBD sample where the NBD intensity and lifetime values decreased to a lesser extent than the monomeric M-K328C-NBD sample. The steady state spectra for the THM2 mutants with and without membranes for the monomeric and SDO species are illustrated in Figure 4.5, and Table 4.5 summarizes the lifetimes obtained for the TMH2 residues.[3]

[3]Please refer to Tables A.8, A.9, A.10 and A.11 for the fit parameters for K328C, A329C, K330C and F331C, respectively.

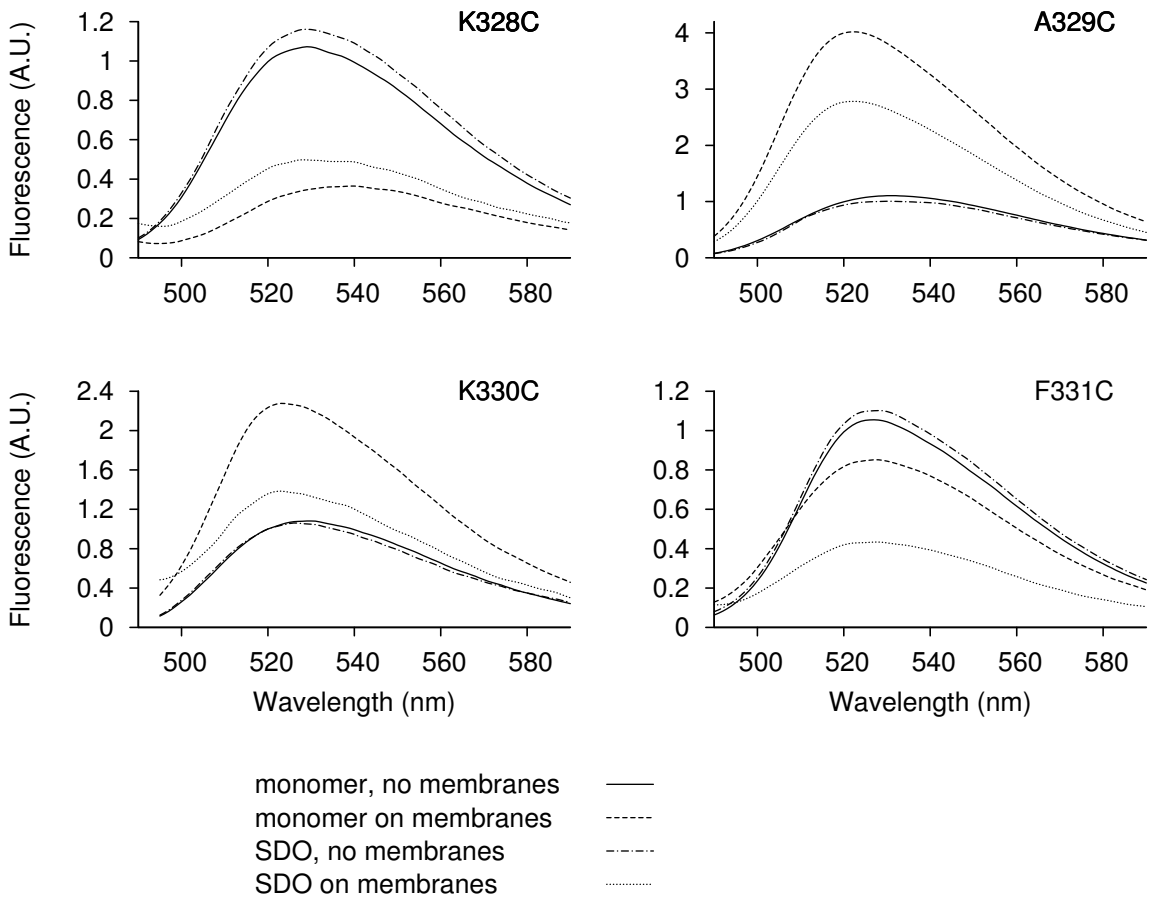

Figure 4.5 Fluorescence emission spectra of NBD-labelled PLO mutants in TMH 2, as monomers and as SDOs, in solution and after incubation with erythrocyte membrane ghosts. With each mutant, the amounts of monomer and SDO were normalized to the same amount of NBD label. The spectra of the membrane-bound samples were corrected for incomplete binding as described in section 2.2.5 on page 24.

4.3.6 Quenching of NBD Fluorescence of Membrane-Inserted Residues

The above fluorescence analyses provide valuable insight into the mechanism of membrane insertion of the SDO as compared to the monomeric toxin, especially with respect to the change in environment the NBD probe experiences upon membrane binding and insertion. In the present study, fluorescence quenching experiments were conducted to further examine the reduced degree of membrane insertion of the SDO compared to monomeric toxin.

Fluorescence quenching tests were done using the spin-labelled hydrophobic quencher, doxyl stearic acid (DSA), which binds to the lipid bilayers of cellular membranes. DSA is labelled with a nitroxide moiety, which is known to be an effective quencher of NBD fluorescence

[20]. Here, both 5- and 16-DSA were used to determine the accessibility of the NBD-labelled SDO to the quencher. The difference between the two reagents is only the positioning of the NO group on the stearic acid acyl chain, where it is positioned on the C_5 carbon in 5-DSA, and on C_{16} in 16-DSA. Samples readily quenched by 5-DSA suggest that the NBD probe is located close to the C_5 of the acyl chain of the stearic acid, while fluorescence intensity that is well-quenched by 16-DSA implies that the NBD probe is close to the C_{16} of the acyl chain. These different reagents have been used in past studies to determine the depth of residue penetration into the membrane bilayer, where 5-DSA quenching may indicate that the NBD fluorophore is found close to the surface of the bilayer, while efficient quenching by 16-DSA would signify a positioning found deeper within the membrane core. However, as it is difficult to determine if the two forms of doxyl strearic acid have the same binding or ability to integrate into membranes, the use of these two reagents cannot yield an exact position of the NBD probe and can only be used for relative measurements.

The effect of increasing quencher concentration on NBD fluorescence can be seen in Figure 4.6. Here, decrease in monomer fluorescence is greater than that for SDO for both 5- and 16-DSA. The fluorescence data for the NBD-labelled monomeric and SDO PLO were also plotted according to the Stern-Volmer equation for collisional quenching (see equation 4.1 on page 59). The Stern-Volmer quenching constant is found from the slope of the plot. A linear plot is expected if all fluorophore molecules are equally accessible to the quencher. However, for almost all PLO mutants tested in both monomeric and SDO forms, a curved Stern Volmer plot was obtained, indicative of two (or more) classes of fluorophores present in the sample each with different accessibility to the quencher. The Stern Volmer quenching plots for M-K231C-NBD and the SDO-K231C-NBD are illustrated in Figure 4.7.

In such cases, the quenching constants must be determined by alternative methods. Referring to equation 4.2, both the kinetic quenching constants k_a and the quenchable fraction of sample intensity, f_q may be determined by fitting the parameters of the equation to experimental data.

For all samples quenching efficiency was considerably greater for both the monomeric and SDO forms for 5-DSA than for the 16-DSA quencher, except for K328C which could not be fitted. Looking at the fraction of quenchable sample, f_q, 5-DSA consistently yields a higher value for both monomer and SDO than does the 16-DSA (although A329C shows only slightly greater accessibility in monomeric form than SDO complexes).

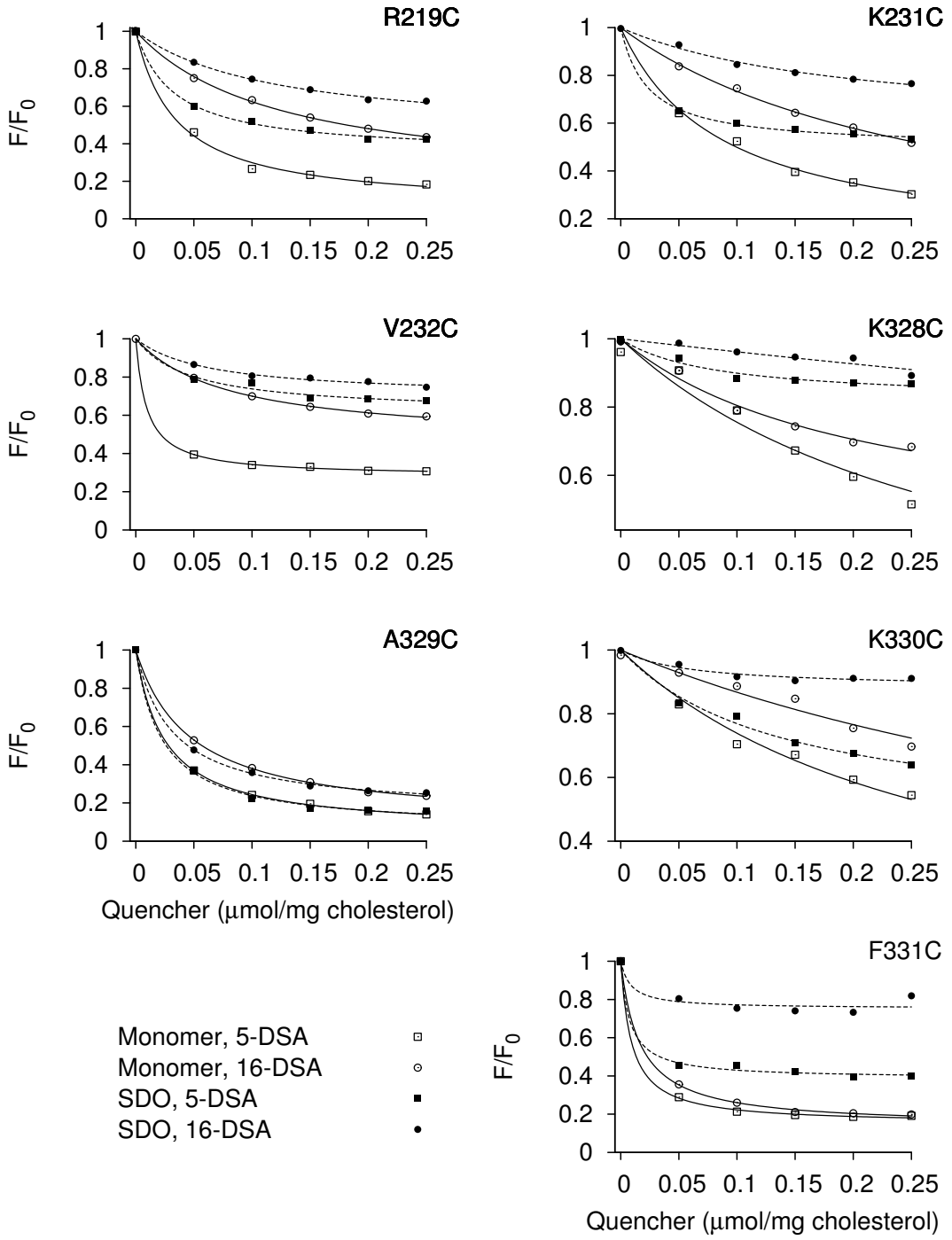

Figure 4.6 The effect of increasing concentrations of doxyl stearic acid on NBD fluorescence intensity. Both 5- and 16-doxyl stearic acid (DSA) were used to quench NBD fluorescence of monomeric and SDO complexes.

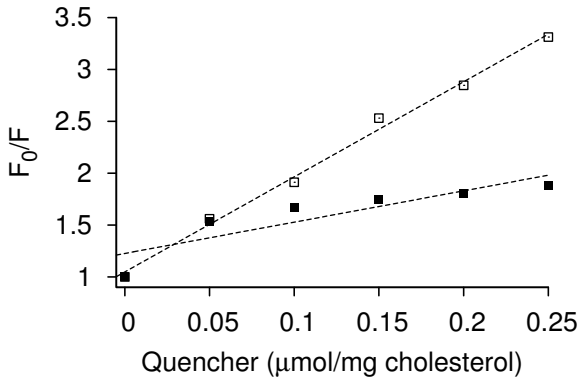

Figure 4.7 Stern-Volmer plot of mutant K231C NBD-labelled monomers (hollow squares) and SDO (solid squares), bound to membranes and quenched by 5-doxylstearate. The straight lines represent linear regression fits.

The values obtained for the quenching constant k_a, however, are surprising and much different than that expected. For mutants R219C, K231C, A329C and K330C, the quenching constants for the SDO were shown to be greater than that of the monomeric forms, although with two samples, K231C monomer quenched with 16-DSA and K330C monomer quenched with both 5- and 16-DSA, meaningful values of k_a could only be determined when fixing the f_q values for the monomeric samples to 1. Table 4.6 lists the quenching constants and the fraction of accessible fluorophores to both 5-DSA and 16-DSA for all monomeric and SDO samples.

Table 4.6 Quenching constants (k_a) and quenchable fractions (f_q) of NBD-labelled mutants by 5-DSA and 16-DSA, bound to membranes. These parameters were obtained from the fits illustrated in Figure 4.6. Where f_q is given as 1^*, the actual fit produced a value of greater than 1. In those cases, f_q was fixed at 1, and the fit was repeated to obtain the given value of k_a.

Mutant		5-DSA		16-DSA	
		Monomer	SDO	Monomer	SDO
R219C	f_{acc}	0.94	0.84	0.65	0.56
	k_a	29.1	8.1	30.7	8.4
K231C	f_{acc}	0.93	1*	0.50	0.43
	k_a	11.6	3.6	43.3	5.0
V232C	f_{acc}	0.72	0.55	0.39	0.31
	k_a	107.1	12.2	20.9	15.8
K328C	ND	ND	ND	ND	ND
A329C	f_{acc}	0.95	0.91	0.94	0.85
	k_a	39.9	21.5	44.0	32.2
K330C	f_{acc}	1*	1*	0.56	0.12
	k_a	3.5	1.5	7.1	17.2
F331C	f_{acc}	0.93	0.50	1 *	0.42
	k_a	11.6	43.3	3.63	5.0

4.4 DISCUSSION

The solution-derived oligomeric complexes of PLO were found to retain haemolytic activity of approximately one-quarter to one-third that of the toxin in monomeric form. This was an unexpected discovery as the oligomeric complexes of other CDC family members are believed to lose haemolytic activity upon their formation [39].

This feature of PLO prompted the current study to determine the pore-forming mechanism of SDO-PLO, and to ascertain if it is similar to the pore-forming mechanism of the monomeric toxin. In the current study, the pore-forming activity of SDO-PLO was examined by analyzing the membrane insertion of key residues in the trans-membrane hairpin regions of domain 3 of PLO.

Using the environmentally sensitive fluorophore NBD, steady-state and time-resolved fluorescence experiments were conducted for mutated residues in the monomeric form before and after incubation with membranes, and the tests repeated for the SDO complexes. The steady state fluorescence intensity of the NBD revealed that, in general, SDO bound to the membrane approximately 30% less efficiently than the monomeric toxins. The change in NBD emission intensity and excited state lifetimes show that the same residues insert into the membrane for both the monomeric and SDO forms. However, the extent of change in intensity and lifetime was much greater for the monomeric toxin than for the oligomer when membrane-insertion occurred; this was especially pronounced in the K231C residue of TMH1 and the A329C residue of TMH2. This finding suggests that only a fraction of the toxin molecules found within the SDO unit are able to insert into the membrane. This is supported by hydrophobic quenching analysis, where monomeric samples were quenched to a larger extent than SDO.

Comparing the two different fluorescence methods, the results of the steady state tests are in good agreement with those obtained for the time resolved experiments, where the change or ratio in the observed steady state intensity between soluble and membrane-bound toxin equaled that seen for the decay values. For both methods, average values are obtained. For the steady state spectra, the observed intensity is the average of the labelled toxins that have inserted into the membrane and those that remain uninserted. Likewise, for the time-resolved analyses, a three-component model is used where the individual lifetimes are averaged to obtain the final fluorescence decay value. In past studies, researchers have attempted to determine physical meaning to each lifetime in order to assign the percentage of the fluorophore found in different environments [105]. However, this is not possible in the current study, as NBD alone in aqueous

solution (with no toxin or membrane) gives a tri-exponential decay. As such, no physical meaning can be assigned to each of the individual lifetimes, and therefore average lifetimes must be used.

Qualitatively, the fluorescence analyses correspond well with the observed decrease in haemolytic activity of the SDO. With the results of the fluorescence analysis, the weakening of the SDO lytic ability may be attributed to two causes: poor binding efficiency of the SDO compared to monomeric toxin, and incomplete insertion of the SDO toxin into the membrane. This also coincides with the results of the quenching experiments, where it was found that the quenchable fraction of monomeric toxin is greater than that of the SDO samples. It is, however, difficult to quantitatively compare the results of the fluorescence and quenching experiments to that of the haemolytic assays, as the values obtained depend on the NBD intensity emitted. As the quantum yield of the fluorophore is greater when in an apolar environment (such as within the lipid bilayer), the intensity of the NBD observed does not quantitatively match the actual fraction of toxin inserted into the membrane. Therefore, no direct correlation between the observed haemolytic activity and the results of the fluorescence and quenching experiments can be obtained.

Previous studies on PLO-SDO have shown that the SDO subunits do not break apart upon membrane binding and form pores with other individual PLO monomeric toxin molecules [27]. FRET analysis showed that little change in donor fluorescence emission occurred with the presence of SDO labelled with a suitable acceptor fluorophore, as compared to the intensity of the donor fluorophore alone. In addition to this, circular dichroism was employed to show that the conformation of the SDO-PLO was much more similar to that of unbound, monomeric PLO than to that of the membrane-bound toxin [27]. These results, combined with the findings of the NBD-fluorescence tests, suggest that a fraction of SDO units retain the ability to bind, and undergo the necessary conformational changes to insert into the membrane bilayer, while the remainder of the SDO complexes may stay trapped in the pre-pore conformation on the surface and are unable to insert.

The self-association of CDC toxin has been known for many years. For monomeric toxins, it has been historically believed that interaction with a cholesterol-containing membrane was necessary in order for the required conformational changes that initiate oligomerization to occur. In fact, in the case of three toxins, cereolysin, PFO and SLO, it was originally speculated that such aggregation was due to sample contamination by cholesterol, or the aggregation was an artifact as a result of the preparation procedures to ready the samples for electron mi-

croscopy analysis [10]. PFO self-oligomerization has been analysed to some extent, and the PFO aggregation may in fact be a result of cholesterol contamination. Other studies involving PFO at very high protein concentrations (>10 $^{mg}/_{mL}$) have shown that PFO does not possess the ability to form oligomeric species in solution of any considerable size [95]. Instead, only an anti-parallel dimer form has been observed upon careful analyses [98]. It was postulated that this positions the individual monomers in such a way that blocks key sites in the protein from further intermolecular interaction that would result in aggregate growth of a significant size [95, 39].

This, however does not seem to be the case for the CDC pneumolysin (PLY). In studies using small angle neutron scattering and analytical centrifugation [37], it was found that PLY forms complexes readily in solution at moderate (1 mg/mL) to low (0.4 mg/mL) concentrations [39, 107], and the weak intermolecular interactions between the monomers initially form dimeric species, and then rapidly add monomers to yield oligomers of many subunits [37]. At higher concentrations, PLY can form helical structures in solution, having approximately 41 subunits per turn [36].

Also, analytical centrifugation tests conducted on PLY aggregates suggest that the oligomers take on a side-by-side orientation, as opposed to an end-to-end configuration [37]. In these experiments, an increase in the sedimentation coefficient (R_g) was observed with increasing molecular weight of the aggregate species, meaning that a large increase in mass resulted in a small increase in size. It was reasoned that if an end-to-end structure resulted from the aggregate formation, a considerable increase in size would occur, and the corresponding increase in frictional forces would result in a very small increase in R_g, if any, thereby slowing the rate of sedimentation. Considering the activity of PLO, and the fact that the conformation of the individual toxin subunits of unbound, soluble SDO complexes is similar to that of the soluble monomeric toxin as determined by circular dichroism experiments, PLO-SDO quite possibly adopts a similar side-to-side orientation as seen with PLY.

In summary, an unusual property of PLO has been investigated. The spontaneously-derived oligomers of pyolysin have been analysed by several fluorescence techniques to supplement previous investigations on CDC aggregates and SDO behaviour and properties. The novel finding that the SDO of PLO retain some of the haemolytic activity of monomeric PLO may be attributed by the discovery that only a fraction of the proteins that make up the SDO insert into the membrane after binding, while the remaining portion of these proteins remain unable

to insert into the lipid bilayer. These results may provide further insight into the many ways CDCs are able to form functional pores.

Chapter 5

Summary

The Cholesterol-Dependent Cytolysins (CDCs) are a large family of toxins expressed by approximately 30 species of Gram-positive bacteria. Important members of this group include listeriolysin (LLO) from *Listeria monocytogenes*, streptolysin O (SLO) from *Streptococcus pyogenes*, and perfringolysin O (PFO) from *Clostridium perfringens*. As these toxins play an important role in the pathogenic mechanism of the organisms that produce them, there is much interest in their characterization and mode of action. The three-dimensional crystal structure has been determined for a number of CDCs, and based on the similarity of these structures and the sequence homology and identity of the entire group of toxins, it can be confidently assumed that all CDCs share a common architecture.

The common architecture of the CDCs translates into similarities in their function. As their name suggests, CDC activity is dependent on the presence of cholesterol in the target membrane, and is thought that for all CDCs the C-terminal domain, or domain 4, is responsible for membrane recognition and binding. After binding, the molecules diffuse laterally on the membrane surface, and upon encountering one another begin the oligomerization process. Oligomerization allows adjacent molecules to align TMHs which allows for their insertion into the membrane. How far along the oligomerization process goes before insertion occurs, however, has been the topic of some debate. One theory postulates that a complete, ring-shaped oligomer is formed before membrane insertion could occur, but this does not account for the presence

of arc-shapes on membrane surfaces and the possibility of these incomplete oligomers to form viable pores. To account for this, another theory suggests that oligomerization does not need to be completed prior to membrane insertion.

Pyolysin (PLO) is a CDC secreted by the bacterial pathogen *Arcanobacterium pyogenes*. First discovered in 1996, PLO is considered a relative new-comer to the CDC family, and as such, little is known about its structure-function relationship. Among all CDCs, pyolysin has the lowest degree of sequence homology relative to the group as a whole. The question therefore arises how much similarity it retains in term of structure and function. Several aspects of the molecular function of pyolysin were addressed in this study. In particular, the role of domain 4 in the oligomerization process, the cooperativity of membrane insertion, and the pore-forming ability of oligomers that have been pre-formed in solution were examined. With this work, a better understanding of the different ways CDCs can work to damage membranes can be achieved.

5.1 DOMAIN 4 OF PYOLYSIN AND OLIGOMERIZATION

Domain 4 (D4) has previously been considered to be responsible only for membrane recognition and binding via a surface receptor, with little evidence to suggest a role in toxin oligomerization [120]. In the present study, however, domain 4 of pyolysin is shown to have a distinctly greater role in the oligomerization process. Pyolysin D4 acts to *enhance*, not inhibit the haemolytic activity of wild type PLO. Since D4 itself remains devoid of haemolytic activity, it must be able to not only associate with wild type toxin but also trigger functionally relevant conformational changes within the latter. Interestingly, the amplification of wild type haemolytic acitivity by D4 was found to be saturable and limited by the amount of wild type toxin present. This suggests that one wild type toxin molecule can productively interact with only a few, or even only one, D4 molecule. In a previous study, the haemolysis of SLO was found to be kinetically limited by an initial step of second order, which was followed by a much more rapid and facile serial polymerization [88]. A possible explanation for the saturable activation by D4 is that it functions in the initial step, which likely involves only two or three molecules, and that at least one of the other partners must remain a wild type molecule, which would subsequently recruit other wild type molecules to form a functional pore. Such a preference of wild type molecules for one another, even in the presence of D4 in excess, is consistent with both EM and fluorescence data.

In addition to this, D4 of PLO is able to self-associate, a feature not seen in other CDCs. This is seen with the electron microscopy images of D4 alone, where distinct oligomers in the form of linear rods were observed on crystalline cholesterol surfaces. EM images of mixtures of D4 and WT also gave images of 'horseshoe' and 'walking-cane' formations, the likes of which have not been observed with any other CDC.

In previous studies on PFO and SLO [114, 120], the C-terminal region was shown to inhibit the haemolytic activity of wild type toxin, where a complex was formed that ceased the oligomerization from forming an active pore. In addition to this, little evidence showing the D4 fragments could form was seen. It was postulated that as each oligomer subunit must contain two separate oligomerization interfaces to allow interaction with the two adjacent molecules, it was proposed that the C-terminal fragments of PFO and SLO would retain only one site of interaction. This would allow the fragment to associate with a growing oligomer, but further growth would be prevented.

These results suggest that PLO-D4, unlike the domains 4 of PFO and SLO, may contain the two sites necessary to promote the oligomerization process. The difference is surprising, considering the similarity of the domains 4 of the three CDCs, in length and primary structure. The difference in the functionality of PLO-D4 may be explained by considering that slight differences in primary structure may translate to more significant differences in secondary structure, or differ in the extent of conformational changes experienced by domain 4 that are conferred to the upper regions of the CDC molecule. Alternatively, the secondary structure may be preserved, but a greater mutual affinity may exist between PLO D4 fragments due to a few more favourably matched amino acid side chains. Fluorescence tests conducted on the domains 4 of the three CDCs may help determine differences in the nature of the conformational change in D4 that occurs upon membrane binding. It would also be beneficial to determine the X-ray crystal structure of PLO to be able to directly visualize differences in secondary structure that would account for the ability for the domain 4 of PLO to play a more profound role in the oligomerization process than originally believed. Absent such a structure, chimeric molecules or site-directed mutagenesis should be able to provide further insight.

5.2 PARTIAL OLIGOMERIZATION INDUCED BY A DISULPHIDE TETHERED MUTANT OF PYOLYSIN

Little research has been conducted on CDCs to determine the extent of the cooperativity of the membrane insertion step, which occurs after the oligomeric pre-pore has been assembled. In this study, this problem has been addressed by designing a mutant that does not have the ability to insert into the membrane, and monitoring its effects on the activity of wild type PLO. As domains 2 and 3 are packed tightly together in the monomeric conformation, they must first uncouple before membrane insertion can occur. It was postulated that a disulphide bridge linking domain 2 to the beginning of the first transmembrane hairpin in domain 3 would prevent membrane insertion. Mutations were made by replacing cysteine for the glycine residue at the 85 position of domain 2, and the arginine residue at the 219 position of domain 3.

This mutant showed no haemolytic activity, and it was also incapable of self-oligomerization; however, it was found to form hybrid oligomers with wild type PLO quite effectively. Formation of such hybrid oligomers inhibited the membrane insertion and pore-formation by wild type toxin in a dose-dependent manner, such that activity was significantly reduced with an equimolar mixture of the two toxin species, and fully suppressed by a tenfold excess. This extent of inhibition fall in between those expected for the two theoretically possible extremes, namely a fully cooperative membrane insertion, in which case even a small fraction of the deficient mutant should prevent it, and a fully un-cooperative insertion, in which case insertion and activity of wild type toxin should persist unchanged regardless of the presence of the disulfide mutant. This conclusion was confirmed by fluorescence measurements on the extent of PLO-DS on the membrane insertion of functional PLO molecules in hybrid oligomers. Residues in both TMH1 and TMH2 showd some degree of membrane insertion with a two-fold molar excess of PLO-DS, but significantly less insertion was achieved compared to active toxin alone. This suggests that membrane-insertion is *partially cooperative*, meaning that it requires cooperation of several, but not all subunits within the oligomer.

PLO-DS, at high concentration, also significantly reduced the size of hybrid oligomers. Osmotic protection experiments on these oligomers confirmed the previously reached conclusion [86] that incomplete, arc-shaped CDC oligomers can indeed form functional pores.

A study on the homologous disulphide mutant of PFO gave surprisingly different results [49]. The disulphide bridge formed between residues homologous to those used for PLO allowed for self-association, and EM images showed ring- and arc-formations on membrane

surfaces similar to that seen with wild type PFO. This disulphide bond worked to trap the toxin in the pre-pore state, leaving it unable to insert into the membrane. In contrast, the similar bond in PLO caused limitations at the oligomerization step. Why this difference occurs may be determined by tests done on active pyolysin to determine the points of contact within domains 2 and 3 between adjacent monomers. In this way, the manner in which the disulphide mutant prevents oligomerization in pyolysin may be deciphered.

5.3 PORE FORMATION PROPERTIES OF SOLUTION-DERIVED OLIGOMERS OF PYOLYSIN

The oligomerization step in the CDC pore-forming mechanism was historically believed to only occur on a membrane surface. But as seen with several CDC members, toxin oligomerization can occur spontaneously in solution at higher protein concentrations. Most of these solution-derived oligomers (SDO) lose their haemolytic activity, yet the SDO from PLO retain approximately one-quarter of the activity obtained from monomeric PLO.

Tests have shown that PLO-SDO binds to membranes less efficiently than monomeric toxin, where SDO binding was shown to be approximately 30% less than that of monomeric PLO. Considering that the SDO haemolytic activity is only 25% that of monomeric toxin, other factors must be involved to account for this difference; it was speculated that the SDO complex may be limited in its ability to insert into the membrane. This hypothesis was tested by monitoring the change in fluorescence intensity of key NBD-labelled membrane-inserting residues of the SDO complex in the presence and absence of membranes, and comparing this with the results obtained from monomeric PLO.

For almost all residues tested, the change in NBD intensity for SDO going from the soluble to membrane-bound state was less than that seen for monomeric PLO. This effect was especially prominent for the TMH1 residue K231C and the TMH2 residue A329C where for the monomeric toxin, the NBD intensity increased greatly with the presence of membranes, while the NBD intensity of the SDO showed only a moderate increase. This suggests that only a fraction of the SDO complexes retain the ability to insert into the membrane. Two scenarios could result in this observation – either all SDO units insert partially into the membrane to the same degree or some oligomers derived by SDO complexes retain the ability to insert into the membrane while others remain inactive on the membrane surface. To test which case is the more plausible, quenching tests using a lipophilic spin-labelled quenching reagent were

conducted. Although the resulting Stern-Volmer curved for the membrane-inserted oligomers derived from monomeric PLO were mostly linear, the plots for the SDO complexes curved toward the x-axis, indicating that more than one class of fluorophore was present in the sample. The quenching data fit reasonably well with a two-site model of fluorophore-quencher accessibility for the SDO samples. Therefore, this evidence supports the view that the reduction in SDO activity is due to the decrease in binding efficiency, and the limited ability of the SDO to insert into the membrane.

This research illustrates that even though there is a great deal of similarity between all CDCs, models of their pore formation and activity have been based on the studies of only a select few. It seems that as more CDCs are discovered, the more changes that need to be made to the model of CDC pore-forming mechanism. This information would be of great value in expanding our breadth of knowledge about CDCs and would help expand on the models that are currently used to describe their mode of action.

Bibliography

[1] J. Alouf and M. Palmer. *"Streptolysin O" in The Comprehensive Soucebook of Bacterial Protein Toxins, Second Edition*. Academic Press, 1999.

[2] J. E. Alouf. Pore-forming bacterial protein toxins: an overview. *Curr Top Microbiol Immunol*, 257:1–14, 2001.

[3] J. E. Alouf. Molecular features of the cytolytic pore-forming bacterial protein toxins. *Folia Microbiol (Praha)*, 48(1):5–16, 2003.

[4] C. Alouf J.E., Geoffroy. Comparative effects of cholesterol and thiocholesterol on streptolysin o. *FEMS Microbiol Lett*, 6:413–16, 1979.

[5] J. B. Alouf J.E., Billington S.J. *"Repertoire and General Features of the Family of Cholesterol-Dependent Cytolysins" in The Comprehensive Soucebook of Bacterial Protein Toxins*. Academic Press, Third Edition, 2006.

[6] C. R. Alving, W. H. Habig, K. A. Urban, and M. C. Hardegree. Cholesterol-dependent tetanolysin damage to liposomes. *Biochim Biophys Acta*, 551(1):224–228, Feb 1979.

[7] J. Arbuthnott. *Bacterial Cytolysins (Membrane-Damaging Toxins)*. Elsevier, 1982.

[8] K. E. Beauregard, K. D. Lee, R. J. Collier, and J. A. Swanson. ph-dependent perforation of macrophage phagosomes by listeriolysin o from listeria monocytogenes. *J Exp Med*, 186(7):1159–1163, Oct 1997.

[9] S. Bhakdi, M. Roth, A. Sziegoleit, and J. Tranum-Jensen. Isolation and identification of two hemolytic forms of streptolysin-o. *Infect Immun*, 46(2):394–400, Nov 1984.

[10] S. Bhakdi and J. Tranum-Jensen. Damage to cell membranes by pore-forming bacterial cytolysins. *Prog Allergy*, 40:1–43, 1988.

[11] S. Bhakdi, J. Tranum-Jensen, and A. Sziegoleit. Mechanism of membrane damage by streptolysin-o. *Infect Immun*, 47(1):52–60, Jan 1985.

[12] S. J. Billington, B. H. Jost, W. A. Cuevas, K. R. Bright, and J. G. Songer. The arcanobacterium (actinomyces) pyogenes hemolysin, pyolysin, is a novel member of the thiol-activated cytolysin family. *J Bacteriol*, 179(19):6100–6106, Oct 1997.

[13] S. J. Billington, B. H. Jost, and J. G. Songer. Thiol-activated cytolysins: structure, function and role in pathogenesis. *FEMS Microbiol Lett*, 182(2):197–205, Jan 2000.

[14] S. J. Billington, K. W. Post, and B. H. Jost. Isolation of arcanobacterium (actinomyces) pyogenes from cases of feline otitis externa and canine cystitis. *J Vet Diagn Invest*, 14(2):159–162, Mar 2002.

[15] S. J. Billington, J. G. Songer, and B. H. Jost. Molecular characterization of the pore-forming toxin, pyolysin, a major virulence determinant of arcanobacterium pyogenes. *Vet Microbiol*, 82(3):261–274, Sep 2001.

[16] S. J. Billington, J. G. Songer, and B. H. Jost. The variant undecapeptide sequence of the arcanobacterium pyogenes haemolysin, pyolysin, is required for full cytolytic activity. *Microbiology*, 148(Pt 12):3947–3954, Dec 2002.

[17] R. W. Bourdeau, E. Malito, A. Chenal, B. L. Bishop, M. W. Musch, M. L. Villereal, E. B. Chang, E. M. Mosser, R. F. Rest, and W.-J. Tang. Cellular functions and x-ray structure of anthrolysin o, a cholesterol-dependent cytolysin secreted by bacillus anthracis. *J Biol Chem*, 284(21):14645–14656, May 2009.

[18] J. Buckley. *"The Channel-forming Toxin Aerolysin", in 'The Comprehensive Soucebook of Bacterial Protein Toxins, Second Edition*. Academic Press, 1999.

[19] A. Chattopadhyay. Chemistry and biology of n-(7-nitrobenz-2-oxa-1,3-diazol-4-yl)-labeled lipids: fluorescent probes of biological and model membranes. *Chem Phys Lipids*, 53(1):1–15, Mar 1990.

[20] A. Chattopadhyay and E. London. Parallax method for direct measurement of membrane penetration depth utilizing fluorescence quenching by spin-labeled phospholipids. *Biochemistry*, 26(1):39–45, Jan 1987.

[21] J. L. Cowell, K. S. Kim, and A. W. Bernheimer. Alteration by cereolysin of the structure of cholesterol-containing membranes. *Biochim Biophys Acta*, 507(2):230–241, Feb 1978.

[22] K. S. Crowley, G. D. Reinhart, and A. E. Johnson. The signal sequence moves through a ribosomal tunnel into a noncytoplasmic aqueous environment at the er membrane early in translocation. *Cell*, 73(6):1101–1115, Jun 1993.

[23] D. M. Czajkowsky, E. M. Hotze, Z. Shao, and R. K. Tweten. Vertical collapse of a cytolysin prepore moves its transmembrane beta-hairpins to the membrane. *EMBO J*, 23(16):3206–3215, Aug 2004.

[24] A. L. Decatur and D. A. Portnoy. A pest-like sequence in listeriolysin o essential for listeria monocytogenes pathogenicity. *Science*, 290(5493):992–995, Nov 2000.

[25] H. Ding and C. Lämmler. Purification and further characterization of a haemolysin of actinomyces pyogenes. *Zentralbl Veterinarmed B*, 43(3):179–188, May 1996.

[26] J. L. Duncan and R. Schlegel. Effect of streptolysin o on erythrocyte membranes, liposomes, and lipid dispersions. a protein-cholesterol interaction. *J Cell Biol*, 67(1):160–174, Oct 1975.

[27] W. el Huneidi. Functional characterization of arcanobacterium pyogenes pyolysin in oligomeric form, and the binding of camp factor to igg. Master's thesis, Department of Chemistry, University of Waterloo, Waterloo ON, 2007.

[28] A. J. Farrand, S. LaChapelle, E. M. Hotze, A. E. Johnson, and R. K. Tweten. Only two amino acids are essential for cytolytic toxin recognition of cholesterol at the membrane surface. *Proc Natl Acad Sci U S A*, 107(9):4341–4346, Mar 2010.

[29] S. C. H. H. Fehrenbach, F.J. Early and long events in streptolysin o-inducing haemolysis. *Toxicon*, 20:233–8, 1982.

[30] J. J. Flanagan, R. K. Tweten, A. E. Johnson, and A. P. Heuck. Cholesterol exposure at the membrane surface is necessary and sufficient to trigger perfringolysin o binding. *Biochemistry*, 48(18):3977–3987, May 2009.

[31] P. G. Funk, J. J. Staats, M. Howe, T. G. Nagaraja, and M. M. Chengappa. Identification and partial characterization of an actinomyces pyogenes hemolysin. *Veterinary Microbiology*, 50(1-2):129 – 142, 1996.

[32] J. L. Gaillard, P. Berche, J. Mounier, S. . Richard, and P. Sansonetti. In vitro model of penetration and intracellular growth of listeria monocytogenes in the human enterocyte-like cell line caco-2. *Infect. Immun.*, 55(3D11):2822–2829, 1987.

[33] C. Geoffroy, J. L. Gaillard, J. E. Alouf, and P. Berche. Purification, characterization, and toxicity of the sulfhydryl-activated hemolysin listeriolysin o from listeria monocytogenes. *Infect Immun*, 55(7):1641–1646, Jul 1987.

[34] K. S. Giddings, A. E. Johnson, and R. K. Tweten. Redefining cholesterol's role in the mechanism of the cholesterol-dependent cytolysins. *Proc Natl Acad Sci U S A*, 100(20):11315–11320, Sep 2003.

[35] K. S. Giddings, J. Zhao, P. J. Sims, and R. K. Tweten. Human cd59 is a receptor for the cholesterol-dependent cytolysin intermedilysin. *Nat Struct Mol Biol*, 11(12):1173–1178, Dec 2004.

[36] R. J. Gilbert, J. L. Jiménez, S. Chen, I. J. Tickle, J. Rossjohn, M. Parker, P. W. Andrew, and H. R. Saibil. Two structural transitions in membrane pore formation by pneumolysin, the pore-forming toxin of streptococcus pneumoniae. *Cell*, 97(5):647–655, May 1999.

[37] R. J. Gilbert, J. Rossjohn, M. W. Parker, R. K. Tweten, P. J. Morgan, T. J. Mitchell, N. Errington, A. J. Rowe, P. W. Andrew, and O. Byron. Self-interaction of pneumolysin, the pore-forming protein toxin of streptococcus pneumoniae. *J Mol Biol*, 284(4):1223–1237, Dec 1998.

[38] R. J. C. Gilbert. Pore-forming toxins. *Cell Mol Life Sci*, 59(5):832–844, May 2002.

[39] R. J. C. Gilbert. Inactivation and activity of cholesterol-dependent cytolysins: what structural studies tell us. *Structure*, 13(8):1097–1106, Aug 2005.

[40] I. J. Glomski, M. M. Gedde, A. W. Tsang, J. A. Swanson, and D. A. Portnoy. The listeria monocytogenes hemolysin has an acidic ph optimum to compartmentalize activity and prevent damage to infected host cells. *J Cell Biol*, 156(6):1029–1038, Mar 2002.

[41] B. J. B. S. Gorbach, S.L. *Infectious Diseases*. W.B. Saunders Company, Toronto Canada, 1998.

[42] E. Gouaux. Channel-forming toxins: tales of transformation. *Curr Opin Struct Biol*, 7(4):566–573, Aug 1997.

[43] Harris, Adrian, Bhakdi, and Palmer. Cholesterol-streptolysin o interaction: An em study of wild-type and mutant streptolysin o. *J Struct Biol*, 121(3):343–355, 1998.

[44] R. W. Harris, P. J. Sims, and R. K. Tweten. Kinetic aspects of the aggregation of clostridium perfringens theta-toxin on erythrocyte membranes. a fluorescence energy transfer study. *J Biol Chem*, 266(11):6936–6941, Apr 1991.

[45] P. Harvey and J. Faber. Some biochemical reactions of teh listerella group. *Journal of Bacteriology*, 41:45–46, 1941.

[46] D. Herbert and E. Todd. Purification and properties of a haemolysin produced by group a streptococci (streptolysin o). *Biochemical Journal*, 35:1124–39, 1941.

[47] A. P. Heuck, E. M. Hotze, R. K. Tweten, and A. E. Johnson. Mechanism of membrane insertion of a multimeric beta-barrel protein: perfringolysin o creates a pore using ordered and coupled conformational changes. *Mol Cell*, 6(5):1233–1242, Nov 2000.

[48] A. P. Heuck, P. C. Moe, and B. B. Johnson. The cholesterol-dependent cytolysin family of gram-positive bacterial toxins. *Subcell Biochem*, 51:551–577, 2010.

[49] E. M. Hotze, E. M. Wilson-Kubalek, J. Rossjohn, M. W. Parker, A. E. Johnson, and R. K. Tweten. Arresting pore formation of a cholesterol-dependent cytolysin by disulfide trapping synchronizes the insertion of the transmembrane beta-sheet from a prepore intermediate. *J Biol Chem*, 276(11):8261–8268, Mar 2001.

[50] S. Howorka and H. Bayley. Improved protocol for high-throughput cysteine scanning mutagenesis. *Biotechniques*, 25(5):764–6, 768, 770 passim, Nov 1998.

[51] M. Ikegami, N. Hashimoto, T. Kaidoh, T. Sekizaki, and S. Takeuchi. Genetic and biochemical properties of a hemolysin (pyolysin) produced by a swine isolate of arcanobacterium (actinomyces) pyogenes. *Microbiol Immunol*, 44(1):1–7, 2000.

[52] K. Imaizumi, K. Matsunaga, H. Higuchi, T. Kaidoh, and S. Takeuchi. Effect of amino acid substitutions in the epitope regions of pyolysin from arcanobacterium pyogenes. *Vet Microbiol*, 91(2-3):205–213, Feb 2003.

[53] K. Imaizumi, A. Serizawa, N. Hashimoto, T. Kaidoh, and S. Takeuchi. Analysis of the functional domains of arcanobacterium pyogenes pyolysin using monoclonal antibodies. *Vet Microbiol*, 81(3):235–242, Aug 2001.

[54] M. Johnson. Cellular location of pneumolysin. *FEMS Microbiology Letters*, 2:243–245, 1977.

[55] M. K. Johnson, C. Geoffroy, and J. E. Alouf. Binding of cholesterol by sulfhydryl-activated cytolysins. *Infect Immun*, 27(1):97–101, Jan 1980.

[56] B. H. Jost and S. J. Billington. Arcanobacterium pyogenes: molecular pathogenesis of an animal opportunist. *Antonie Van Leeuwenhoek*, 88(2):87–102, Aug 2005.

[57] B. H. Jost, K. W. Post, J. G. Songer, and S. J. Billington. Isolation of arcanobacterium pyogenes from the porcine gastric mucosa. *Vet Res Commun*, 26(6):419–425, Aug 2002.

[58] B. H. Jost, J. G. Songer, and S. J. Billington. An arcanobacterium (actinomyces) pyogenes mutant deficient in production of the pore-forming cytolysin pyolysin has reduced virulence. *Infect Immun*, 67(4):1723–1728, Apr 1999.

[59] K. Kanclerski and R. Möllby. Production and purification of streptococcus pneumoniae hemolysin (pneumolysin). *J Clin Microbiol*, 25(2):222–225, Feb 1987.

[60] G. C. Kingdon and C. P. Sword. Effects of listeria monocytogenes hemolysin on phagocytic cells and lysosomes. *Infect Immun*, 1(4):356–362, Apr 1970.

[61] U. K. Laemmli. Cleavage of structural proteins during the assembly of the head of bacteriophage t4. *Nature*, 227(5259):680–685, Aug 1970.

[62] J. R. Lakowicz. *Principles of Fluorescence Spectroscopy, Third Edition*. Springer Scientific and Business Media, 2006.

[63] E. Libman. A pneumococcus producing a peculiar form of hemolysis. *Proceedings of the New York Pathological Society*, 5:168, 1905.

[64] R. Lovell. Studies on corynebacterium pyogenes, with special reference to toxin production. *Journal of Patholological Bacteriology*, 45:339–355, 1937.

[65] J. C. Madden, N. Ruiz, and M. Caparon. Cytolysin-mediated translocation (cmt): a functional equivalent of type iii secretion in gram-positive bacteria. *Cell*, 104(1):143–152, Jan 2001.

[66] A. Marmorek. La toxine streptococcique. *Annales de l'Institut Pasteur*, 16:169–177, 1902.

[67] M. A. Meehl and M. G. Caparon. Specificity of streptolysin o in cytolysin-mediated translocation. *Mol Microbiol*, 52(6):1665–1676, Jun 2004.

[68] T. J. Mitchell, P. W. Andrew, F. K. Saunders, A. N. Smith, and G. J. Boulnois. Complement activation and antibody binding by pneumolysin via a region of the toxin homologous to a human acute-phase protein. *Mol Microbiol*, 5(8):1883–1888, Aug 1991.

[69] K. Mitsui, Y. Saeki, and J. Hase. Effects of cholesterol evulsion on susceptibility to perfringolysin o of human erythrocytes. *Biochim Biophys Acta*, 686(2):177–181, Apr 1982.

[70] K. Mitsui, T. Sekiya, S. Okamura, Y. Nozawa, and J. Hase. Ring formation of perfringolysin o as revealed by negative stain electron microscopy. *Biochim Biophys Acta*, 558(3):307–313, Dec 1979.

[71] N. Mitsui, K. Mitsui, and J. Hase. Purification and some properties of tetanolysin. *Microbiol Immunol*, 24(7):575–584, 1980.

[72] P. J. Morgan, S. C. Hyman, O. Byron, P. W. Andrew, T. J. Mitchell, and A. J. Rowe. Modeling the bacterial protein toxin, pneumolysin, in its monomeric and oligomeric form. *J Biol Chem*, 269(41):25315–25320, Oct 1994.

[73] M. T. Morgan P.J., Andrew P.W. Thiol-activated cytolysins. *Rev. Med. Microbiol.*, 7:221–9, 1996.

[74] H. Nagamune, K. Ohkura, A. Sukeno, G. Cowan, T. J. Mitchell, W. Ito, O. Ohnishi, K. Hattori, M. Yamato, K. Hirota, Y. Miyake, T. Maeda, and H. Kourai. The human-specific action of intermedilysin, a homolog of streptolysin o, is dictated by domain 4 of the protein. *Microbiol Immunol*, 48(9):677–692, 2004.

[75] H. Nagamune, C. Ohnishi, A. Katsuura, K. Fushitani, R. A. Whiley, A. Tsuji, and Y. Matsuda. Intermedilysin, a novel cytotoxin specific for human cells secreted by streptococcus intermedius uns46 isolated from a human liver abscess. *Infect Immun*, 64(8):3093–3100, Aug 1996.

[76] H. Nagamune, C. Ohnishi, A. Katsuura, Y. Taoka, K. Fushitani, R. A. Whiley, K. Yamashita, A. Tsuji, Y. Matsuda, T. Maeda, H. Korai, and S. Kitamura. Intermedilysin. a cytolytic toxin specific for human cells of a streptococcus intermedius isolated from human liver abscess. *Adv Exp Med Biol*, 418:773–775, 1997.

[77] L. D. Nelson, A. E. Johnson, and E. London. How interaction of perfringolysin o with membranes is controlled by sterol structure, lipid structure, and physiological low ph: insights into the origin of perfringolysin o-lipid raft interaction. *J Biol Chem*, 283(8):4632–4642, Feb 2008.

[78] W. Niedermeyer. Interaction of streptolysin-o with biomembranes: kinetic and morphological studies on erythrocyte membranes. *Toxicon*, 23(3):425–439, 1985.

[79] T. Oberley and J. Duncan. Characteristics of streptolysin o action. *Infection and Immunity*, 4:683–7, 1971.

[80] Y. Ohno-Iwashita, M. Iwamoto, S. Ando, and S. Iwashita. Effect of lipidic factors on membrane cholesterol topology–mode of binding of theta-toxin to cholesterol in liposomes. *Biochim Biophys Acta*, 1109(1):81–90, Aug 1992.

[81] Y. Ohno-Iwashita, M. Iwamoto, S. Ando, K. Mitsui, and S. Iwashita. A modified theta-toxin produced by limited proteolysis and methylation: a probe for the functional study of membrane cholesterol. *Biochim Biophys Acta*, 1023(3):441–448, Apr 1990.

[82] Y. Ohno-Iwashita, M. Iwamoto, K. Mitsui, S. Ando, and Y. Nagai. Protease-nicked theta-toxin of clostridium perfringens, a new membrane probe with no cytolytic effect, reveals two classes of cholesterol as toxin-binding sites on sheep erythrocytes. *Eur J Biochem*, 176(1):95–101, Sep 1988.

[83] Y. Ohno-Iwashita, M. Iwamoto, K. Mitsui, H. Kawasaki, and S. Ando. Cold-labile hemolysin produced by limited proteolysis of theta-toxin from clostridium perfringens. *Biochemistry*, 25(20):6048–6053, Oct 1986.

[84] A. Olofsson, H. Hebert, and M. Thelestam. The projection structure of perfringolysin o (clostridium perfringens theta-toxin). *FEBS Lett*, 319(1-2):125–127, Mar 1993.

[85] A. Ortqvist. Pneumococcal vaccination: current and future issues. *Eur Respir J*, 18(1):184–195, Jul 2001.

[86] M. Palmer, R. Harris, C. Freytag, M. Kehoe, J. Tranum-Jensen, and S. Bhakdi. Assembly mechanism of the oligomeric streptolysin o pore: the early membrane lesion is lined by a free edge of the lipid membrane and is extended gradually during oligomerization. *EMBO J*, 17(6):1598–1605, Mar 1998.

[87] M. Palmer, P. Saweljew, I. Vulicevic, A. Valeva, M. Kehoe, and S. Bhakdi. Membrane-penetrating domain of streptolysin o identified by cysteine scanning mutagenesis. *J Biol Chem*, 271(43):26664–26667, Oct 1996.

[88] M. Palmer, A. Valeva, M. Kehoe, and S. Bhakdi. Kinetics of streptolysin o self-assembly. *European Journal of Biochemistry*, 231(2):388–395, 1995.

[89] M. Palmer, I. Vulicevic, P. Saweljew, A. Valeva, M. Kehoe, and S. Bhakdi. Streptolysin o: a proposed model of allosteric interaction between a pore-forming protein and its target lipid bilayer. *Biochemistry*, 37(8):2378–2383, Feb 1998.

[90] J. C. Paton, R. A. Lock, and D. J. Hansman. Effect of immunization with pneumolysin on survival time of mice challenged with streptococcus pneumoniae. *Infect Immun*, 40(2):548–552, May 1983.

[91] C. Petosa, R. J. Collier, K. R. Klimpel, S. H. Leppla, and R. C. Liddington. Crystal structure of the anthrax toxin protective antigen. *Nature*, 385(6619):833–838, Feb 1997.

[92] G. Polekhina, K. S. Giddings, R. K. Tweten, and M. W. Parker. Insights into the action of the superfamily of cholesterol-dependent cytolysins from studies of intermedilysin. *Proc Natl Acad Sci U S A*, 102(3):600–605, Jan 2005.

[93] A. J. Pringent, D. Interaction of streptolysin o with sterols. *Biochimica et Biophysica Acta (BBA)*, 443:288–300, 1976.

[94] R. Ramachandran, A. P. Heuck, R. K. Tweten, and A. E. Johnson. Structural insights into the membrane-anchoring mechanism of a cholesterol-dependent cytolysin. *Nat Struct Biol*, 9(11):823–827, Nov 2002.

[95] R. Ramachandran, R. K. Tweten, and A. E. Johnson. Membrane-dependent conformational changes initiate cholesterol-dependent cytolysin oligomerization and intersubunit beta-strand alignment. *Nat Struct Mol Biol*, 11(8):697–705, Aug 2004.

[96] R. Ramachandran, R. K. Tweten, and A. E. Johnson. The domains of a cholesterol-dependent cytolysin undergo a major fret-detected rearrangement during pore formation. *Proc Natl Acad Sci U S A*, 102(20):7139–7144, May 2005.

[97] C. J. Rosado, S. Kondos, T. E. Bull, M. J. Kuiper, R. H. P. Law, A. M. Buckle, I. Voskoboinik, P. I. Bird, J. A. Trapani, J. C. Whisstock, and M. A. Dunstone. The macpf/cdc family of pore-forming toxins. *Cellular Microbiology*, 10(9):1765–1774, 2008.

[98] J. Rossjohn, S. C. Feil, W. J. McKinstry, R. K. Tweten, and M. W. Parker. Structure of a cholesterol-binding, thiol-activated cytolysin and a model of its membrane form. *Cell*, 89(5):685–692, May 1997.

[99] U. K. RS Brown, JD Brennan. Self-quenching of nitrobenzoxadiazole labelled phospholipids in lipid-membranes. *Journal of Chemical Physics*, 100:6019–27, 1994.

[100] R. Scherrer and P. Gerhardt. Molecular sieving by the bacillus megaterium cell wall and protoplast. *J Bacteriol*, 107(3):718–735, Sep 1971.

[101] N. Sekino-Suzuki, M. Nakamura, K. I. Mitsui, and Y. Ohno-Iwashita. Contribution of individual tryptophan residues to the structure and activity of theta-toxin (perfringolysin o), a cholesterol-binding cytolysin. *Eur J Biochem*, 241(3):941–947, Nov 1996.

[102] K. Sekiya, R. Satoh, H. Danbara, and Y. Futaesaku. A ring-shaped structure with a crown formed by streptolysin o on the erythrocyte membrane. *J Bacteriol*, 175(18):5953–5961, Sep 1993.

[103] S. Shany, A. W. Bernheimer, P. S. Grushoff, and K. S. Kim. Evidence for membrane cholesterol as the common binding site for cereolysin, streptolysin o and saponin. *Mol Cell Biochem*, 3(3):179–186, May 1974.

[104] O. Shatursky, A. P. Heuck, L. A. Shepard, J. Rossjohn, M. W. Parker, A. E. Johnson, and R. K. Tweten. The mechanism of membrane insertion for a cholesterol-dependent cytolysin: a novel paradigm for pore-forming toxins. *Cell*, 99(3):293–299, Oct 1999.

[105] L. A. Shepard, A. P. Heuck, B. D. Hamman, J. Rossjohn, M. W. Parker, K. R. Ryan, A. E. Johnson, and R. K. Tweten. Identification of a membrane-spanning domain of the thiol-activated pore-forming toxin clostridium perfringens perfringolysin o: An α-helical to β-sheet transition identified by fluorescence spectroscopy. *Biochemistry*, 37(41):14563–14574, 1998. PMID: 9772185.

[106] L. A. Shepard, O. Shatursky, A. E. Johnson, and R. K. Tweten. The mechanism of pore assembly for a cholesterol-dependent cytolysin: formation of a large prepore complex precedes the insertion of the transmembrane beta-hairpins. *Biochemistry*, 39(33):10284–10293, Aug 2000.

[107] A. S. Solovyova, M. Nöllmann, T. J. Mitchell, and O. Byron. The solution structure and oligomerization behavior of two bacterial toxins: pneumolysin and perfringolysin o. *Biophys J*, 87(1):540–552, Jul 2004.

[108] C. E. Soltani, E. M. Hotze, A. E. Johnson, and R. K. Tweten. Structural elements of the cholesterol-dependent cytolysins that are responsible for their cholesterol-sensitive membrane interactions. *Proc Natl Acad Sci U S A*, 104(51):20226–20231, Dec 2007.

[109] L. Song, M. R. Hobaugh, C. Shustak, S. Cheley, H. Bayley, and J. E. Gouaux. Structure of staphylococcal alpha-hemolysin, a heptameric transmembrane pore. *Science*, 274(5294):1859–1866, Dec 1996.

[110] S. J. Tilley, E. V. Orlova, R. J. C. Gilbert, P. W. Andrew, and H. R. Saibil. Structural basis of pore formation by the bacterial toxin pneumolysin. *Cell*, 121(2):247–256, Apr 2005.

[111] E. Todd. Antigenic streptococcal hemolysin. *Journal of Experimental Medicine*, 55:267–280, 1932.

[112] E. Todd. The differenciation of two distinct serological varieties of streptolysin o and streptolysin s. *Journal of Patholological Bacteriology*, 47:423–45, 1938.

[113] R. K. Tweten. Cholesterol-dependent cytolysins, a family of versatile pore-forming toxins. *Infect Immun*, 73(10):6199–6209, Oct 2005.

[114] R. K. Tweten, R. W. Harris, and P. J. Sims. Isolation of a tryptic fragment from clostridium perfringens theta-toxin that contains sites for membrane binding and self-aggregation. *J Biol Chem*, 266(19):12449–12454, Jul 1991.

[115] R. K. Tweten, M. W. Parker, and A. E. Johnson. The cholesterol-dependent cytolysins. *Curr Top Microbiol Immunol*, 257:15–33, 2001.

[116] F. G. van der Goot. *Pore-Forming Toxins*. Springer-Verlag, 2001.

[117] A. A. Waheed, Y. Shimada, H. F. Heijnen, M. Nakamura, M. Inomata, M. Hayashi, S. Iwashita, J. W. Slot, and Y. Ohno-Iwashita. Selective binding of perfringolysin o derivative to cholesterol-rich membrane microdomains (rafts). *Proc Natl Acad Sci U S A*, 98(9):4926–4931, Apr 2001.

[118] K. C. Watson and E. J. Kerr. Sterol structural requirements for inhibition of streptolysin o activity. *Biochem J*, 140(1):95–98, Apr 1974.

[119] K. C. Watson, T. P. Rose, and E. J. Kerr. Some factors influencing the effect of cholesterol on streptolysin o activity. *J Clin Pathol*, 25(10):885–891, Oct 1972.

[120] S. Weis and M. Palmer. Streptolysin o: the c-terminal, tryptophan-rich domain carries functional sites for both membrane binding and self-interaction but not for stable oligomerization. *Biochimica et Biophysica Acta (BBA) - Biomembranes*, 1510(1-2):292 – 299, 2001.

[121] J. Weld. The toxic properties of serum extracts of hemolytic streptococci. *J. Exp. Med.*, 59:83–95, 1934.

[122] P. Wu and L. Brand. Resonance energy transfer: methods and applications. *Anal Biochem*, 218(1):1–13, Apr 1994.

Appendix A

Fitted Parameters for Time-Resolved Fluorescence Analyses

As stated in the previous chapters, time-resolved fluroescence decays were fitted with a three-exponential model, from which the average lifetimes were obtained according to equation 2.2 on page 25. Here, the pre-exponential (α_i) and lifetime (τ_I) values for the individual components obtained from the fits are given.

A.1 LIFETIME PARAMETERS FOR CHAPTER 2

Table A.1 Fitted lifetime components N90C-F oligomers and for hybrid oligomers formed from an equimolar mixture of N90C-F and N90C-R, without domain 4 or with 1, 2 or 4 equivalents of domain 4 fragment added (see section 2.3.4 on page 29).

Parameter	N90C-F	N90C-F+R, no D4	D4 1 eq.	D4 2 eq.	D4 4 eq.
α_1	4579	11042	10620	10192	10284
τ_1	0.571	0.372	0.384	0.380	0.41
α_2	6205	7867	7596	7834	7721
τ_2	2.512	1.65	1.605	1.54	1.66
α_3	5066	2418	2577	2793	2486
τ_3	5.071	3.64	3.59	3.62	3.76
$< \tau >$	2.77	1.10	1.23	1.25	1.29
χ^2	1.03	1.12	1.12	1.07	1.15

Table A.2 Fitted lifetime components N90C-F oligomers and for hybrid oligomers formed from an equimolar mixture of N90C-F and N90C-R, without unlabelled wild type PLO or with 1, 2 or 4 equivalents of wild type PLO added (see section 2.3.4 on page 29).

Parameter	N90C-F	N90C-F+R, no wt	wt 1 eq.	wt 2 eq.	wt 4 eq.
α_1	4579	11042	8681	8927	8626
τ_1	0.571	0.372	0.62	0.79	0.66
α_2	6205	7867	5664	6909	5745
τ_2	2.512	1.65	2.26	3.35	2.26
α_3	5066	2418	3420	1155	3368
τ_3	5.071	3.64	5.06	6.78	5.05
$< \tau >$	2.77	1.10	1.87	2.23	2.14
χ^2	1.03	1.12	1.11	1.06	1.13

A.2 LIFETIME PARAMETERS FOR CHAPTER 3

Table A.3 K231C-NBD fluorescence membrane insertion of domain 3 in hybrid oligomers. Fitted lifetime components of K231C-NBD without membranes, and for 1:2 mixtures of NBD-K231C and unlabelled disulphide mutant or unlabelled wild type PLO.

Parameter	+WT	+DS	no membranes
α_1 6897	6505	11509	
τ_1	0.93	1.07	0.52
α_2	5121	4485	7001
τ_2	3.32	3.84	2.19
α_3	4483	1957	1982
τ_3	9.38	9.84	7.58
$< \tau >$	4.04	3.2	1.7
χ^2	1.20	1.08	1.19

Table A.4 A329C-NBD fluorescence membrane insertion of domain 3 in hybrid oligomers. Fitted lifetime components of A329C-NBD without membranes, and for 1:2 mixtures of NBD-K231C and unlabelled disulphide mutant or unlabelled wild type PLO.

Parameter	+WT	+DS	no membranes
α_1	2975	8050	7885
τ_1	1.46	0.56	0.62
α_2	4587	6245	4691
τ_2	4.99	2.64	2.24
α_3	4446	3573	1851
τ_3	10.60	8.76	8.68
$< \tau >$	6.2	2.9	2.1
χ^2	1.09	1.17	1.18

A.3 LIFETIME PARAMETERS FOR CHAPTER 4

Table A.5 R219C-NBD fluorescence lifetime parameters of membrane-bound and -unbound monomers and SDO

Parameter	Monomer	Monomer on Membranes	SDO	SDO on Membranes
α_1	13053	7915	11180	10545
τ_1	0.65	0.78	0.47	0.39
α_2	5301	6451	8272	7119
τ_2	2.28	2.87	1.61	2.24
α_3	907	1845	1255	1885
τ_3	7.10	8.34	6.03	7.43
$< \tau >$	1.4	2.5	1.3	1.9
χ^2	1.07	1.08	1.17	1.19

Table A.6 K231C-NBD fluorescence lifetime parameters of membrane-bound and -unbound monomers and SDO

Parameter	Monomer	Monomer on Membranes	SDO	SDO on Membranes
α_1	9718	6458	12185	8423
τ_1	0.59	0.74	0.78	0.86
α_2	6153	5322	7791	5368
τ_2	2.54	3.65	2.80	3.46
α_3	2314	3930	2757	2380
τ_3	7.92	9.33	8.01	9.27
$< \tau >$	2.2	3.9	2.4	2.9
χ^2	1.09	1.05	1.10	1.04

Table A.7 V232C-NBD fluorescence lifetime parameters of membrane-bound and -unbound monomers and SDO

Parameter	Monomer	Monomer on Membranes	SDO	SDO on Membranes
α_1	7654	13611	7091	12899
τ_1	0.55	0.64	0.84	0.69
α_2	5523	4544	5217	4562
τ_2	2.97	2.38	3.14	2.65
α_3	3908	958	2842	1016
τ_3	9.33	7.93	9.63	8.52
$< \tau >$	3.4	1.4	3.3	1.6
χ^2	1.14	1.06	1.14	1.03

Table A.8 K328C-NBD Fluorescence Lifetime Parameters of Membrane-bound and -unbound monomers and SDO

Parameter	Monomer	Monomer on Membranes	SDO	SDO on Membranes
α_1	9659	13481	9189	11003
τ_1	0.69	0.49	0.51	0.59
α_2	5478	6072	7005	6355
τ_2	2.92	1.70	2.26	2.30
α_3	1825	1280	2294	1325
τ_3	8.45	5.67	7.75	6.63
$< \tau >$	2.2	1.3	2.1	1.6
χ^2	1.10	1.12	1.18	1.04

Table A.9 A329C-NBD fluorescence lifetime parameters of membrane-bound and -unbound monomers and SDO

Mutant	Monomer	Monomer on Membranes	SDO	SDO on Membranes
α_1	12271	3284	11991	4182
τ_1	0.65	1.87	0.66	0.15
α_2	4288	4880	4480	6463
τ_2	2.98	4.35	2.88	2.70
α_3	1992	5165	1934	5872
τ_3	9.67	9.22	9.44	8.56
$< \tau >$	2.2	6.7	2.1	4.1
χ^2	1.15	1.13	1.05	1.19

Table A.10 K330C-NBD fluorescence lifetime parameters of membrane-bound and -unbound monomers and SDO

Parameter	Monomer	Monomer on Membranes	SDO	SDO on Membranes
α_1	8007	8098	9062	12247
τ_1	0.29	0.86	0.53	0.51
α_2	10228	5014	8421	6656
τ_2	1.56	2.96	1.57	2.08
α_3	2136	2579	1431	579
τ_3	6.68	8.35	4.75	6.15
$< \tau >$	1.6	2.7	1.3	1.3
χ^2	1.20	1.19	1.16	1.05

Table A.11 F331C-NBD Fluorescence Lifetime Parameters of Membrane-bound and -unbound monomers and SDO

Parameter	Monomer	Monomer on Membranes	SDO	SDO on Membranes
α_1	5932	5876	5756	5956
τ_1	0.96	0.83	0.778	0.81
α_2	5097	6189	5609	5625
τ_2	3.84	3.59	3.39	2.68
α_3	3689	3118	3713	3324
τ_3	9.83	8.96	9.59	7.71
$< \tau >$	4.1	3.7	3.9	2.3
χ^2	1.05	1.09	1.03	1.11